UNIVERSITY OF COSTA RICA
GRADUATE STUDIES SYSTEM

IMPACT OF DIETARY FIBER FROM COSTA RICAN BEANS ON THE GUT MICROBIOTA IN A CHEMICALLY INDUCED COLORECTAL CARCINOGENESIS MODEL IN WISTAR RATS.

Impacto de la fibra dietética de tres variedades de frijoles costarricenses sobre la microbiota intestinal de un modelo de carcinogénesis colorrectal en ratas Wistar

Thesis submitted for the consideration of the Committee of the Graduate Program in Microbiology, Parasitology, Clinical Chemistry, and Immunology in partial fulfillment of the requirements for the degree and title of Academic Master's in Immunology

MARIA JOSE CARVAJAL CARVAJAL

Rodrigo Facio University Campus, Costa Rica

2026

DEDICATION

To God, for His infinite love and guidance, and for carrying me through every step of this journey.

To my husband, for his love and support.

To my children, Pío, María Paulina, and Josemaría, my endless source of motivation, strength and joy.

"At the right time, I, the Lord, will make it happen."
— Isaiah 60:22

ACKNOWLEDGMENTS

I wish to express my deepest and most sincere gratitude to my thesis director, Dr. Gabriel Vargas Asensio, for granting me the opportunity to undertake this project and for his exceptional guidance throughout every stage of this research. Working under his supervision has been a true privilege. His vision and rigorous scientific approach were fundamental to the development of this thesis. His confidence in my ability to independently conduct the analyses and successfully complete this work was a constant source of motivation. I am especially grateful for his thoughtful counsel, clarity of judgment, and constructive guidance, which not only strengthened this research but also contributed significantly to my academic and professional growth.

I am deeply grateful to my advisor, Dr. Ernesto Vargas Méndez, whose patience, support, and encouragement were invaluable throughout this process. Beyond his remarkable knowledge and teaching ability, he has been an outstanding mentor who inspired me to strive for the highest standards. His ability to analyze situations from diverse perspectives enriched my work, and his warmth and generosity have left a lasting impression on both my professional and personal development.

I also wish to express my sincere gratitude to Dra. Silvia Molina Castro for the opportunity to participate in this project and for her valuable guidance in the development and successful implementation of the carcinogenesis model. Her dedication, expertise, and support were fundamental to the execution of the experimental work. I am particularly grateful for her insightful contributions, and for her openness in sharing her knowledge.

My sincere thanks also go to Dr. David Loria Masis for his guidance during the initial stages of this thesis. His advice and support provided an important foundation for the development of this work.

I extend my gratitude to all collaborators who contributed to the execution of the assay, particularly Kimberly, Ana, and the participating students, whose dedication and commitment were essential to the completion of this research.

I am especially grateful to Iván León for his guidance and generous support in the longitudinal analysis of the microbiota, as well as for his valuable contributions and willingness to share his knowledge throughout this work.

I acknowledge the support of the Molecular Techniques Laboratory of the Faculty of Agronomy, whose assistance and collaborative environment were greatly appreciated.

To my husband, Pío, for fostering my growth both personally and professionally throughout this academic journey. His encouragement, support, and strength sustained me through challenging moments and were fundamental to the completion of this degree.

To my children, Pío, María Paulina, and Josemaría, who are my endless source of love, strength and inspiration. You motivate me every day to give the best of myself. This achievement is as much yours as it is mine, for your joy and resilience gave me the courage to persevere.

To my parents, Rita and Vinicio, for their unconditional love, support, and faith in me. Thank you for teaching me the meaning of perseverance and dedication, and for the sacrifices you made that shaped who I am today.

Finally, I express my gratitude to the Academic Master's Program in Microbiology, Parasitology, Immunology, and Clinical Chemistry at the University of Costa Rica— particularly Dr. Carlos Chacón— and to its faculty for providing an opportunity that contributed significantly to my professional and scientific development.

HOJA DE APROBACIONES

Esta tesis fue aceptada por la Comisión del Programa de Posgrado en Microbiología, Parasitología, Química Clínica e Inmunología de la Universidad de Costa Rica, como requisito parcial para optar al grado y título de Maestría Académica en Inmunología.

PhD. Javier Mora Rodríguez
Representante de la Decanatura
Sistema de Estudios de Posgrado

PhD. Gabriel Vargas Asencio
Director de Tesis

PhD. Ernesto Vargas Méndez
Asesor

PhD. Silvia Molina Castro
Asesora

PhD. Cynthia Arroyo Portilla
Representante del Director del Programa de Posgrado

María José Carvajal Carvajal
Candidata

TABLE OF CONTENTS

ABSTRACT

Colorectal cancer (CRC) represents a major global health burden, and dietary modulation of the gut microbiota (GM) has emerged as a promising preventive strategy. This study evaluated the impact of dietary fiber derived from three native Costa Rican varieties of *Phaseolus vulgaris* (Cabecar, Mantequilla, and Nambi) on GM composition during chemically induced colorectal carcinogenesis in Wistar rats. Sixty-four animals were randomized to receive flour obtained from whole cooked beans, isolated dietary fiber derived from whole cooked beans, or high-fructose corn syrup (HFCS) for 12 weeks. Carcinogenesis was induced at week 3 with 1,2-dimethylhydrazine (1,2-DMH) and dextran sulfate sodium (DSS), and fecal samples were collected at baseline, pre-carcinogen, mid-intervention, and endpoint (weeks 1, 3, 9, and 12).

Gut microbiome profiling was performed by metagenomic sequencing of the 16S rRNA gene (V3–V4 region) to characterize taxonomic composition and differential abundance. Carcinogen exposure alone did not induce significant dysbiosis, indicating that microbial shifts were primarily driven by dietary interventions. Bean fiber supplementation enriched the GM with fermentative and short-chain fatty acids (SCFAs)–producing taxa such as *Eubacterium ventriosum* group, while suppressing opportunists including Eggerthellaceae, Planococcaceae, and *Corynebacterium*. In contrast, HFCS intake promoted inflammation-associated taxa (Enterobacteriaceae, *Enterococcus, Helicobacter, Kosakonia*) and depleted butyrate producers (*Eubacterium xylanophilum* group, Lachnospiraceae NK4A136 group), fostering a pro-inflammatory environment.

These findings confirm that Wistar rats harbor GM responsive to dietary fiber and are suitable for studying diet–microbiome–carcinogenesis interactions. Bean fiber supplementation demonstrates protective effects against colorectal carcinogenesis by modulating GM toward anti-inflammatory and immune-regulatory profiles. Further research is needed to understand the molecular mechanisms associated with these GM shifts. In conclusion, native Costa Rican beans can beneficially modulate the GM during colorectal carcinogenesis, supporting their role as preventive nutritional strategy against colorectal cancer while adding economic and social value to local bean production and strengthening food security in Costa Rica.

RESUMEN EN ESPAÑOL

El cáncer colorrectal (CRC) constituye una de las principales causas de incidencia y mortalidad por cáncer a nivel mundial, y la modulación dietética de la microbiota intestinal (MI) se ha consolidado como una estrategia preventiva prometedora. El presente estudio evaluó el efecto de la fibra dietética derivada de tres variedades nativas costarricenses de *Phaseolus vulgaris* (Cabecar, Mantequilla y Nambi) sobre la composición de la MI durante la carcinogénesis colorrectal en un modelo de inducción química en ratas Wistar con 1,2-dimetilhidrazina (1,2-DMH) y dextrán sulfato de sodio (DSS). Se administró harina de los frijoles cocidos enteros, fibra dietética aislada de frijoles cocidos enteros o jarabe de maíz alto en fructosa (HFCS), según los grupos experimentales, durante 12 semanas, recolectándose muestras fecales en las semanas 1, 3, 9 y 12.

La microbiota intestinal se analizó mediante secuenciación del gen del ARNr 16S (región V3–V4), lo que permitió estudiar su composición y abundancia. La exposición al carcinógeno no generó disbiosis significativa, evidenciando que las variaciones observadas fueron atribuibles principalmente a las intervenciones dietéticas. La suplementación con frijol promovió la proliferación de taxones fermentativos y productores de ácidos grasos de cadena corta (AGCC), como el grupo *Eubacterium ventriosum,* y redujo la presencia de oportunistas como Eggerthellaceae, Planococcaceae y *Corynebacterium*. En contraste, el consumo de HFCS favoreció la expansión de taxones asociados a inflamación (*Enterococcus, Helicobacter, Kosakonia*) y disminuyó productores clave de butirato (*Eubacterium xylanophilum y* Lachnospiraceae NK4A136), favoreciendo un entorno proinflamatorio.

Estos hallazgos confirman que la MI de ratas Wistar tiene especies capaces de responder a intervenciones con fibra dietética y constituye un modelo experimental valioso para estudiar las interacciones dieta–microbiota intestinal–carcinogénesis. La suplementación con fibra de los frijoles demostró efectos protectores al modular la MI hacia perfiles anti-inflamatorios e inmunoreguladores. En conclusión, los frijoles nativos de Costa Rica pueden modificar beneficiosamente la MI en el contexto de la carcinogénesis colorrectal, respaldando su papel como intervención dietética para la prevención del CRC y aportando, además, valor económico y social a la producción local de frijoles, fortaleciendo la seguridad alimentaria y la sostenibilidad agrícola del país.

LIST OF TABLES

LIST OF FIGURES

LIST OF ABBREVIATIONS

1,2-DMH: 1,2-dimethylhydrazine

ACF: Aberrant crypt foci

AGCC: Ácidos grasos de cadena corta

AhR: Aryl hydrocarbon receptor

ANCOM-BC: Analysis of Compositions of Microbiomes with Bias Correction

ANOSIM: Analysis of Similarities

AOM: Azoxymethane

ASR: Age-standardized incidence rate

ASVs: Amplicon sequence variants

BAs: Bile acids

BFT: *Bacteroides fragilis* toxin

Bregs: Regulatory B cells

CAZymes: Carbohydrate-active enzymes

CCL17: C-C chemokine ligand 17

CCL22: C-C chemokine ligand 22

CCL25: C-C chemokine ligand 25

CCR9: C-C chemokine receptor type 9

CD8+ Tregs: Regulatory CD8+ cells

CIMP: CpG island methylator phenotype

CIN: Chromosomal instability

CITA: Research Center for Food Science and Technology

CLR: Centered log-ratio

CNS1: Conserved non-coding sequence 1

CoPEC*:* Colibactin-producing *Escherichia coli*

COX-2: Cyclooxygenase-2

CRC: Colorectal cancer

DCregs: Regulatory dendritic cells

DMAB: 3,2′-Dimethyl-4-Aminobiphenyl

DNA: Deoxyribonucleic acid

DSS: Dextran Sulfate sodium

EOCRC: Early-onset of colorectal cancer

ETBF: Enterotoxigenic *Bacteroides fragilis*

FOS: Fructo-oligosaccharides

Gal-3: Galectin-3

GM: Gut microbiota

GOS: Galacto-oligossacharides

GPCR: G protein coupled receptor

H_2S: Hydrogen sulfide

HDACs: Histone deacetylases

HFCS: High fructose corn syrup

HFD: High fat diet

IBD: Irritable Bowel Disease

IECs: Intestinal epithelial cells

IL-1: Interleukin-1

IL-22: Interleukin-22 (IL-22)

IL-8: Interleukin-8

IL-10: Interleukin 10

ILCregs: Regulatory innate lymphoid cells

ILCs: Innate lymphoid cells

IOM: Immuno-oncology-microbiome axis

LFC: Log fold changes

LOESS: Locally Estimated Scatterplot Smoothing

MAM: Methylazoxymethanol

MDSCs: Myeloid-derived suppressor cells

METTL3: Methyltransferase-like 3

MI: Microbiota intestinal

MSI: Microsatellite instability

NDCs: Non- digestible carbohydrates

NF-kB: Nuclear factor-kappa B

NKregs: Regulatory natural killer cells

NTBF: Non-toxigenic *Bacteroides fragilis*

PCoA: Principal Coordinate Analysis

PERMANOVA: Permutational Multivariate Analysis of Variance

PRRs: Pattern recognition receptors

PULS: Polysaccharide utilization loci

RNA: Ribonucleic acid

rRNA: Ribosomal RNA

SCFAs: Short-chain fatty acids

SGG: *Streptococcus gallolyticus subespecies gallolyticus*

SRB: Sulfate-reducing bacteria

SUS: Starch utilization system

T regs: regulatory T cells

TDF: total dietary fiber

TGF-β: transforming growth factor-beta

TLR2: Toll-Like Receptor 2

TLR4Toll-Like Receptor 4

TME: tumor microenvironment

TNF-α: tumor necrosis factor-alpha

UC: Ulcerative Colitis

UCR: University of Costa Rica

CHAPTER I. INTRODUCTION

1.1 Colorectal cancer

Cancer is defined as uncontrolled cell proliferation leading to the formation of neoplasms. These neoplasms can spread systemically via the blood and lymphatic circulation, a process termed metastasis. Colorectal cancer (CRC) is defined as cancer of the large intestine and/or rectum. It is the third most frequently diagnosed cancer worldwide and the second leading cause of cancer-related deaths. In Costa Rica, CRC ranks second in mortality and fourth in incidence (Bray et al., 2024).

In recent years, a marked increase incidence of CRC has been observed among young people. The epidemiology of CRC is evolving. There is an increasing incidence of early onset of CRC in people under 50 years of age affecting all ethnic groups. Currently, there is a decline in CRC incidence among individuals over 70 years old. The distribution of CRC among Hispanic population has increase from 8.8% in 1992 to 16.0% in 2019 of the total CRC cases (Dharwadkar et al., 2022; Gupta et al., 2024).

The development of colorectal cancer (CRC) is a multistep process that begins with a mutagenic event known as tumor initiation. This is followed by additional mutagenic and/or epigenetic changes, referred to as tumor promotion, which drive the expansion of the mutated cell clone and the proliferation of tumor cells. In response to these stimuli, normal colonic epithelial cells undergo transformation into aberrant crypt foci (ACF), the earliest identifiable preneoplastic lesions. ACF are considered precursors that can progress into adenomatous intermediates (precancerous polyps), thereby linking these two concepts within the continuum of colorectal carcinogenesis. As these lesions accumulate further genetic alterations, they evolve into early and advanced adenomas. The next critical step is the transition to carcinoma *in situ*, characterized by malignant cellular atypia confined to the mucosa. Invasion into the submucosa marks the progression to invasive adenocarcinoma, which may subsequently metastasize to secondary organs, most commonly the liver (Alzahrani et al., 2022; Testa et al., 2018). Histologically, colorectal adenocarcinoma constitutes approximately 90% of CRCs, followed by mucinous colorectal adenocarcinoma, medullary CRC, and, albeit infrequently, signet ring cell CRC (Nitsche et al., 2013).

Colorectal carcinogenesis refers to the initiation and progression of colorectal cancer through the accumulation of molecular changes. These changes disrupt normal cell growth,

differentiation, and apoptosis, ultimately leading to tumor formation. Despite the genetic heterogeneity exhibited by colorectal tumors, their development appears to proceed through multiple discrete pathways, which include the following: Chromosomal instability (CIN), is defined as large-scale genetic alterations including gains, losses, or translocations of chromosomes; Microsatellite instability (MSI), is characterized by defects in DNA mismatch repair leading to an accumulation of mutations in short repetitive DNA sequences. The CpG island methylator phenotype (CIMP), is an epigenetic silencing of tumor suppressor genes through abnormal DNA methylation. Oncogene activation and tumor suppressor loss, mutations in genes such as APC, KRAS, TP53, and MLH1 drive progression from adenoma to carcinoma (Nguyen et al., 2020)

Colorectal carcinogenesis is a complex process influenced by host-related factors such as age, sex, and genetics, as well as environmental factors including diet, obesity, and tobacco use (Keum & Giovannucci, 2019). The increasing incidence of CRC suggests that risk factors during childhood and adolescence may contribute to its development. These factors include a sedentary lifestyle, higher consumption of animal-based foods, the rising prevalence of childhood obesity, and early antibiotic exposure, which may disrupt the gut microbiota and promote colorectal carcinogenesis. Conversely, the consumption of whole grains, dietary fiber, and dairy products, together with regular physical activity, has been shown to exert a protective effect against CRC. Costa Rica, a country undergoing a transition with relatively low risk of CRC, has exhibited increasing trends in age-standardized incidence rate (ASR) during the last decades, showing greater early-onset of CRC (EOCRC) (Roshandel et al., 2024).

While the carcinogenic effects of high-fat, high-calorie diets have been extensively studied, recent research has focused on the role of specific nutrients—such as dietary fiber, vitamins, minerals—and the intestinal microbiota in CRC development (Kato & Sun, 2023). Emerging evidence shows the critical role of the gut microbiota (GM), an essential component of the tumor microenvironment, in the development of colorectal carcinogenesis. Gut dysbiosis, characterized by imbalance in bacterial, fungal, viral and archaeal communities has been strongly implicated in colorectal carcinogenesis through direct and indirect interactions with host epithelial and immune cells via metabolites, proteins and macromolecules (Kim & Lee, 2022).

1.2 Gut Microbiota

The GM is defined as the community of microorganisms residing in the gastrointestinal tract, including bacteria, fungi, viruses, archaea, and protozoa. This community plays a critical role in nutrient metabolism, vitamin K synthesis, maintenance of the epithelial barrier, systemic and local immunomodulation, and prevention of colonization by enteropathogenic bacteria (Tudela et al., 2021). The definition of a healthy GM has changed over time. A healthy GM is characterized by a diverse and balanced community of microorganisms that perform vital functions for the host. Several key markers have been proposed to assess a healthy GM, including microbial diversity, composition, functionality, and resilience. Production of important metabolites like Short Chain Fatty Acids (SCFAs), conjugation and deconjugation of bile acids and tryptophan derivatives, as well as gases (hydrogen, hydrogen sulfide, methane), pH levels and presence of inflammation markers are also potential indicators of healthy GM (Van Hul et al., 2024).

The main phyla of the human GM are Bacillota (formerly Firmicutes), Bacteroidota (formerly Bacteroidetes), Actinomycetota, Pseudomonadota (formerly Proteobacteria) and Verrucomicrobiota, with the top two phyla Bacillota and Bacteroidota representing roughly 90% of gut microbiota. However, the exact proportion of each of these phyla varies significantly between healthy subjects and does not constitute a major marker of diseases. The phylum Bacillota includes relevant genera such as *Ruminococcus*, *Clostridium*, and butyrate producers like *Eubacterium, Faecalibacterium,* and *Roseburia*. Rather than merely focusing on diversity, the current literature predominantly examines the specific composition of gut microbiota in diseased versus healthy states. This approach provides deeper insights into the microbial alterations associated with various health conditions, enabling researchers to identify specific bacterial taxa that may contribute to or protect against disease (Van Hul et al., 2024).

Dysbiosis is any change to the composition of resident commensal communities relative to the community found in healthy individuals. Dysbiosis has been categorized into three types: 1) loss of beneficial microbial organisms, (2) expansion of pathobionts or potentially harmful microorganisms and (3) loss of overall microbial diversity (Petersen & Round, 2014). Dysbiosis modulates colorectal carcinogenesis by reprogramming regulatory T cells (Tregs) abundance and function: pathogenic communities can drive pro-tumor,

IL-17–biased or immunosuppressive Treg responses, whereas a balanced SCFAs-rich microbiota supports Tregs that restrain chronic inflammation and thereby lower cancer risk (Garvey, 2024).

The intestinal microbiota is essential for shaping immune responses, balancing the inflammation required to fight pathogens with tolerance mechanisms that prevent harmful reactions against self-tissues and commensals. Immune tolerance is maintained through central and peripheral mechanisms. Central tolerance eliminates autoreactive clones in primary lymphoid organs, while peripheral tolerance operates in tissues once lymphocytes are mature and circulating. Peripheral tolerance relies on mechanisms such as anergy, clonal deletion, and suppression mediated by regulatory cells. Several cell types contribute to this network, including CD4+ regulatory subsets (Foxp3+ Tregs, Tr1, Th3), regulatory CD8+ cells (CD8+Tregs), regulatory B cells (Bregs), myeloid-derived suppressor cells (MDSCs), regulatory dendritic cells (DCregs), regulatory innate lymphoid cells (ILCregs),regulatory natural killer cells (NKregs) and tolerogenic dendritic cells (P. Shi et al., 2025). Together, these populations orchestrate immune balance, which is essential for preventing autoimmunity but can also be co-opted by tumors to evade immune surveillance. Among these, CD4+ Foxp3+ IL-10+ Tregs are the most studied and abundant subset. They produce IL-10 and TGF-β, suppressing excessive inflammatory responses and maintaining homeostasis against commensals and self-antigens (Ge et al., 2024).

Microbial metabolites such as SCFAs—particularly butyrate and propionate—expand colonic Treg populations and protect against colitis through several mechanisms. Two of the most prominent are: inhibition of histone deacetylases (HDACs), that promote chromatin condensation and can thereby regulate gene expression; by inhibiting HDACs, butyrate facilitates a more open chromatin structure, enhancing the expression of genes involved in Treg differentiation and IL-10 production (Cheong & Trefely, 2025; J. Wang et al., 2025); and (2) activation of G-protein-coupled receptors (GPCRs), including GPCR43 (FFAR2) and GPR109a (HCAR2). These receptors are expressed on intestinal epithelial cells and Tregs, where they sense SCFAs and initiate intracellular signaling cascades. GPCR43 activation promotes anti-inflammatory responses by modulating ERK and AKT pathways while dampening NF-κB activity, thereby favoring Treg expansion and cytokine production. GPR109a signaling similarly induces anti-inflammatory pathways and supports epithelial

integrity. Notably, GPCR43 expression is increased specifically on intestinal Tregs, and genetic loss of these receptors predisposes animals to colonic inflammation and colorectal cancer (Arpaia et al., 2013; Furusawa et al., 2013; Z. Liu et al., 2025; Round & Mazmanian, 2010; Smith et al., 2013).

In colorectal carcinogenesis, Tregs play a dual role. On one hand, they are indispensable for preventing chronic inflammation and maintaining mucosal integrity, which can reduce the risk of tumor initiation. In colitis-associated cancer models, Treg-derived IL-10 dampens microbiota-driven inflammation, reducing tissue damage and polyposis, thereby showing a protective side. On the other hand, tumor-infiltrating Foxp3+ Tregs can accumulate in CRC, suppress cytotoxic CD8+ and Th1 responses, favor immune evasion, and are linked to poorer prognosis and reduced efficacy of immunotherapy. This apparent contradiction reflects the functional heterogeneity of Tregs. Distinct subsets exert opposing effects: IL-10+ Tregs can suppress IL-17–driven tumor growth and exert anti-tumor activity, whereas IL-10– or CCR8+/Helios– Tregs are strongly pro-tumor and correlate with worse outcomes. Chemokine axes such as CCR9/CCL25 and CCL17/CCL22 orchestrate Treg recruitment into tumors; altering these pathways (e.g., CCR9 deficiency) increases the CD8+/Treg ratio and enhances antitumor immunity in mouse CRC models (Martínez-Ríos et al., 2025; Yu et al., 2025).

Beyond Treg induction, commensals have evolved direct anti-inflammatory strategies. Patients with IBD often exhibit elevated cytokines such as TNF-α and CXCL10, normally counterbalanced by Tregs. However, certain bacteria can antagonize these cytokines directly. *Lactobacillus paracasei* and *Lacticaseibacillus casei* encode a protease, lactoceptin, that selectively degrades IP-10, reducing lymphocyte recruitment in animal models of ileitis. This demonstrates that commensals not only promote tolerance through immune cell modulation but also directly suppress inflammatory mediators, reinforcing intestinal homeostasis (von Schillde et al., 2012). Beneficial genera including *Lactobacillus* and *Bifidobacterium* have been associated with anticancer effects in CRC (Louis & Flint, 2017).

Pathobionts are groups of microbes within the microbiota that are generally innocuous but can revert to a pathogenic under certain host and/or environmental conditions. Repeated exposure to pathobionts may damage the epithelial barrier of the host by inducing

an exacerbated innate inflammatory response through activation of proinflammatory cytokines, the inflammasome, induction of TH17 cells, and recruitment of neutrophils to the site of infection. Pathobiont proliferation depends on imbalances in the homeostasis of symbiotic communities caused by host genetic factors, dietary changes, and excessive use of antibiotics or other medications, among other factors. Important gastrointestinal pathobionts include *Clostridioides difficile*, *Helicobacter hepaticus*, *Helicobacter pylori*, invasive *Escherichia coli*, *Proteus mirabilis*, and *Klebsiella pneumoniae*, among others, which are implicated in pathological conditions such as Crohn's disease and Ulcerative Colitis (Chandra et al., 2021).

Mechanisms of colorectal carcinogenesis linked to the intestinal microbiota include: (1) inflammation and immune regulation, mentioned above (2) production of genotoxins, and (3) metabolism of dietary components (Tortora et al., 2022). Chronic inflammation is an established risk factor for CRC, and patients with IBD have an increased risk of developing CRC (Beaugerie & Itzkowitz, 2015). In CRC patients, enrichment of proinflammatory bacteria such as *Fusobacterium* has been observed, which is also overrepresented in IBD patients, along with reduced abundance of butyrate-producing species (N. Wu et al., 2013). Proinflammatory bacteria are thought to inhibit, alter, or exacerbate normal host responses, leading to abnormal apoptosis, cell proliferation, and inflammation.

Several bacterial species have been implicated in colorectal carcinogenesis through diverse mechanisms. *Fusobacterium nucleatum*, an oral commensal that translocate to the gut, promotes CRC by activating oncogenic Wnt/β-catenin signaling via its adhesion protein FadA, suppressing immune cytotoxicity through Fap2–TIGIT interactions, and inducing inflammation via outer membrane vesicles (Pignatelli et al., 2023). Similarly, Enterotoxigenic *Bacteroides fragilis* (ETBF) produces *B. fragilis* toxin (BFT), which disrupts epithelial barriers and activates NF-κB and STAT3 signaling, driving Th17-mediated inflammation and tumorigenesis (Chung et al., 2018; S. Wu et al., 2009). While non-toxigenic strains (NTBF) can promote tolerance through polysaccharide A–induced Tregs (Round & Mazmanian, 2010), some NTBF isolates have been linked to pro-inflammatory responses and polyp growth (Kordahi et al., 2021).

Colibactin-producing *Escherichia coli* (CoPEC) strains harbor the *pks* gene cluster, generating DNA damage, oxidative stress, and metabolic reprogramming that promote

tumorigenesis (Bonnet et al., 2014; Devaux et al., 2025). *Streptococcus gallolyticus subspecies gallolyticus* (SGG) is strongly associated with colonic neoplasia, with bloodstream infections often revealing undiagnosed tumors; its pathogenicity involves inflammatory mediators such as IL-1, COX-2, and IL-8 (Biarc et al., 2004). *Peptostreptococcus anaerobius* fosters a pro-inflammatory microenvironment by recruiting myeloid-derived suppressor cells and increasing reactive oxygen species, which activate TLR2/TLR4 signaling, cholesterol synthesis, and epithelial dysplasia (Long et al., 2019; Tsoi et al., 2017).

Beyond the gut, *Helicobacter pylori*, long recognized for its role in gastric cancer, has been linked to CRC. Large-scale epidemiological studies show that *H. pylori* infection increases CRC risk and mortality (Shah et al., 2024). Mechanistically, its VacA toxin disrupts epithelial proliferation, reduces regulatory T cells, activates STAT3 signaling, and depletes goblet cells, contributing to oncogenesis (Ralser et al., 2023). Collectively, these findings highlight how diverse bacterial species—through genotoxicity, immune modulation, and inflammatory signaling—can drive CRC development, underscoring the microbiota complex role in cancer pathogenesis.

Recent studies show that the intratumor microbiome is a key part of the tumor microenvironment (TME). Intratumor bacteria, often found inside tumor and immune cells, may originate from the gut microbiome. These microbes influence tumor biology by regulating immune cells, shaping inflammatory responses, and interacting with host metabolism, especially in gastrointestinal cancers such as esophageal, gastric, liver, colorectal, and pancreatic malignancies. To explain this interplay, researchers have proposed the immuno-oncology-microbiome (IOM) axis, which describes how gut and intratumor microbes together modulate immunity and metabolism within the TME, thereby affecting tumor progression and therapeutic outcomes. This concept positions the microbiome as an active regulator of cancer development and a potential target for new immunotherapy strategies, offering new insights into colorectal malignancy research (Lin et al., 2023).

Microbial diversity is critical for host health because different organisms contribute unique and non-redundant functions, ranging from promoting anti-inflammatory networks to inducing protective immune responses. Loss of diversity, therefore, represents a key aspect of dysbiosis. Experiments in germfree animals show that colonization with complex

communities of Clostridia—over 30 strains—induces a threefold expansion of Tregs, while colonization with only one or a few strains results in diminished Treg induction (Atarashi et al., 2011). This indicates that even within the same bacterial family, diversity enhances immune development. The requirement for diversity is further highlighted by experiments showing that colonization with a single species, such as *E. coli*, or even a few species, fails to suppress IgE, while colonization with up to 40 strains successfully reduces hyper-IgE production (Cahenzli et al., 2013). Taken together, the evidence indicates that increased microbial diversity maximizes host benefits, and dysbiosis likely involves multiple manifestations—including reduced diversity, altered abundance, and disrupted function—that collectively drive disease.

Products such as SCFAs, bile acids (BAs) and tryptophan metabolites are frequently referred to when assessing gut health and optimal gut microbiota composition. Particularly, SCFAs, including acetate, propionate and butyrate, which are directly produced by gut microbes during the fermentation of dietary fibers, have been extensively studied due to their pivotal roles in maintaining gut barrier integrity, modulating immune responses and serving as an energy source for colonic cells. BAs, synthesized from cholesterol in the liver and subsequently modified by gut bacteria, are also valuable indicators of microbial influence on host metabolism and gut integrity. BAs are metabolized into secondary forms such as deoxycholic acid, which are abundant in individuals consuming high-fat diets and correlate with increased CRC risk (Ma et al., 2022). Another significant group is tryptophan metabolites, such as indole and kynurenine which activate aryl hydrocarbon receptor (AhR) on immune cells, triggering protective effects like boosting IL-22 for mucosal defense and reducing inflammation (De Vos et al., 2022).

The intestinal microbiota metabolizes dietary carbohydrates, converting them into oligo- and monosaccharides to obtain energy. A healthy microbiota harbors genes that enable degradation and utilization of the wide variety of dietary fiber structures present in food, such that a mixture of fibers is required to meet the metabolic needs of the microbial community. Within the genome of each bacterial strain, polysaccharide utilization loci (PULs) are encoded. These gene clusters contain the genetic information required to synthesize and assemble outer membrane complexes analogous to the starch utilization system (SUS) (Foley et al., 2016). Bacteria of the phylum Bacteroidota access dietary fiber polymers through outer

membrane complexes that physically bind carbohydrates, digest them into small oligosaccharides, and transport the fragments into the periplasmic space. Subsequent enzymatic activity further digests oligosaccharides into monosaccharides, which are transported into the cytoplasm for metabolic processing (Rastall et al., 2022).

Similarly, Bacillota and Actinomycetota employ diverse mechanisms to access and metabolize dietary carbohydrates. The genus *Ruminococcus*, which resides prominently in the colonic mucosa, produces cellulosomes—extracellular appendages that bind and degrade carbohydrates. Cellulosomes can be exchanged with different carbohydrate-degrading enzymes and binding proteins and are presumably directed toward insoluble fiber matrices for degradation and fermentation. Bacillota species employ mechanisms such as SUS-like complexes analogous to those of Gram-negative bacteria and secretion of extracellular enzymes. The phylum Actinomycetota includes *Bifidobacterium* species that utilize oligosaccharides transported across the membrane, and their growth is promoted by prebiotic oligosaccharides such as galacto-oligosaccharides (GOS) and fructo-oligosaccharides (FOS) (Rastall et al., 2022).

1.3 Dietary Fiber of Beans

Metabolism of dietary components represents a key area of interaction between the intestinal microbiota and the host. Although associations between microbiota-derived metabolites and CRC risk have been extensively investigated, the impact of diet on the intestinal microbiota in CRC has been less studied. Given the global increase in CRC incidence, dietary changes are believed to contribute significantly to current trends. Increased consumption of red and processed meats is consistent with alterations in microbiota composition and elevated CRC risk (E. Kim et al., 2013).

Carbohydrates, along with proteins and fats, are the primary macronutrients in the human diet. Carbohydrates are classified by their degree of polymerization into digestible and non-digestible forms. Non-digestible carbohydrates (NDCs), categorized as dietary fiber, include: (1) low molecular weight compounds such as oligosaccharides and inulin; and (2) high molecular weight compounds such as non-starch polysaccharides (e.g., cellulose, hemicellulose, pectin), resistant starch, and lignin (Stribling & Ibrahim, 2023).

NDCs exert protective effects against CRC through three proposed mechanisms: (1) physicochemical interactions that reduce nutrient absorption and limit contact between carcinogens and the intestinal epithelium; (2) fermentation by intestinal microbiota producing SCFAs and other metabolites that influence intestinal epithelial cells (IECs), immune cells, and cancer cells; and (3) direct interactions with cellular components such as pattern recognition receptors (PRRs) and galectin-3 (Gal-3), triggering intracellular signaling pathways that affect cancer cell adhesion and invasion (Prado et al., 2019).

Acetate, propionate, and butyrate are the primary SCFAs generated by microbial fermentation of dietary fiber. These SCFAs enter cells via diffusion or the SLC5A8 transporter and act through three mechanisms: (1) epigenetic regulation via inhibition of HDACs in IECs and immune cells; (2) activation of GPCRs, including GPR43, GPR41 (also known as FFAR2 and FFAR3), and GPR109A (Tudela et al., 2021); and (3) agonism of the AhR. Butyrate promotes extrathymic differentiation of Tregs via the conserved non-coding sequence 1 (CNS1) (Arpaia et al., 2013).

Butyrate serves as a key energy source for colonocytes and is a critical regulator of intestinal barrier integrity and mucosal immune homeostasis (H. Wang et al., 2016). It signals through GPR43 and GPR109A in IECs to stimulate inflammasome-dependent IL-18 production, essential for maintaining epithelial integrity (Macia et al., 2015). Butyrate also protects against colonic inflammation by inhibiting HDACs, thereby attenuating inflammatory signaling in lamina propria macrophages (Chang et al., 2014), modulating dendritic cell differentiation (B. Wang et al., 2008), and promoting Treg generation via FoxP3 locus acetylation (Furusawa et al., 2013). Additionally, it induces IL-22 expression in CD4+ T cells and innate lymphoid cells (ILCs) through GPR41 and HDAC inhibition (W. Yang et al., 2020).

Butyrate contributes to normal epithelial turnover by promoting IEC proliferation in colonic crypts and inducing apoptosis in villus cells. In cancer cells, this proliferative effect is diminished due to a metabolic shift from oxidative phosphorylation to anaerobic glycolysis (Warburg effect), resulting in lactate accumulation. Since cancer cells preferentially utilize glucose over butyrate, nuclear accumulation of butyrate leads to HDAC inhibition and epigenetic dysregulation of genes involved in proliferation, apoptosis, and differentiation (Donohoe et al., 2012).

Phaseolus vulgaris, the biggest group of the Fabaceae family, has been proposed to have many health benefits due to their nutritional profile. Beans contain high levels of dietary fiber and polyphenols (flavonoids, phenolic acids, and tannins). The major fibers present in beans are resistant starch, non-starch polysaccharides (pectin, cellulose, hemicellulose), lignin, and highly soluble raffinose family oligosaccharides (a class of GOS). The human genome cannot encode carbohydrate-active enzymes (CAZymes) capable of breaking down glycosidic bonds found in fibers, such as β-1,4 linked glucose units in cellulose or α-1,4 linked galacturonic acid units in pectin. Instead, the human genome is limited to only 17 CAZymes for the digestion of starch, glucose, and lactose, while the gut microbial genome can encode a high quantity of CAZyme. The CAZyme-encoding genes are mostly present in the dominant bacterial phyla of Bacteroidota, Bacillota, and Actinomycetota (Cantarel et al., 2012).

The polyphenols and gut microbes reveal an interaction whereby gut microbiota metabolize complex (poly)phenols to simpler phenolic compounds, and at the same time, the produced phenolic metabolites aid the growth of certain bacteria while suppressing certain pathogenic species (Le et al., 2024). Findings from *in vivo* studies showed that speckled kidney bean (poly)phenols increased the abundance of Bacteroidota, Pseudomonadota and Verrucomicrobiota, while decreasing the Bacillota and Actinomycetota populations compared to high fat diet (HFD) fed Wistar rats (Zuo et al., 2023).

In Costa Rica, beans represent an important part of traditional cuisine and plays a central role in the diet of populations at socioeconomic risk, providing affordable access to essential nutrients and dietary fiber. Costa Rica, as part of the Mesoamerican region, possesses a diversity of species of *Phaseolus*. Three local varieties of *Phaseolus vulgaris L*. (Cabecar, Mantequilla and Nambi) are of particular interest due to their affordability, nutrient composition, and adaptability (González & Fernandez-Rojas, 2015)

1.4 Animal model for colorectal carcinogenesis

The mechanisms by which dietary changes, including fiber deprivation or ingestion, affect the microbiota and its association with CRC have been studied using experimental rodent models. Laboratory rodents are widely used in experimental animal models because they are easy to maintain, their physiology and genetics are well characterized, and they are

mammals, like humans. The intestine of rats and mice is similar to that of humans in terms of development, structure, and function. The large intestine of rodents comprises the cecum, colon, rectum, and anus. The rodent colon has the same histological structure as the human gastrointestinal tract (mucosa, submucosa, muscularis mucosa, serosa), with the difference that rodents lack adipose tissue in the submucosa. The colon is divided into ascending, transverse, and descending segments. The rectum is relatively short and indistinguishable from the distal colon (Vdoviaková et al., 2016).

Although no animal model replicates all aspects of human disease, rodents are suitable models for studying colorectal carcinogenesis due to their physiological similarity, reproducibility in tumor induction, and the possibility of studying pathology and testing strategies for cancer treatment and prevention. Rats, along with mice, have been among the most widely used laboratory species for research since the late 1940s and have been bred specifically for biological experimentation. Wistar rats, *Rattus norvegicus*, are an outbred strain developed at the Wistar Institute in Pennsylvania, USA, derived from the wild Norway rat. Wistar rats, together with F344 and Sprague-Dawley strains, are currently the three most used strains in carcinogenesis studies. Their larger size compared to mice allows for a wider range of experimental procedures. The growth rate and terminal body weight of Wistar rats are intermediate between F344 and Sprague-Dawley rats, with an average weight of approximately 650 g (range 472–987 g) for males at the end of two-year carcinogenesis studies (Foster & Frost, 2018)

An ideal murine model of colorectal carcinogenesis should allow the development of carcinomas in the colon and rectum, with high incidence in a short period, enabling non-invasive monitoring of disease progression and containing the histological and molecular characteristics of human CRC. Murine models used for CRC studies include spontaneous models, chemically induced models, genetically modified models, xenograft models, and syngeneic models. In chemically induced models, carcinogenic compounds are administered alone or in combination and can be of two types: direct carcinogens, which do not require metabolic activation to induce cancer, and indirect carcinogens, which are administered in an inactive form and acquire carcinogenic activity after biotransformation in the liver (Tanaka, 2009). Among indirect carcinogens, 3,2′-Dimethyl-4-Aminobiphenyl (DMAB), 1,2-Dimethylhydrazine (DMH), Azoxymethane (AOM), and PhiP have been used. DMH is

an alkylating agent oxidized in the liver to AOM and subsequently hydroxylated to methylazoxymethanol (MAM). MAM is converted to formalin and the methyldiazonium ion, which can methylate DNA, RNA, and proteins. Cancer induction with DMH in the distal colon is histopathological similar to human CRC, as confirmed in several studies using male Wistar rats. DMH can be administered via different routes, including subcutaneous, intraperitoneal, oral, and intrarectal, with the subcutaneous route being the most effective and therefore the most widely used (Nascimento-Gonçalves et al., 2021; Tanaka et al., 2003). Additionally, dextran sulfate sodium (DSS) is an inflammatory compound that damages the colonic epithelium and induces colitis and has been used to promote CRC in murine models employing DMH or AOM (Tanaka et al., 2003).

Significant differences in intestinal microbiota composition have been observed in Wistar rats in CRC models induced with DMH. Rats with CRC showed increased abundance of Bacillota, Pseudomonadota, and Actinomycetota, while Bacteroidota and Spirochetes were reduced. At the genus level, *Prevotella*, *Lactobacillus,* and *Treponema* were significantly more abundant in healthy rats. A marked reduction of butyrate-producing bacteria such as *Roseburia* and *Eubacterium* was observed in CRC rats, along with significant increases in *Desulfovibrio, Erysipelotrichaceae*, and *Fusobacterium*. Probiotic species such as *Ruminococcus* and *Lactobacillus* were decreased in the CRC group. The higher abundance of *Bacteroides*, *Desulfovibrio*, and *Fusobacterium* in the intestinal lumen of CRC rats supports the hypothesis that these bacteria play an important role in CRC development and progression (Zhu et al., 2014). The intestinal microbiota of Wistar rats with CRC also showed increased abundance of Bacillota, Clostridia*, Clostridiales,* Peptostreptococcaceae*, Blautia, Romboutsia,* and *Clostridium* sensu stricto compared to healthy controls, while Prevotellaceae*, Prevotella, Akkermansia,* and *Lactobacillus* were more prevalent in healthy animals (Silva-Reis et al., 2022).

In a CRC model induced with AOM in gnotobiotic BALB/c mice colonized with wild-type or mutant butyrate-producing bacterial strains, dietary fiber consumption was shown to exert a protective effect against CRC through the butyrate-producing microbiome. Due to the Warburg effect, butyrate was less metabolized in tumors, where it accumulated and functioned as HDAC inhibitor, stimulating histone acetylation and affecting apoptosis and cell proliferation (Donohoe et al., 2015).

The effect of Nigerian beans in a colorectal carcinogenesis model in Wistar rats showed variations in colonic inflammation and reduced incidence of dysplasia with the consumption of *Spenostyles stenocarpa, Cajanus cajan, Phaseolus lunatus, Mucuna cochindunum,* and *Phaseolus vulgaris*. Rats fed *Spenostyles stenocarpa* and *Cajanus cajan* exhibited lower dysplasia incidence compared to other groups (Awoyinka et al., 2016).

Consumption of condensed tannins from *Phaseolus vulgaris L.* modulated the expression of genes in the *Tp53* signaling pathway in early stages of CRC in a Sprague-Dawley rat model induced with AOM, contributing to a chemoprotective effect. Significant differences were detected in the expression of 72 *Tp53* pathway genes involved in apoptosis, cell cycle regulation and arrest, inhibition of proliferation, inflammation, and DNA repair. This suggests that prevention of ACF formation is due to cell cycle arrest and induction of apoptosis (Haydé et al., 2012).

The differential impacts on gut microbiota diversity depend on the composition of dietary fiber and physicochemical properties, including solubility, sugar composition, branching, chain length, or degree of polymerization (Kilua et al., 2020). However, current studies have usually used whole beans to observe the effect of gut microbiota modulation, assuming synergy of various fibers in common beans, such as cellulose, resistant starch, pectin, soluble fibers and other components, such as protein or (poly)phenols. The effect of cooked black beans with and without high fat and sugar for 2 months showed at phylum level a decrease in Proteobacteria and increased Cyanobacteria and Clostridia; at genus level increased *Ruminococcus, Coprococcus, Prevotella* ; and at species level increased *C. eutactus, R. callidus, R. bromii, B. pullicaecorum, R. flavefaciens* (Sánchez-Tapia et al., 2020).

According to the National Nutrition Survey of 1996, 96.7% of Costa Ricans consumed beans; however, intake has since declined by 35.1%, with higher consumption in rural areas compared to urban zones (Fernández Rojas, 2008). In parallel, local bean production has decreased, and Costa Rica currently imports approximately 75% of the beans consumed, primarily from Asia (Valerin, 2020). Given the nutritional and cultural importance of beans, the present work seeks to investigate the association between dietary fiber derived from native beans and changes in the gut microbiota during colorectal carcinogenesis in a murine model. By focusing on the preventive potential of bean fiber

against colorectal cancer, this project aims not only to generate scientific evidence on diet–microbiota interactions but also to highlight the value of locally produced beans, thereby promoting their consumption and supporting national producers while contributing to public health.

Grounded in the preceding context, the central question of this investigation is whether supplementation with dietary fiber obtained from whole beans can modulate the composition of the intestinal microbiota during the development of preneoplastic lesions in a Wistar rat model of colorectal carcinogenesis. The working hypothesis proposes that the intestinal microbiota will undergo variations in both diversity and composition because of carcinogenesis induction and in response to dietary fiber derived from three Costa Rican bean varieties. These shifts are anticipated to contribute to a protective microbial profile, characterized by the preservation of diversity and the enrichment of beneficial taxa associated with intestinal health, thereby potentially mitigating the onset and severity of preneoplastic lesions.

CHAPTER II. OBJETIVES

2. General Objective

Characterize the composition of the gut microbiota of Wistar Rats in a colorectal carcinogenesis model, to evaluate the impact of dietary fiber from Costa Rican beans during the induction of preneoplastic lesions.

Specific Objectives

In a colorectal carcinogenesis model in Wistar rats induced with 1,2-dimethylhydrazine (DMH) and dextran sulfate sodium (DSS), this study aims to:

2.1 Validate the colorectal carcinogenesis model, by monitoring food and water intake, body weight, and overall health status, ensuring that subsequent analyses of gut microbiota composition are not confounded by nutritional distress or systemic impairment.

2.2 Characterize the basal intestinal microbiota of Wistar rats at the beginning of the study, providing a reference framework for comparative analyses of its composition during colorectal carcinogenesis.

2.3. Evaluate the effect of DMH and DSS on the composition of the gut microbiota, determining whether carcinogen exposure induces dysbiosis.

2.4 Determine the effect of the consumption of dietary fiber from three Costa Rican bean varieties, considering both total dietary fiber and cooked whole-bean flour, on the composition of the intestinal microbiota during colorectal carcinogenesis, with the aim of establishing whether bean consumption promotes microbial profiles that are beneficial and potentially protective against preneoplastic lesion development.

CHAPTER III. MATERIALS AND METHODS

3.1 Dietary Fiber of Beans

The processing of beans and extraction of total dietary fiber (TDF) was performed at the Research Center for Food Science and Technology (CITA), University of Costa Rica (UCR), within project code 742-C4-512: *Characterization of Indigestible Carbohydrates (Dietary Fiber) Present in Traditional High-Consumption Foods in Costa Rica and Their Effect on the Development of Precancerous Colonic Lesions: Analysis of Histological Features, Molecular Markers, and Microbiome*.

The study used cooked whole-bean flour and TDF derived from three local varieties of *Phaseolus vulgaris* L. (Nambi, Cabecar, and Mantequilla), obtained from a single producer in Upala, Huetar Norte region of Costa Rica. This producer is affiliated with the Social Solidarity Economy Program of the University of Costa Rica.

Briefly, before cooking, beans were washed once with distilled water; no soaking step was applied. Cooking was performed in a 4-L stainless-steel pot containing 1.5 L of distilled water, brought to a boil before adding 500 g of beans. Once boiling resumed, the pot was covered, and water volume was monitored every 10 min to be maintained between 1.7 and 2.0 L. Cooking times depended on the bean variety: Mantequilla (65 min), Nambi (80 min), and Cabecar (95 min). At the end of cooking, beans were removed and the cooking water was discarded. Cooked beans were packed in metallized doypack bags to minimize environmental exposure and microbial contamination, then stored at −20 °C until further processing.

For subsequent preparation, beans were vacuum-dried and pulverized under freezing conditions to obtain particles suitable for administration by cannulation. TDF, defined as the sum of soluble and insoluble fractions, was isolated from whole beans and lyophilized after separation. Both the cooked whole-bean flour and the TDF were stored at −80 °C until use.

3.2 Ethical Management of Laboratory Animals

Male Wistar rats (Crl:WI), between three and four weeks of age, were obtained from the colony of the Biological Testing Laboratory (LEBI) at the University of Costa Rica. During the experiment, all protocols, procedures, and guidelines established by legislation for the use and handling of laboratory animals were strictly followed, as well as the guidelines of the Institutional Committee for the Care and Use of Laboratory Animals (CICUA) of the University of Costa Rica.

The rats were housed in individual cages with autoclaved wood shaving as bedding and provided with food and tap water *ad libitum*. They received a standard rodent diet and were maintained under a 12-hour light/dark cycle. A total of eight animals were randomly assigned to each experimental group after a one-week acclimatization period. During this acclimatization week, the animals were not subjected to any treatment. Handling sessions were also conducted prior to the experimental procedures so that both the personnel responsible for handling and the animals became accustomed to the procedures, thereby minimizing stress and discomfort.

Each experimental group was assigned separately to 15-minute play sessions in a large cage with autoclaved wood shavings prior to the study and after each oral gavage procedure during the 12-week study period. Play sessions were supervised to ensure that coprophagy did not occur. The cages used for the play sessions were washed and disinfected after each use.

To avoid unnecessary stress and ensure animal welfare, animals were handled firmly but gently, without abrupt movements, avoiding noise from cages and carts, speaking only when strictly necessary and in a low tone of voice, thereby creating a calm environment. Acrylic tube shelters were used as environmental enrichment. Daily health monitoring was routinely performed. All animals were euthanized at the end of the study.

The cages were meticulously cleaned on a weekly basis. To ensure that cages were not shared between experimental groups, two cages were assigned to each animal. On designated cage-cleaning days, each animal was transferred together along with its acrylic tube and water bottle into a clean cage containing sterile wood shaving.

The animals were weighed on two times per week, with the objective of monitoring their weight gain and the quantity of food and water consumed. The water was changed three

times per week, on alternating days. During this study, each animal was assigned an individual water bottle, which was washed at every water change day and refilled with tab water from the LEBI. For the High Fructose Corn Syrup (HFCS) group, bottles were replenished with 250 g of a 10% (w/w) high fructose corn syrup suspension, prepared by mixing 200 g of HFCS with 1800 g of water.

To control potential positional effects within the animal facility, cages were rotated every three days. This procedure ensured that environmental variables associated with cage location did not influence experimental outcomes.

3.3 Animal Model of Chemical Induction of Colorectal Carcinogenesis with 1,2-Dimethylhydrazine (1,2-DMH) and Dextran Sodium Sulfate (DSS) in Wistar Rats

A chemical induction model of precancerous colorectal lesions using DMH and DSS was used in male Wistar rats (Figure 1). The selection of males was based on evidence indicating that early androgen exposure and the resulting hormonal milieu modulate susceptibility to DMH-induced carcinogenesis (Smirnova & Turusov, 1988), in addition to the fact that the incidence and mortality of CRC is higher in men than in women (Bray et al., 2024). At week 3 of the experiment, the animals received three subcutaneous doses of DMH (40 mg/kg body weight) over the course of one week as an initiating agent for precancerous lesions. Subsequently, the inflammation promoting agent, DSS, was administered *ad libitum* (1% w/v) in the drinking water during week 3.

Microbiome fecal samples were collected weekly using sterile tweezers. The fecal samples were transferred to 2mL cryotubes and snap-frozen with liquid nitrogen. The samples were stored at –80C. At the end of the protocol, all animals were euthanized by exsanguination under isoflurane anesthesia. The colon was excised and rinsed with cold saline solution using a syringe to remove fecal residues. The intestine was opened longitudinally along the mesenteric border using fine scissors. The mucosa was examined macroscopically for visible lesions. Finally, the tissue was stretched and fixed in 10% neutral buffered formalin for 24 hours for further studies.

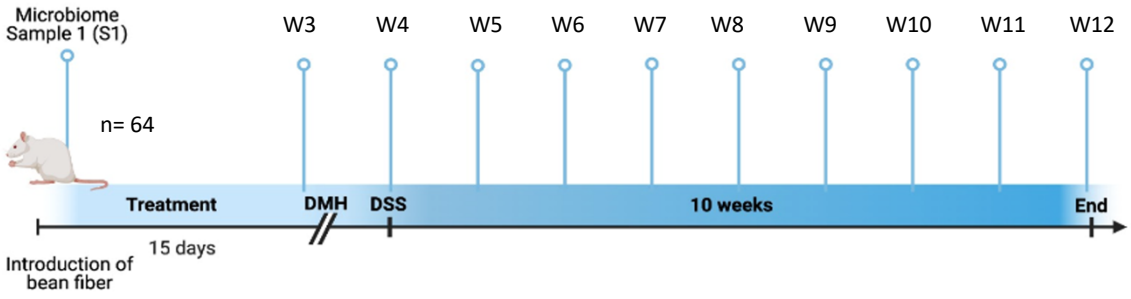

Figure 1. Experimental timeline for colorectal carcinogenesis model and dietary intervention. After one week of acclimatization, dietary supplementation total dietary fiber, whole bean flour or high fructose corn syrup was initiated via oral gavage. At week 3, colorectal carcinogenesis was induced with DMH, followed by *ad libitum* administration of DSS in drinking tap water. Bean fiber supplementation continued throughout the subsequent 9 weeks. Microbiome samples were collected at four key timepoints: baseline (week 1), pre-carcinogen (week 3), mid-intervention (week 9), and endpoint (week 12). This design enabled longitudinal assessment of gut microbiota dynamics in response to dietary fiber during chemically induced colorectal carcinogenesis.

3.4 Treatment groups

All rats in this experiment were fed with regular rodent chow diet. Supplemental suspensions of total fiber, as well as whole beans, were administered by oral gavage once daily for a period of 12 weeks. This procedure was initiated two weeks prior to the induction of carcinogenesis and continued until the time of euthanasia, which occurred at 10 weeks following the induction. The experimental groups were assigned as follows (**Table *1***):

- Control group (Control): no carcinogenesis induction. This group did not receive any nutritional supplementation including bean, fiber or HFCS (n = 8).
- Positive carcinogenesis control group (Colorectal carcinogenesis): carcinogenesis was induced with DMH and DSS. No bean preparations, fiber, or HFCS supplementation was administered (n = 8).
- Hypercaloric diet group (HFCS): carcinogenesis was induced with DMH and DSS. A 10% (w/w) HFCS55 suspension was prepared by dissolving 200 g of HFCS55 in 1800 g of tap water and was administered in the water bottles (n = 8) *ad libitum*. The hypercaloric diet will be used to evaluate the effect of a pro-inflammatory dietary environment associated with colorectal carcinogenesis.
- Dietary fiber treatment groups: carcinogenesis was induced with DHM and DSS, and whole bean or TDF supplementation was administered as shown in Table 1.

Table 1.Summary of the experimental groups used in this study.

Group	Cancer Induction	Supplementation	n
Control	None	None	8
Colorectal cancer	DMH + DSS	None	8
HFCS	DMH + DSS	HFCS suspensión	8
Nambi Fiber	DMH + DSS	Total dietary fiber from Nambi beans	8
Cabecar Fiber	DMH + DSS	Total dietary fiber from Cabecar beans	8
Mantequilla Fiber	DMH + DSS	Total dietary fiber from Mantequilla beans	8
Nambi	DMH + DSS	Cooked whole-bean flour from Nambi beans	8
Mantequilla	DMH + DSS	Cooked whole-bean flour from Mantequilla beans	8

3.5 Sampling of Intestinal Microbiota

Stool samples were collected under sterile conditions following a standardized protocol on cage-cleaning days, directly deposited onto autoclaved wood shaving and free from urine contamination. Prior to sampling, all working surfaces were disinfected with 70% ethanol. Each animal was placed in a clean cage containing fresh autoclaved wood shaving, and a small amount of wood shaving from the previous cage was transferred to the new one to maintain environmental familiarity, taking care not to transfer fecal or urine matter. Stainless steel tweezers were kept in a beaker containing 96% ethanol with the tips fully submerged. Immediately after defecation, the tweezers were removed from the ethanol and briefly passed through a flame. The tweezers were then allowed to cool before handling the stool sample. Fecal pellets were collected with the cooled tweezer and placed into sterile 2 mL cryovials assigned to each animal, with a minimum of two pellets per cryovial and ideally three. Cryovials were immediately sealed and submerged in liquid nitrogen for 10 seconds and placed in an icebox, ensuring complete immersion in ice. Sampling details were recorded in the laboratory logbook, including the consistency of the feces according to the Bristol Stool Scale and the date and hour of collection. Cryovials were transported under cold chain conditions, and all samples were stored at −80 °C until the DNA extraction.

Stool samples used in this thesis include the following four time points:

1. Beginning of the experiment (Week 1)
2. Before administration of DMH and DSS but after climatization (Week 3)
3. Seven weeks after carcinogenesis induction (Week 9)
4. Fina timepoint of the study (Week 12).

DNA Extraction and Quality Control

Metagenomic DNA was extracted using the DNeasy PowerLyzer PowerSoil Kit (Qiagen, USA) following the manufacturer's protocol with some modifications. Between 0.25 and 0.35 g of fecal pellets were placed in a PowerBead Tube, to which 750 µL of PowerBead Solution and 60 µL of Solution C1 were added. Tubes were incubated for 10 min at room temperature (25 °C), then vortexed horizontally at maximum speed for 10 min and centrifuged at 10,000 × g for 3 min. The supernatant was transferred to a clean tube, mixed with 250 µL of Solution C2, vortexed briefly, and incubated at 2–8 °C for 5 min. After

centrifugation at 10,000 × g for 1 min, the supernatant was transferred to a new collection tube, combined with 200 µL of Solution C3, vortexed, and incubated at 2–8 °C for 5 min. Following centrifugation at 10,000 × g for 1 min, the supernatant was transferred again to a clean tube.

Subsequently, 1200 µL of Solution C4 was added, vortexed for 5 s, and loaded in three sequential aliquots of 675 µL onto an MB Spin Column, each centrifuged at 10,000 × g for 1 min. The flow-through was discarded after each step. The column was then washed twice with 300 µL of Solution C5, centrifuged at 10,000 × g for 30 s each time, followed by an additional centrifugation at 10,000 × g for 1 min to remove residual wash buffer. The column was placed in a clean collection tube, and DNA was eluted twice with 30 µL of Solution C6, incubated for 1 min before centrifugation at 10,000 × g for 30 s.

DNA concentration and purity were assessed using a Nanodrop spectrophotometer. Sample quality was evaluated based on DNA yield and absorbance ratios (A260/A230 and A260/A280). DNA samples were stored at -80°C until further analysis.

Library Preparation and Sequencing

The purified DNA samples were sent to SeqCenter (Pittsburgh, USA) for library construction and amplicon sequencing of the hypervariable V3–V4 region of the 16S rRNA gene. The raw fastq files were transferred and stored in the University of Costa Rica HPC computing cluster.

Bioinformatics Analysis

Raw sequence quality was evaluated using FastQC and Trimmomatic. Sequences were filtered, trimmed, and denoised using DADA2 as implemented in QIIME2. Taxonomic assignment of amplicon sequence variants (ASVs) was performed using the latest version of the SILVA classifier. ASVs were aligned with MAFFT, and a phylogenetic tree was constructed using FastTree within QIIME2. ASV, taxonomy, and phylogeny files were imported into the Phyloseq package in R for diversity and statistical analyses. Alpha diversity metrics: Shannon, Simpson, and richness indices were calculated in Phyloseq. Beta diversity metrics were computed in Phyloseq and visualized in R using ggplot2.

Differentially abundant taxa between groups were identified using ANCOM-BC in QIIME2. Treatment effects were analyzed using ANOSIM in QIIME2. Additional abundance analyses were performed with the ggpubr package in R.

Statistical Analysis

Statistical analyses of gut microbiota comparisons and treatment effects were performed using QIIME2 tools and the Phyloseq package in R. To detect changes in genera over time, a generalized mixed-effects model (GLMM) was performed, assuming a Poisson distribution for the read counts for each family. This response was normalized by the total read counts. Then, we performed a deviance analysis to study whether treatment and time were causing changes in the read counts. If so, we performed a pairwise Z-test and obtained a compact letter display for all comparisons. We used the statistical programming language R (v4.5.2. ;R Core Team, 2025) under the integrated development environment RStudio (v2026.01.0+392; Posit Team, 2025), and the packages glmmTMB (McGillycuddy et al., 2025) for modelling, tidyverse (Wickham et al., 2019) for data wrangling and plotting, emmeans (Lenth & Piaskowski, 2017) for pairwise comparisons, and multcomp to get the compact letters.

CHAPTER IV. RESULTS

4.1 Validation of the animal Model of Chemical Induction of Colorectal Carcinogenesis with DMH and DSS in Wistar Rats.

The experimental groups consisted of 8 animals each for a total of 64 rats. Two animals in the Mantequilla group did not survive the 12-week experimental period. Both deaths occurred within 24 hours of cannulation and were attributed to procedural complications, specifically movement-induced injury during the intervention. No further mortality was observed in the remaining cohort.

Figure 2 illustrates the progression of average body weight across all experimental groups from January 16 to April 10, 2025. Each group—control, colorectal carcinogenesis (CRC), High Fructose Corn Syrup, Mantequilla, Mantequilla Fiber, Nambi, Nambi Fiber and Cabecar Fiber)—demonstrated a consistent upward trend in body weight throughout the study period. The absence of significant weight loss or growth impairment across groups indicates that the animals maintained normal physiological development, supporting the tolerability and robustness of the assay conditions.

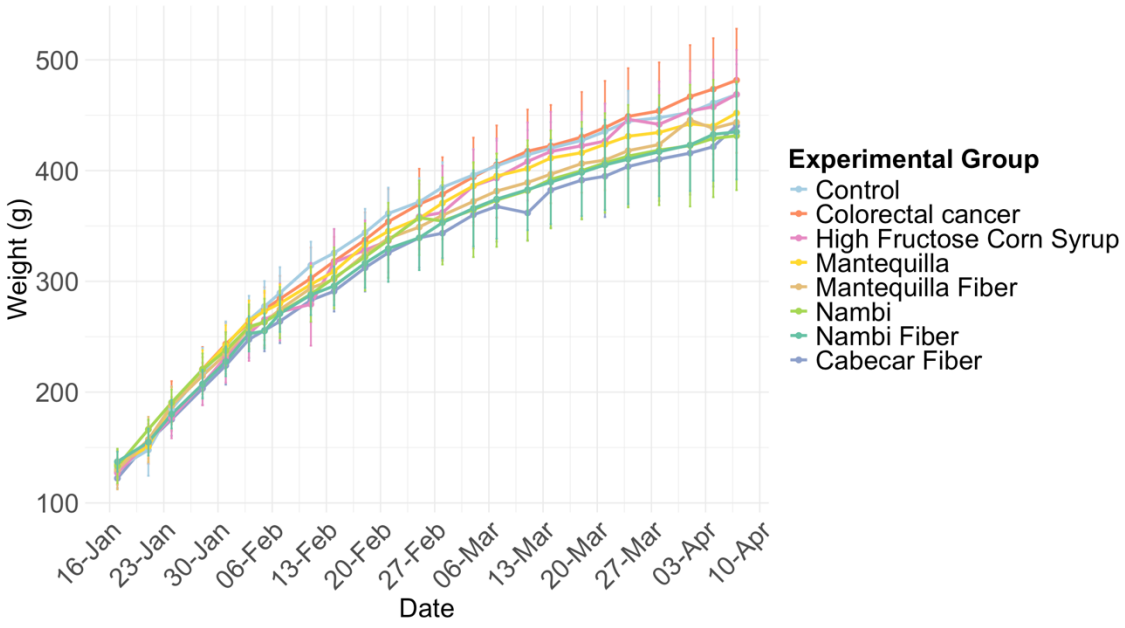

Figure 2. Mean body weight per experimental group over time. Average body weight (± standard deviation) for all experimental groups during colorectal carcinogenesis induced with 1,2-DMH and DSS during 12 weeks of study.

At the end of the assay, mean body weights did not differ significantly among experimental groups (Kruskal–Wallis, $p > 0.05$; pairwise Wilcoxon tests, BH-adjusted $p > 0.05$). Compact letter display analysis assigned all groups to the same statistical category ('a'), indicating no detectable differences in body weight at this time point (Figure 3).

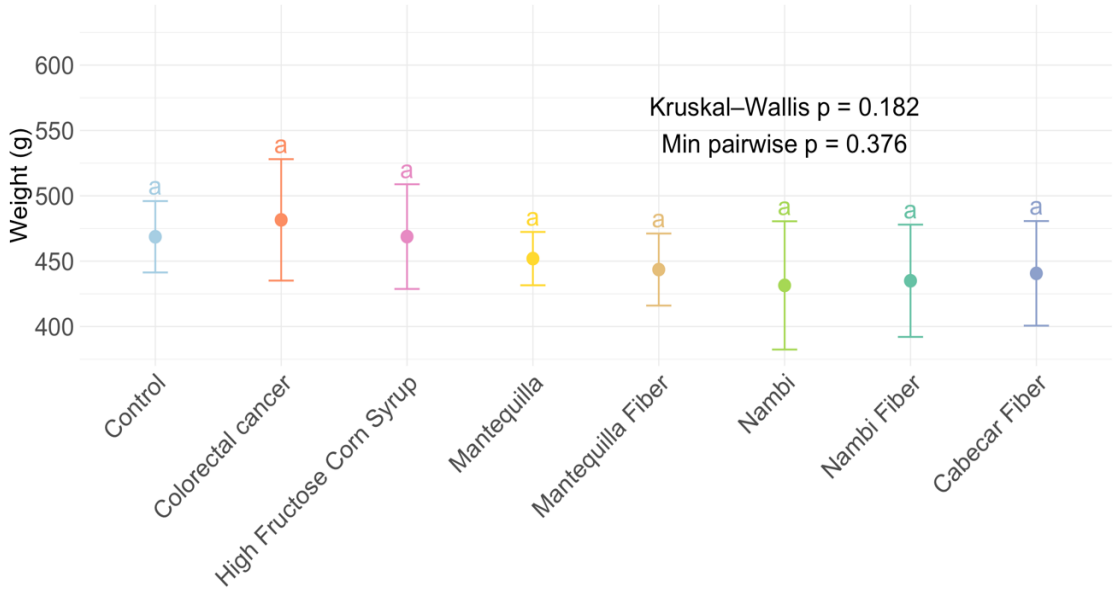

Figure 3. Final body weight per experimental group at Week 12. Average body weight (± standard deviation) of animals in each experimental group at the end of the 12-week intervention period. Statistical analysis using the Kruskal–Wallis test indicated no significant differences among groups ($p > 0.05$). Pairwise comparisons performed with the Wilcoxon test and Benjamini–Hochberg correction revealed no significant differences ($p > 0.05$).mar

Food intake was measured weekly and expressed as grams (g). The average daily food intake (± standard deviation) across all experimental groups varied over time, with fluctuations observed in all groups. A decline in food intake was noted during the induction of carcinogenesis with DMH and DSS (Figure 4).

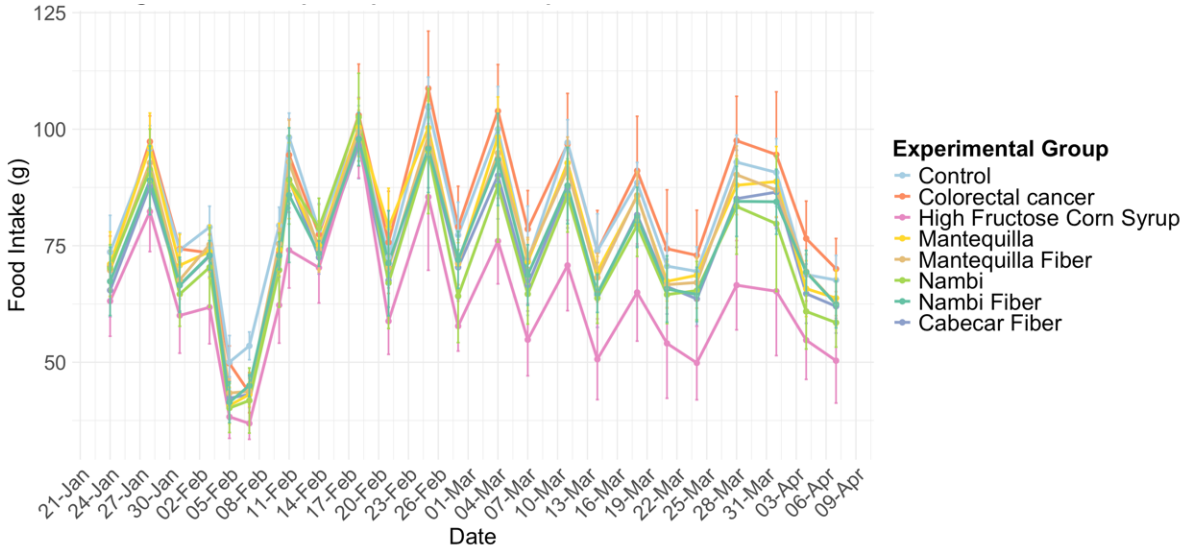

Figure 4. Average food intake per experimental group across time. Average daily food intake (± standard deviation) per experimental group from January 21 to April 9. All experimental groups Control, Colorectal, HFCS, Mantequilla, Mantequilla Fiber, Nambi, Nambi Fiber, and Cabecar Fiber exhibited dynamic consumption patterns over time.

To see the dynamic feeding behavior over time and underlying patterns beyond daily fluctuation a Locally Estimated Scatterplot Smoothing (LOESS) was performed showing that the HFCS group has the lowest food intake while the colorectal cancer group has the highest. The whole bean and whole fiber consumption showed similar trends (Figure 5).

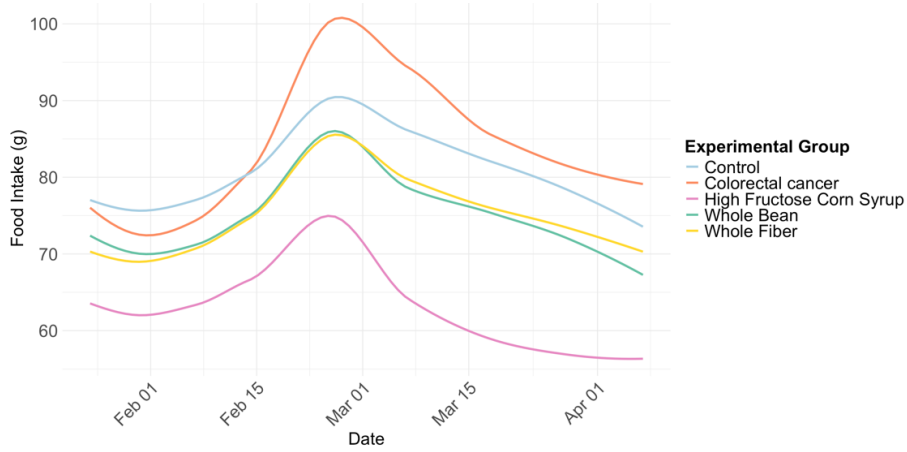

Figure 5. LOESS-Smoothed Trend of Food Intake over time. LOESS-smoothed trajectories of daily food intake (in grams) for groups Control, Colorectal Cancer, HFCS, cooked whole bean flour(Mantequilla and Nambi group) and whole fiber (Mantequilla fiber, Nambi fiber and Cabecar fiber).

At Week 12, food intake differed significantly among groups (Kruskal–Wallis p = 0.000177). Post hoc comparisons indicated that the whole bean and whole fiber group consumed significantly less food than Control and Colorectal Cancer groups (group “a” vs. “c”), while HFCS group showed the lowest intake overall (group “b”) (Figure 6).

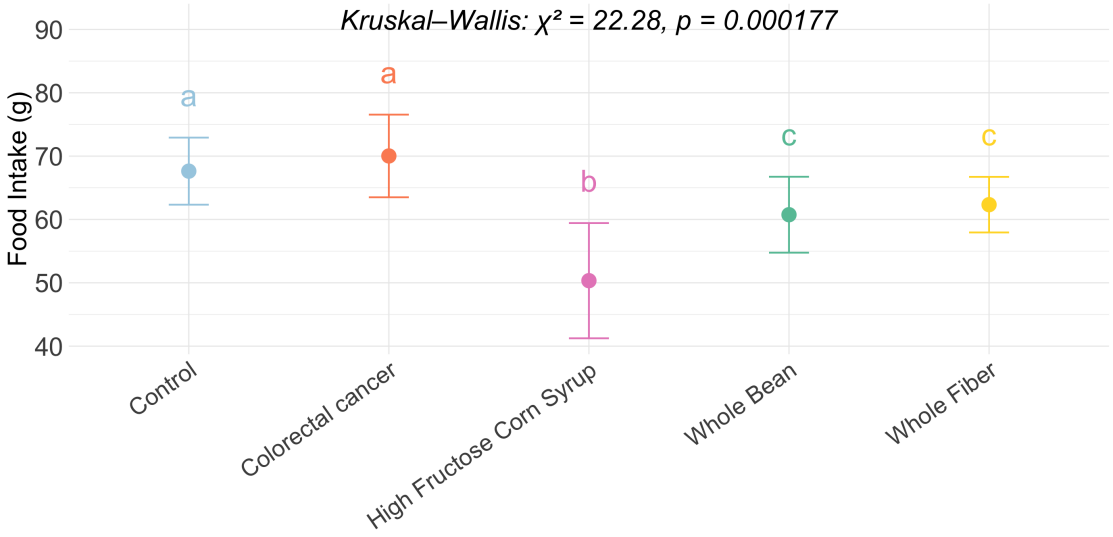

Figure 6. Food intake at week 12. Average food intake (g ± SD) for five experimental groups at the end of the 12-week intervention. Groups included Control, Colorectal Cancer, High Fructose Corn Syrup (HFCS), Whole Bean (whole cooked bean flour), and Whole Fiber (Mantequilla Fiber, Nambi Fiber and Cabecar Fiber). Statistical analysis using the Kruskal–Wallis test revealed significant differences among groups ($p < 0.05$).

Water intake varied over time for all experimental groups. The HFCS group showed consistently elevated consumption, compared to other groups (Figure 7).

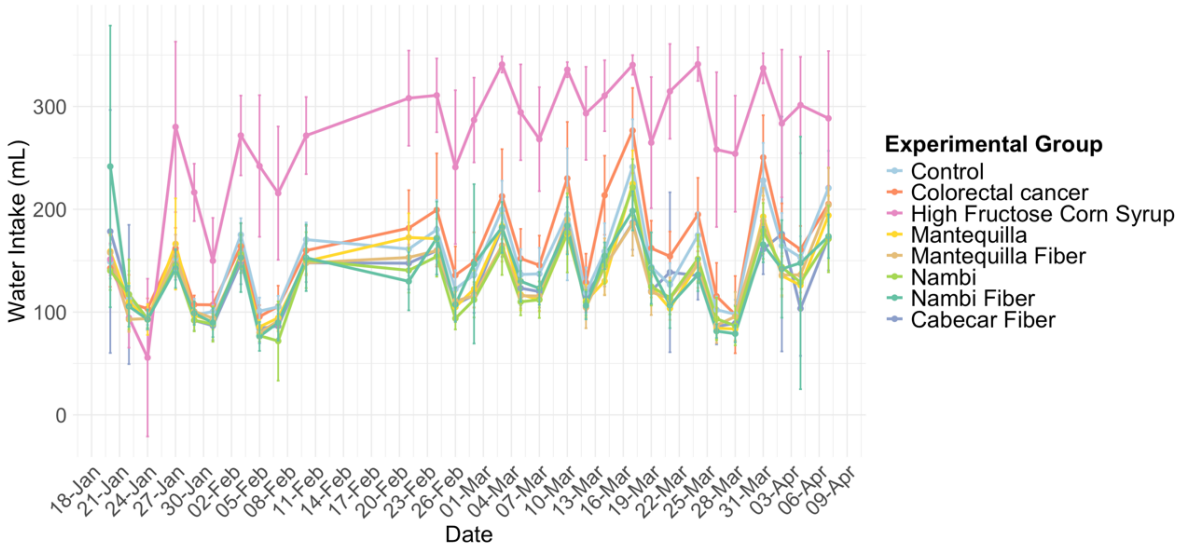

Figure 7. Water intake per Experimental Group across time. Average daily water intake (± standard deviation) for each experimental group from January 18 to April 9. Experimental groups included control, colorectal cancer and dietary interventions (HFCS, Mantequilla, Mantequilla Fiber, Nambi, Nambi Fiber, and Cabecar Fiber). Temporal fluctuations in water consumption were observed across all groups.

The HFCS group consistently exhibited the highest water intake, peaking above 300 mL around mid-March. In contrast, the cooked whole bean flour and TDF groups maintained lower and nearly overlapping intake patterns. Control and Colorectal Cancer groups showed intermediate intake levels with stable trends (Figure 8).

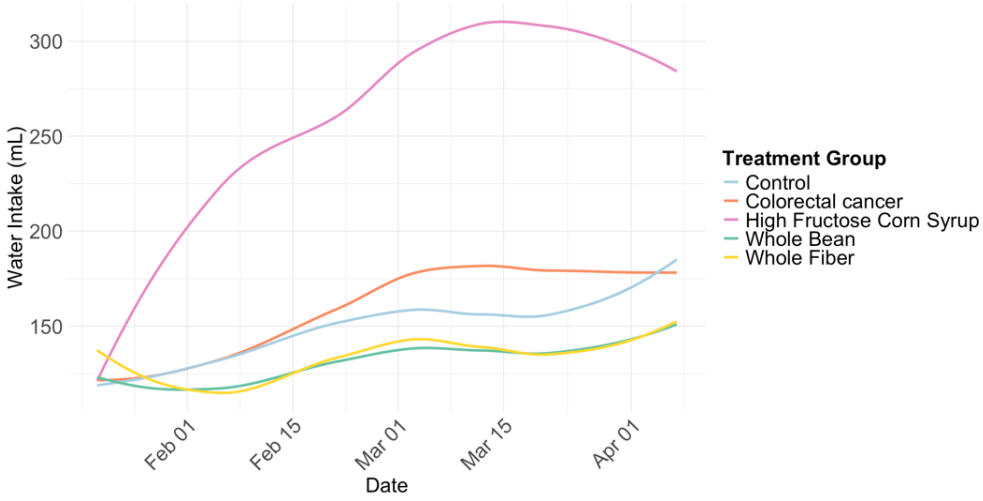

Figure 8. LOESS-Smoothed trend of Water intake per Treatment group over time. Daily water intake (in mL) for five groups—Control, Colorectal Cancer, High Fructose Corn Syrup, cooked whole bean flour, and total dietary fiber—during the 12 weeks of study.

At the end of the study, the HFCS group showed the highest water intake compared to other treatments. In contrast, the colorectal cancer, mantequilla and mantequilla fiber groups reflected intermediate intake and partial overlap with other groups. Fiber-containing treatments Nambi, Nambi Fiber and Cabecar Fiber tended to have lower water intake and statistical similarity among fiber-rich interventions (Figure 9).

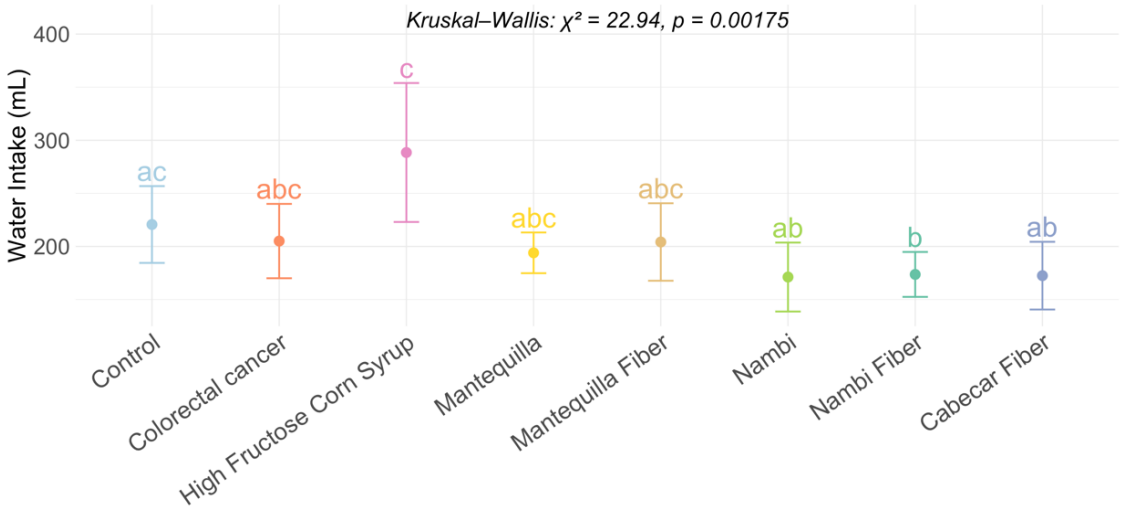

Figure 9. Water intake per experimental group at Week 12. Average water intake (mL ± SD) for eight experimental groups at the end of the 12-week intervention. Statistical analysis using the Kruskal–Wallis test revealed significant differences in water consumption among groups ($p < 0.05$). Letter annotations above each data point indicate statistical groupings derived from post hoc comparisons.

4.2 Basal gut microbiome of Wistar rats at Week 1 of the study

Samples and Illumina sequencing

The analysis was performed using a subset of six stool samples per experimental group, randomly chosen, for each of the four timepoints. Illumina pair-end sequencing returned a total of 28,937,093 sequences across 194 samples from 48 rats and wood shaving, after denoising with DADA2 protocol. A total of 8,290 ASV were detected across all samples, with a mean frequency per feature of 3,490.6.

A subset of samples with less than 57900 reads per sample were excluded from the analysis. The analysis of the sequencing´s depth showed that our methodology produced enough reads to cover the diversity of the samples. The rarefaction curves for all samples grew rapidly at first, as the most common species are found, and subsequently showed a plateau, as only the rarest species remain to be sampled (Figure 10). The plateau was observed at about 10,000 reads of sequencing depth for most of the samples.

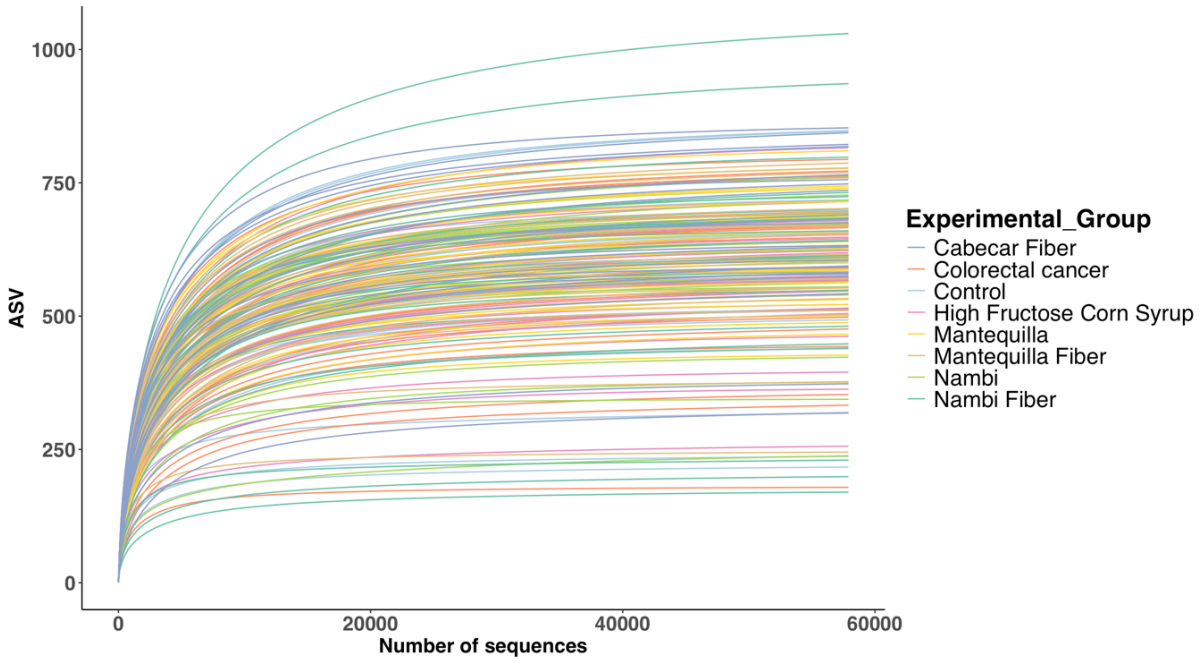

Figure 10. Rarefaction curve of the gut microbiome of laboratory Wistar rats from the stool samples of experimental groups. Rarefaction curves showing amplicon sequence variant (ASV) richness as a function of sequencing depth across experimental groups. Each line represents an individual sample, and colors indicate the corresponding experimental group. Most curves approach a plateau, suggesting adequate sequencing depth to capture the majority of microbial diversity within samples.

Fecal microbiome diversity and composition analysis

The Shannon index and Chao1 index were used to evaluate community diversity for each sample. The analysis of alpha diversity at the beginning of the study demonstrated that the Shannon index was higher in the HFCS group followed by Mantequilla Fiber and Nambi. The Nambi Fiber group showed the lowest values of the Shannon index. However, the Kruskal-Wallis test indicated no statistically significant differences in microbial diversity among the groups (p = 0.1819). The Chao1 index revealed no statistically significant differences among experimental groups (Kruskal-Wallis test, p = 0.3374). Notably, the diversity was higher in the Nambi and Mantequilla Fiber groups, while the Nambi Fiber group showed the lowest values (Figure 11).

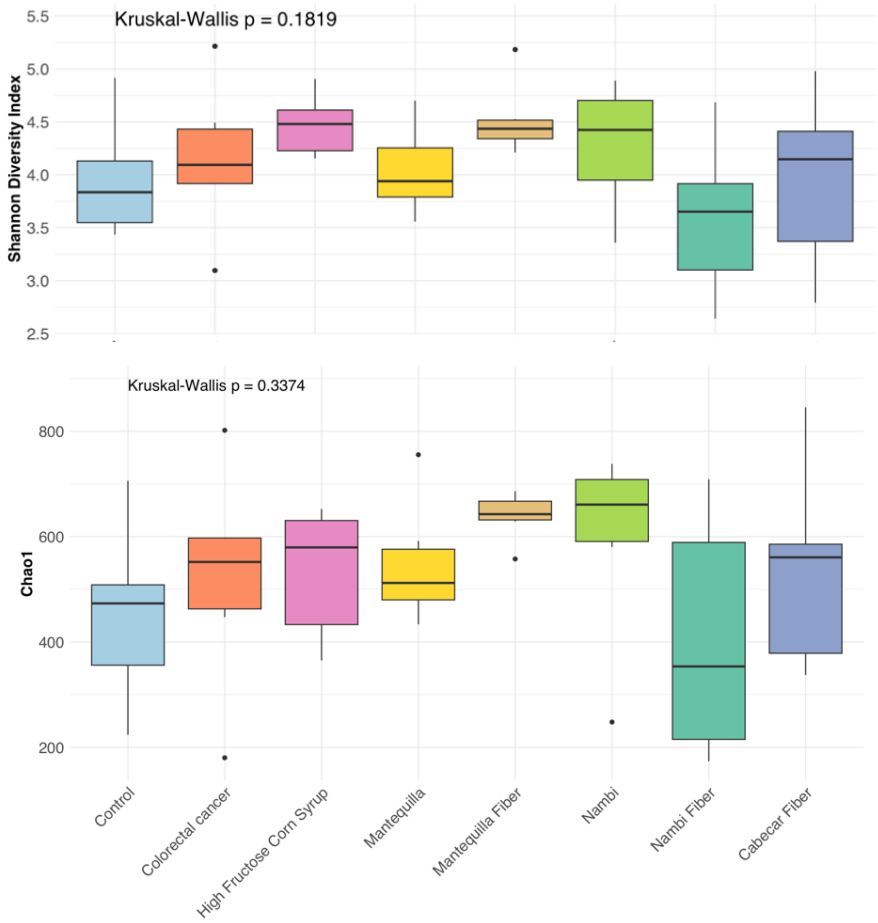

Figure 11. Indices representing alpha diversity of the gut microbiota in eight experimental groups at Week 1. Alpha diversity was assessed using Shannon and Chao1 indices. Statistical comparisons across groups were performed with the Kruskal–Wallis test, which did not reveal significant differences ($p > 0.05$).

Beta diversity was evaluated using Principal Coordinates Analysis (PcoA) based on both Weighted and Unweighted UniFrac distances. The Weighted UniFrac analysis, which considers the relative abundance of taxa, showed that the first two principal coordinates explained 48% and 23% of the variation, respectively. No statistically significant differences in microbial community composition were detected among groups (ADONIS $p = 0.082$), indicating overall similarity in microbiota structure at baseline. In contrast, the Unweighted UniFrac analysis, which accounts only for the presence or absence of taxa, explained 15.7% and 6.7% of the variation in the first two coordinates and revealed statistically significant differences among groups (ADONIS $p = 0.015$) (Figure 12).

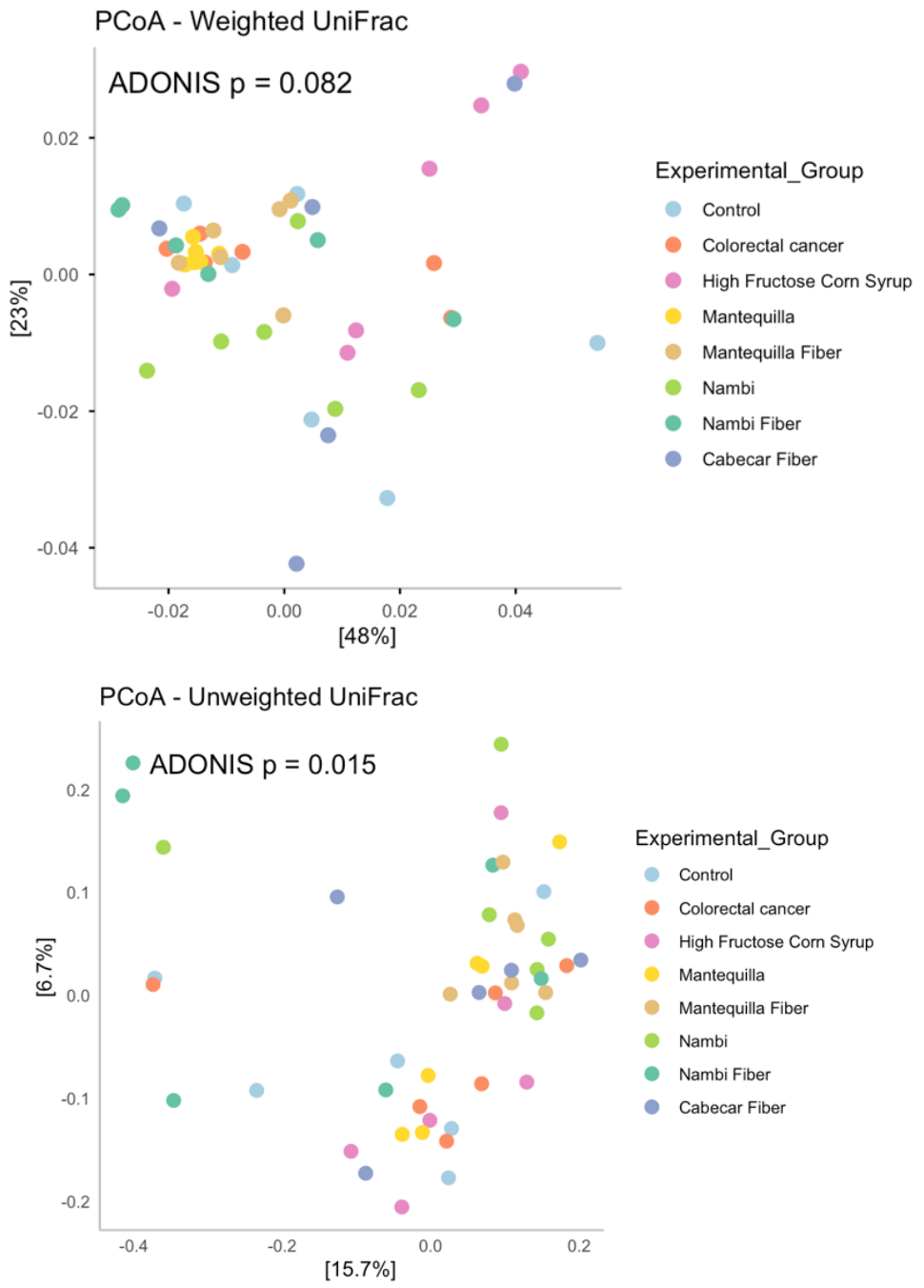

Figure 12. Principal Coordinates Analysis (PcoA) of weighted and unweighted UniFrac distances representing beta diversity of the gut microbiota at Week 1 across all experimental groups. Differences in community composition were assessed using permutational multivariate analysis of variance (Adonis test), which did not reveal statistically significant separation among groups ($p > 0.5$ for all comparisons).

At the end of the acclimatization period (Week 1), analysis of the basal fecal microbiota revealed the presence of 12 distinct bacterial phyla across all samples. The most abundant phylum was Bacillota (formerly Firmicutes), representing 54.05 ± 15.51% of the total microbial community. This phylum was consistently dominant in all samples. The second and third most prevalent phyla were Bacteroidota (formerly Bacteroidetes) at 20.86 ± 15.31%, and Actinomycetota (formerly Actinobacteriota) at 14.72 ± 11.29%. In addition to these dominant groups, other phyla such as Campylobacterota, Pseudomonadota, and Cyanobacteriota were detected at lower relative abundances. These results provide a baseline characterization of the gut microbiota prior to any dietary or experimental interventions (**Table *2***).

Table 2. Phylogenetic distribution at phylum level of the basal gut microbiome of laboratory Wistar rats at Week 1.

Phylum	Mean	Max.Val	Min.Val	Median	SD
Bacillota	54,05	82,18	21,01	53,48	15,51
Bacteroidota	20,68	63,84	3,00	15,68	15,31
Actinomycetota	14,72	51,02	0,27	14,31	11,29
Campylobacterota	7,18	40,34	0,27	3,19	9,12
Pseudomonadota	2,40	9,69	0,17	1,50	2,08
Cyanobacteriota	0,36	2,52	0,00	0,13	0,58
Patescibacteria	0,33	1,47	0,00	0,26	0,30
Desulfobacterota	0,18	0,59	0,00	0,15	0,15
Methanobacteriota	0,05	0,39	0,00	0,01	0,09
Deferribacterota	0,02	0,16	0,00	0,01	0,03

At the family level, a total of 91 distinct taxonomic groups were identified in the fecal microbiota of Wistar rats at the end of the acclimatization week. The most predominant families were Lactobacillaceae (18.81 ± 11.73%), Lachnospiraceae (15.30 ± 11.86%), and Bifidobacteriaceae (13.76 ± 10.74%), which together accounted for a substantial proportion of the community. In addition to these dominant groups, other families such as

Muribaculaceae, Helicobacteraceae, Prevotellaceae, and Erysipelotrichaceae were also detected, albeit at lower relative abundances. These findings provide a detailed baseline characterization of the gut microbiota composition at the family level prior to the introduction of dietary or experimental interventions (**Table *3***).

Table 3. Phylogenetic distribution at Family level of the gut microbiome of laboratory Wistar rats on Week 1.

Family	Mean	Max.Val	Min.Val	Median	SD
Lactobacillaceae	18,81	56,87	1,05	16,34	11,73
Lachnospiraceae	15,30	39,46	0,50	12,05	11,86
Bifidobacteriaceae	13,76	50,49	0,21	10,93	10,74
Muribaculaceae	10,40	42,31	1,42	7,92	7,86
Helicobacteraceae	6,92	40,38	0,27	3,00	8,92
Prevotellaceae	6,47	28,65	0,25	4,37	6,74
Erysipelotrichaceae	6,14	14,78	0,44	5,30	3,66
Peptostreptococcaceae	3,88	10,50	0,10	3,38	2,16
Ruminococcaceae	3,20	10,77	0,19	2,99	2,06
Oscillospiraceae	3,18	11,67	0,16	2,80	2,43

At the genus level, a total of 208 distinct taxonomic groups were identified in the fecal microbiota of Wistar rats at the end of the acclimatization week. The most abundant genera were *Lactobacillus* (17.81 ± 11.46%), *Bifidobacterium* (15.40 ± 11.43%), *Muribaculaceae* (11.36 ± 8.35%), *Helicobacter* (8.25 ± 10.37%), and Prevotellaceae (6.59 ± 6.99%). Several genera associated with fiber fermentation were detected, including *Bacteroides*, *Bifidobacterium, Lactobacillus*, *Prevotella,* and *Rombutsia* (**Table *4***). In addition, SCFA producers such as *Eubacterium*, *Ruminococcus***,** *Barnesiella***,** *Roseburia***,** and *Blautia* were identified.

Table 4. Phylogenetic distribution at Genus level of the gut microbiome of laboratory Wistar rats on Week 1.

Genus	Mean	Max.Val	Min.Val	Median	SD
Lactobacillus	17,81	48,18	0,82	15,96	11,46
Bifidobacterium	15,40	52,15	0,25	15,95	11,43
Muribaculaceae	11,36	42,68	1,66	8,69	8,35
Helicobacter	8,25	46,64	0,27	3,67	10,37
Prevotellaceae_UCG-001	6,59	32,08	0,27	4,59	6,99
Romboutsia	4,37	10,89	0,10	3,76	2,45
Lachnospiraceae_NK4A136	4,02	23,11	0,00	2,86	4,28
Dubosiella	3,59	12,37	0,10	3,03	3,06
Bacteroides	2,52	10,92	0,16	1,85	2,20
Lactobacillaceae *HT002*	2,29	6,73	0,15	1,87	1,37

4.3 Effect of DHM and DSS on the GM composition

Alpha diversity was evaluated to compare microbial richness and diversity between the Control and Colorectal cancer group at the end of the study (Week 12). The Shannon Diversity Index, which accounts for both richness and evenness, revealed a slightly higher median in the Control group relative to the Colorectal cancer group. Yet this difference was also not statistically significant (Kruskal–Wallis p = 0.2623). Similarly, the Chao1 index, which estimates species richness, showed a higher median value and broader distribution in the Control group compared to the Colorectal cancer group. However, this difference was not statistically significant (Kruskal–Wallis p = 0.7488) (Figure 13).

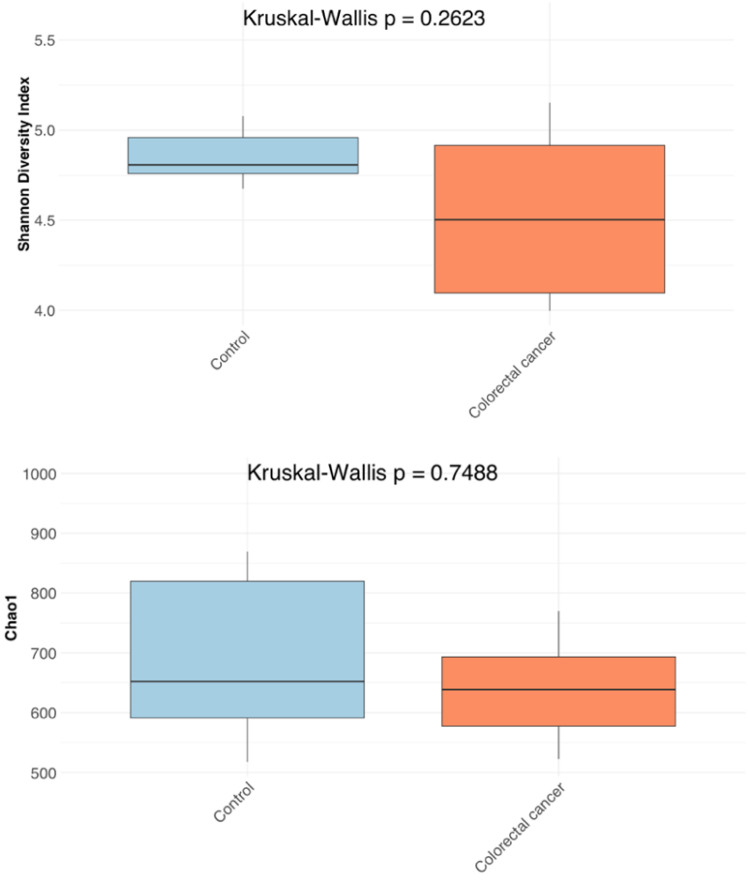

Figure 13. Indices representing alpha diversity of the gut microbiota of the Control and Colorectal cancer group at the end of the study. Shannon Index and Chao1 Index are shown. No statistically significant differences were observed among experimental groups (Kruskal–Wallis test, $p > 0.05$ for all comparisons).

The beta diversity was analyzed using PCoA based on Weighted and Unweighted UniFrac distances to compare microbial community composition between the Control and Colorectal cancer groups. The Weighted UniFrac PCoA, which accounts for both taxonomic presence and relative abundance, showed no statistically significant differences between groups (ADONIS $p = 0.705$, $R^2 = 0.058$). The first two principal coordinates explained 46.7% and 18.1% of the total variation, respectively. In contrast, the Unweighted UniFrac PCoA, which considers only the presence or absence of taxa, revealed a marginally non-significant difference between groups (ADONIS $p = 0.065$, $R^2 = 0.11$). The first two principal coordinates accounted for 16.2% and 13.2% of the variation (Figure 14).

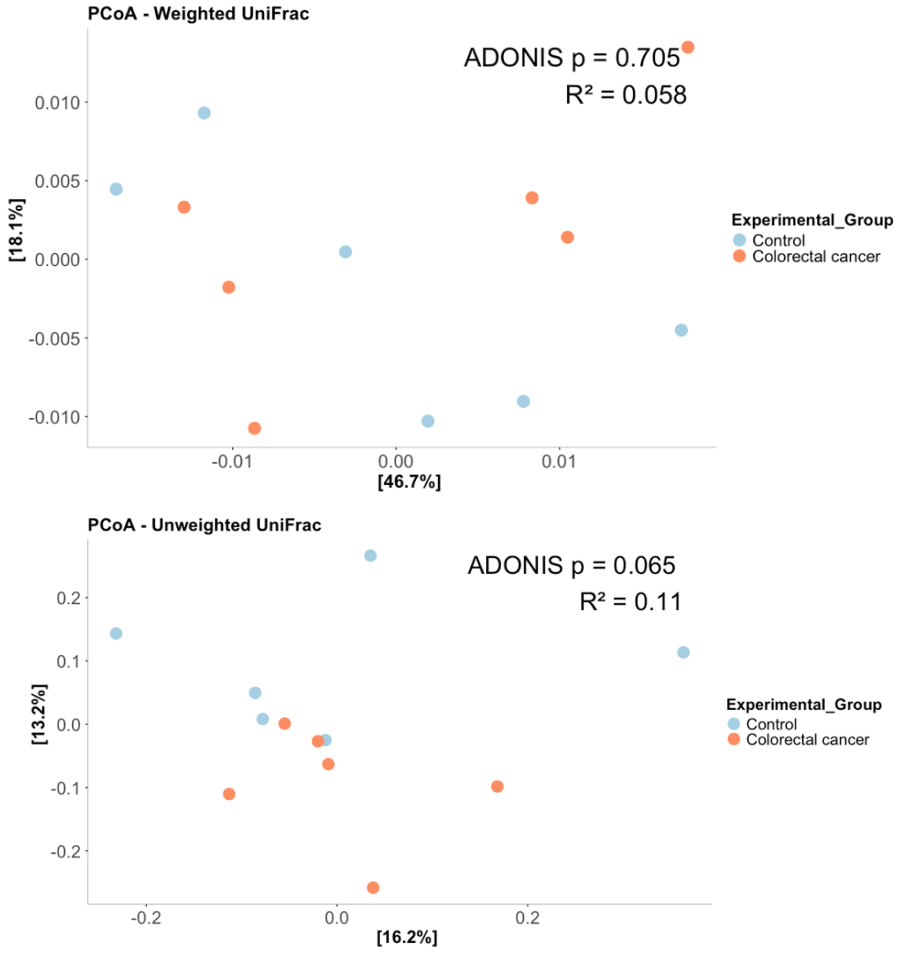

Figure 14. PCoA based on Weighted and Unweighted Unifrac distances comparing microbial community composition between Control and Colorectal cancer group. Each point represents an individual sample, colored by experimental group. In the Weighted UniFrac analysis no statistically significant differences between groups were observed (ADONIS $p = 0.705$, $R^2 = 0.058$). In the Unweighted UniFrac analysis, a non-significant difference between groups was observed (ADONIS $p = 0.065$, $R^2 = 0.11$).

To assess taxonomic shifts at the genus level, the centered log-ratio (CLR) transformed abundances of the ten most prevalent genera were compared between the Control and Colorectal cancer groups at Week 12. The genera analyzed included *Bacteroides*, *Bifidobacterium*, *Clostridia_UCG-014*, Lactobacillaceaea *HT002*, Lachnospiraceae_NK4A136, *Lactobacillus*, *Muribaculaceae*, Prevotellaceae_UCG-001, *Romboutsia*, and *Ruminococcus*. Boxplot analysis revealed no statistically significant differences in CLR-transformed abundance for any of the genera examined (Kruskal–Wallis $p > 0.6$ for all comparisons) (Figure 15).

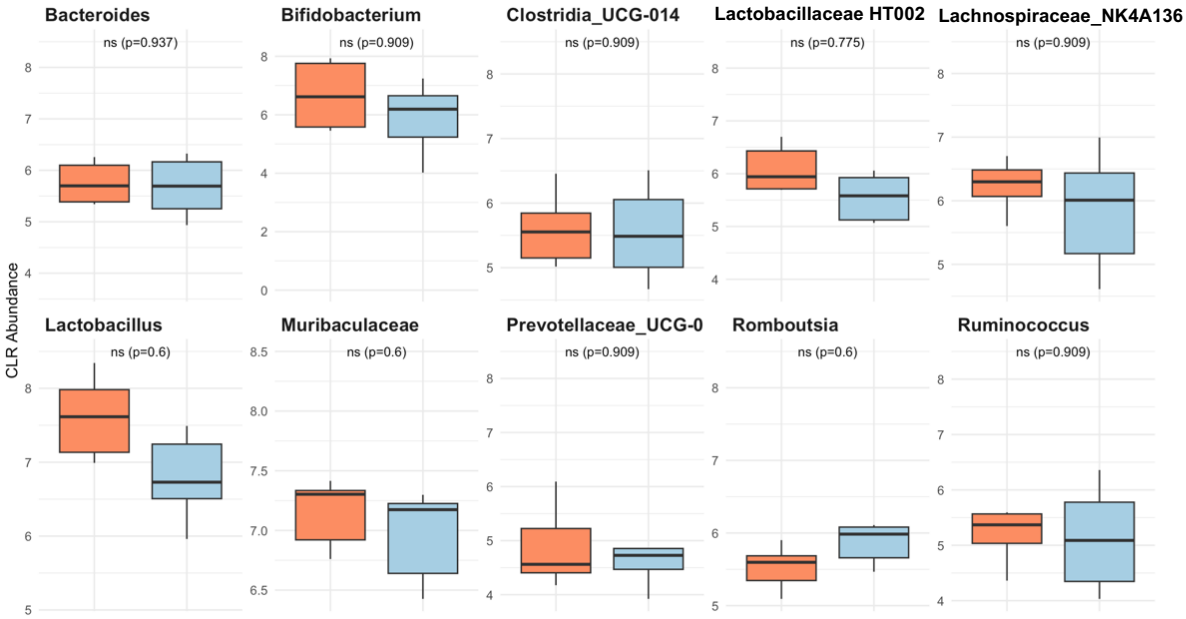

Figure 15. Centered log-ratio (CLR) transformed abundance of the top 10 bacterial genera in Control and Colorectal cancer group at Week 12. Each panel displays the distribution of CLR-transformed abundance values for a specific genus, comparing samples from the Control (blue) and Colorectal cancer (orange) groups. No statistically significant differences were observed for any genus (Kruskal–Wallis $p > 0.6$ for all comparisons).

4.4 Effect of dietary fiber on the GM composition during colorectal carcinogenesis

To assess how microbial community structure evolved over time in response to colorectal carcinogenesis and dietary fiber interventions, the beta diversity was analyzed using PCoA based on Weighted and Unweighted UniFrac distances across four timepoints (Weeks 1, 3, 9, and 12). The Weighted UniFrac PCoA showed overlapping distributions across experimental groups and timepoints. The first two principal coordinates explained 47.4% and 12.8% of the total variation. ADONIS analysis revealed no statistically significant differences ($p = 0.21$, $R^2 = 0.045$), indicating that the overall abundance-weighted microbial community structure remained broadly conserved throughout the study. In contrast, the Unweighted UniFrac PCoA, revealed clearer separation among groups and timepoints. The first two axes explained 12.2% and 7.0% of the variation, respectively. ADONIS analysis showed statistically significant differences ($p = 0.001$, $R^2 = 0.053$), suggesting that dietary fiber interventions and carcinogen exposure influenced the composition of low-abundance or rare taxa over time (Figure 16).

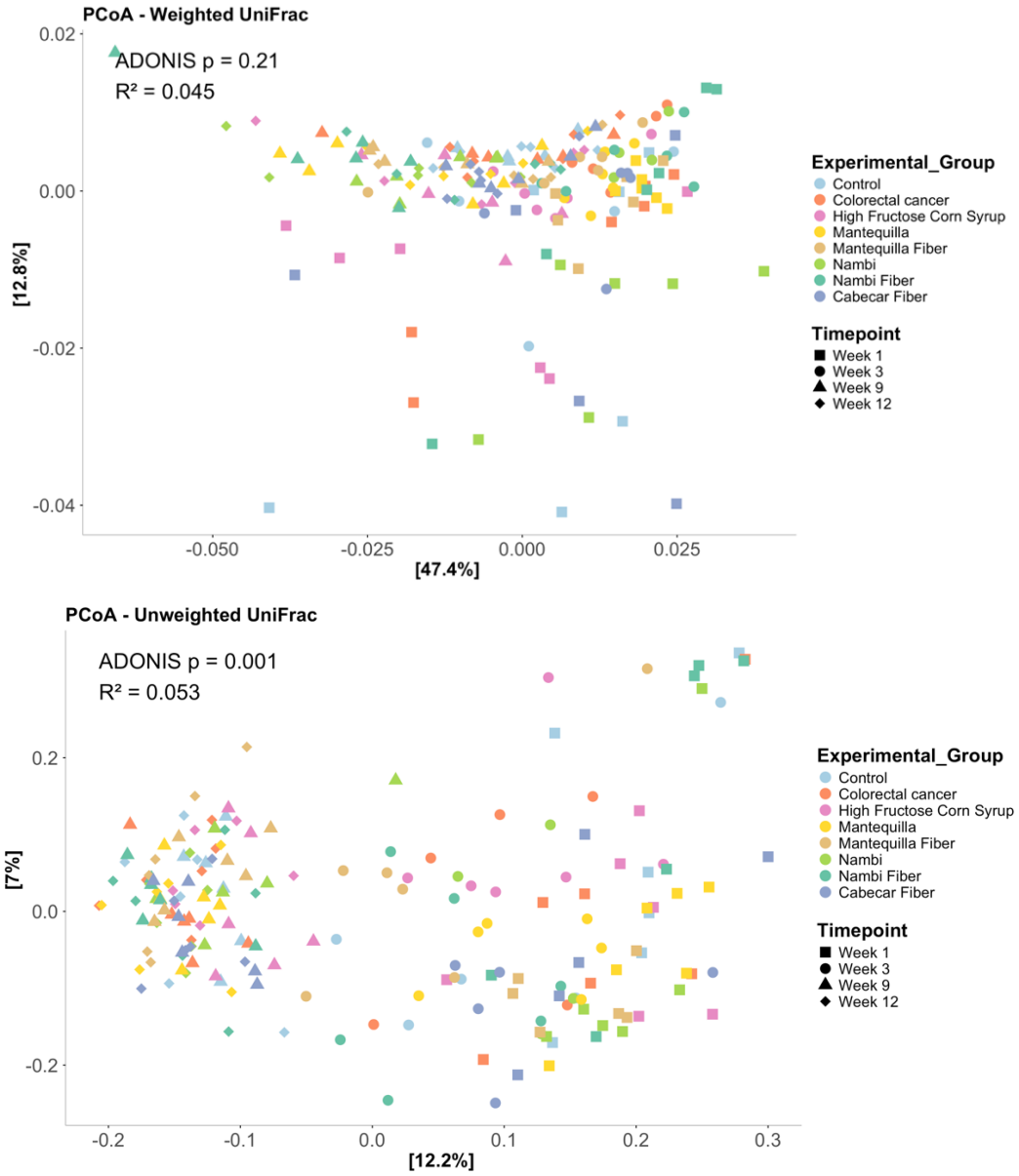

Figure 16. PCoA of gut microbial community composition across experimental groups and timepoints. PCoA plots based on Weighted UniFrac (top) and Unweighted UniFrac (bottom) distances illustrate microbial community structure of all experimental groups at Weeks 1, 3, 9, and 12. Each point represents a sample, color-coded by experimental group (Control, Colorectal cancer, High Fructose Corn Syrup, Mantequilla, Mantequilla Fiber, Nambi, Nambi Fiber, Cabécar Fiber) and shaped by timepoint (Week 1 = square, Week 3 = circle, Week 9 = diamond, Week 12 = triangle).The Weighted UniFrac ADONIS analysis showed no significant differences ($p = 0.21$, $R^2 = 0.045$). The Unweighted ADONIS analysis revealed significant differences among groups and timepoints ($p = 0.001$, $R^2 = 0.053$).

To evaluate longitudinal changes in gut microbiota composition during colorectal carcinogenesis and dietary fiber intervention, the relative abundance of key bacterial families was analyzed across four timepoints: Week 1, Week 3, Week 9, and Week 12. At the phylum level, Bacteroidota, Bacillota, and Actinomycetota were predominant across all groups. Colorectal cancer and High Fructose Corn Syrup groups showed shifts in composition, while fiber interventions helped preserve phylum-level balance, especially in Week 12 (Figure 17).

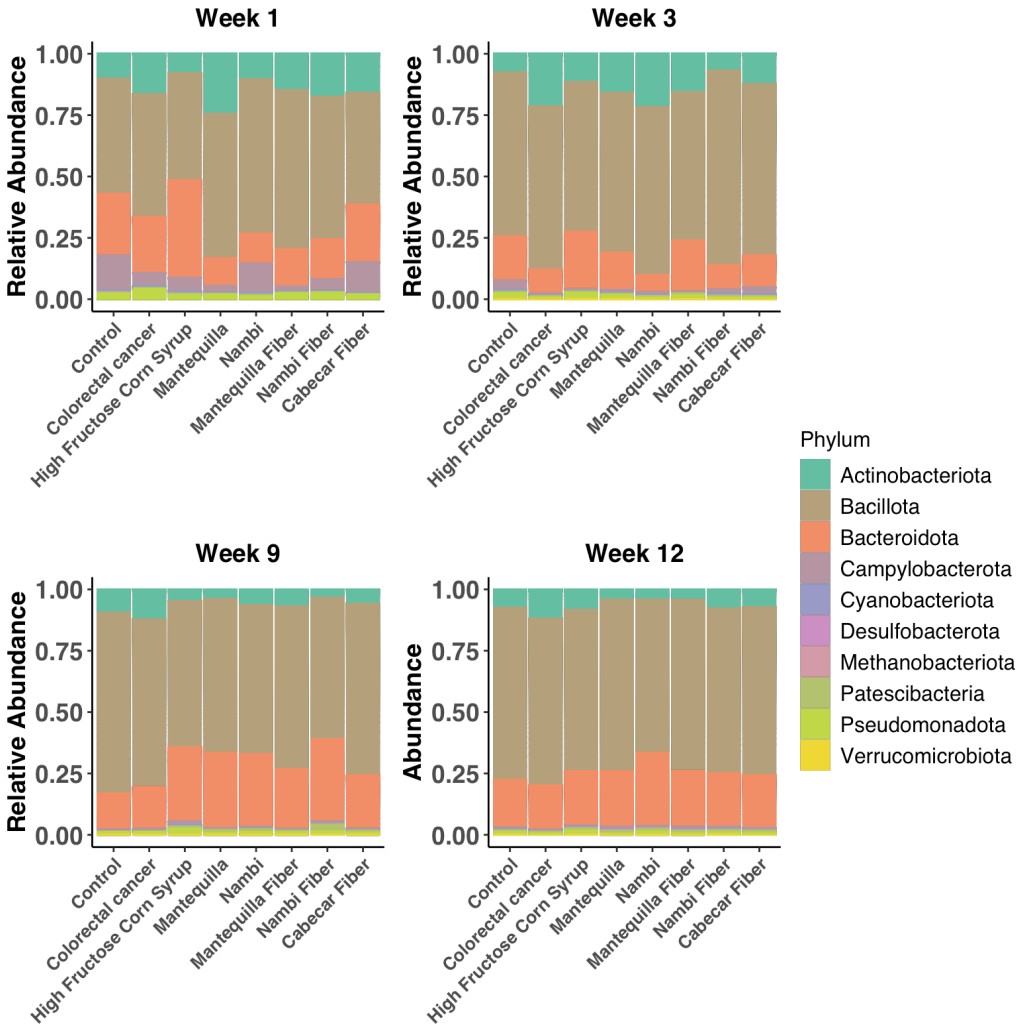

Figure 17. Relative abundance of bacterial phyla across experimental groups at weeks 1, 3 , 9, 12. Stacked bar plots display the composition of gut microbiota at the phylum level across the eight experimental groups: Control, Colorectal cancer, High Fructose Corn Syrup, Mantequilla, Nambi, Mantequilla Fiber, Nambi Fiber, and Cabecar Fiber.

At the family level, dominant taxa included Muribaculaceae, Lachnospiraceae, Ruminococcaceae, and Bacteroidaceae. Fiber-supplemented groups, particularly Cabecar and Nambi Fiber, maintained or increased the relative abundance of these beneficial families over time. The Control group maintained a relatively stable family-level profile, while the Colorectal carcinogenesis and High Fructose Corn Syrup groups showed progressive reductions in Muribaculaceae, suggesting disruption of fiber-degrading taxa. Notably, Lachnospiraceae and Bacteroidaceae remained consistently abundant across most groups, while Helicobacteraceae and Erysipelotrichaceae showed a decrease across all groups (Figure 18).

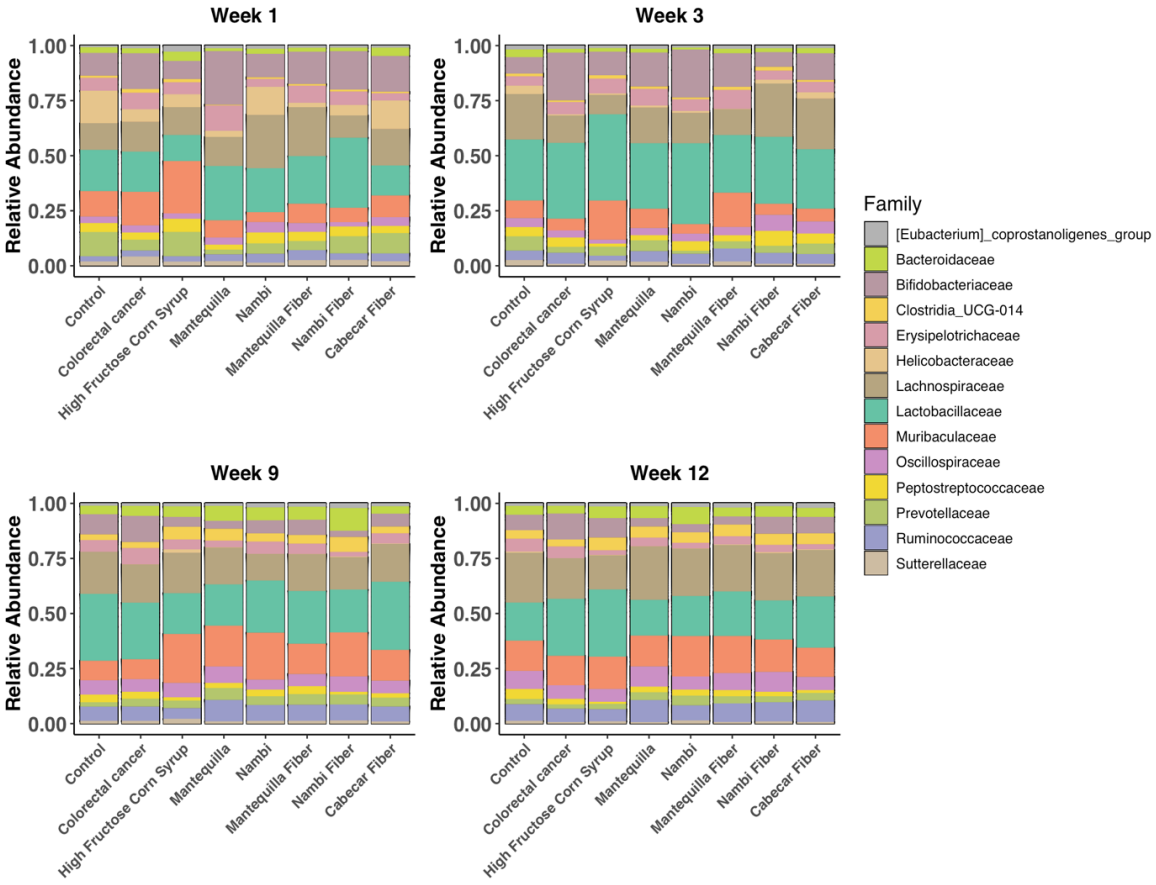

Figure 18. Relative abundance of bacterial families of experimental groups at weeks 1, 3, 9 and 12. Stacked bar plots display the composition of gut microbiota at the family level in Control, Colorectal cancer, High Fructose Corn Syrup, Mantequilla, Nambi, Mantequilla Fiber, Nambi Fiber, and Cabecar Fiber.

Among the most represented taxa at genus level, *Muribaculaceae*, *Lactobacillus* and Lachnospiraceae NK4A136 show broad distribution across groups, with fluctuations suggesting sensitivity to dietary treatments and temporal changes (Figure 19). *Bacteroides* and *Romboutsia* exhibit more specific patterns: *Bacteroides* showed an increasing trend, and *Rombutsia* a decreasing trend over time. *Dubosiella* appear intermittently, the latter with a stronger presence in later stages of the experiment. Other genera, such as *Helicobacter* showed higher abundance at Week 1 and then decreased over time. *Turicibacter* showed stable profiles across the four timepoints. *Lactobacillus* and *Ligilactobacillus* are detected across multiple treatments but without a consistent trend. *Clostridia UCG-014* seemed to increase its abundance across time, contrary to Prevotellaceae UCG-001 with decreased abundance over time.

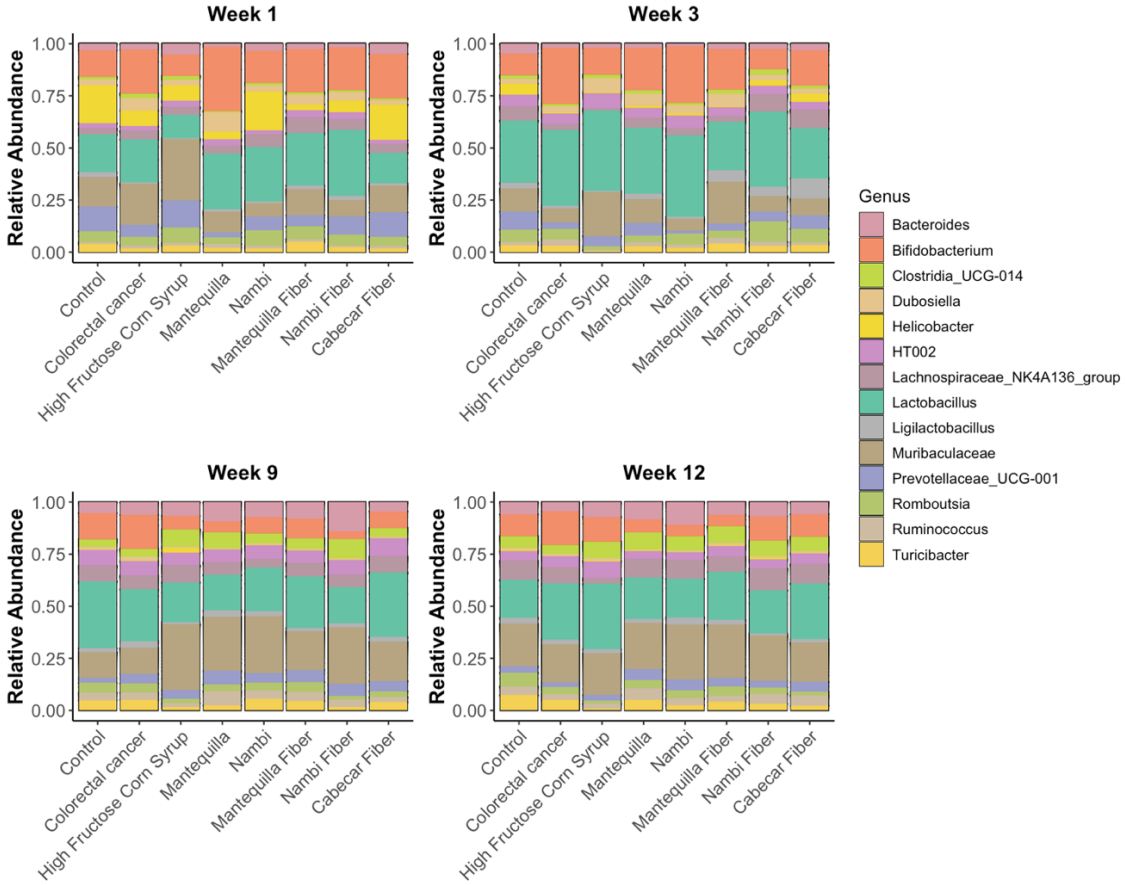

Figure 19. Relative abundance of bacterial genera across experimental groups at weeks 1,3,9 and 12. Stacked bar plots display genus-level gut microbiota composition in Control, Colorectal cancer, High Fructose Corn Syrup, Mantequilla, Nambi, Mantequilla Fiber, Nambi Fiber, and Cabecar Fiber groups.

The following analysis assesses whether specific dietary fibers can induce compositional shifts, enhance microbial richness or promote beneficial taxa capable of counteracting carcinogenesis-associated preneoplastic lesions.

Alpha diversity at the end of the study (Week 12) was assessed using the Chao1 and Shannon indices to evaluate microbial richness and diversity across all experimental groups. The Chao1 index showed no statistically significant differences among groups (Kruskal–Wallis p = 0.6402). Similarly, the Shannon Diversity Index also revealed no significant differences (Kruskal–Wallis p = 0.5963) (Figure 20).

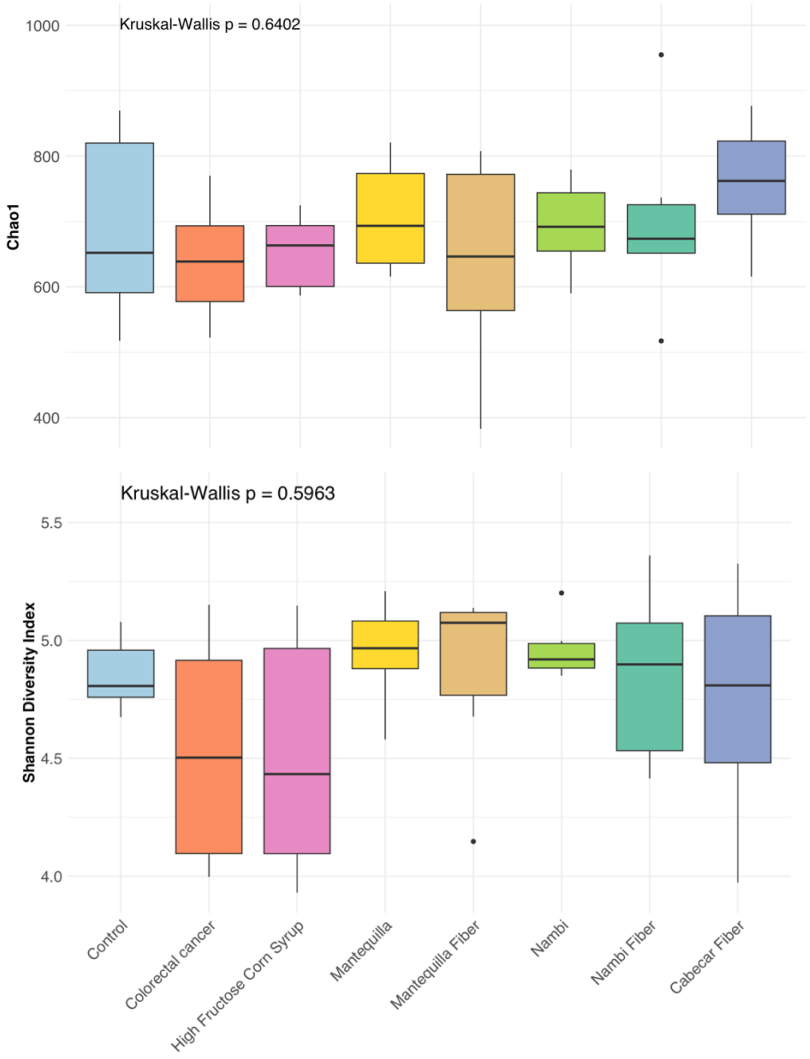

Figure 20. Alpha diversity across experimental groups at week 12. Boxplots display the distribution of microbial richness (Chao1 index) and diversity (Shannon index). No statistically significant differences were observed among groups for either metric (Kruskal–Wallis p = 0.6402 for Chao1; p = 0.5963 for Shannon).

The Weighted UniFrac PCoA, which incorporates both taxonomic presence and relative abundance, revealed partial separation among experimental groups. The first two principal coordinates explained 51.9% and 9.6% of the total variation. ADONIS analysis did not detect statistically significant differences across groups ($p = 0.071$, $R^2 = 0.213$). In contrast, the Unweighted UniFrac PCoA showed clearer group separation. The first two axes explained 8.9% and 6.3% of the variation, respectively. ADONIS analysis revealed statistically significant differences among groups ($p = 0.001$, $R^2 = 0.196$) (Figure 21).

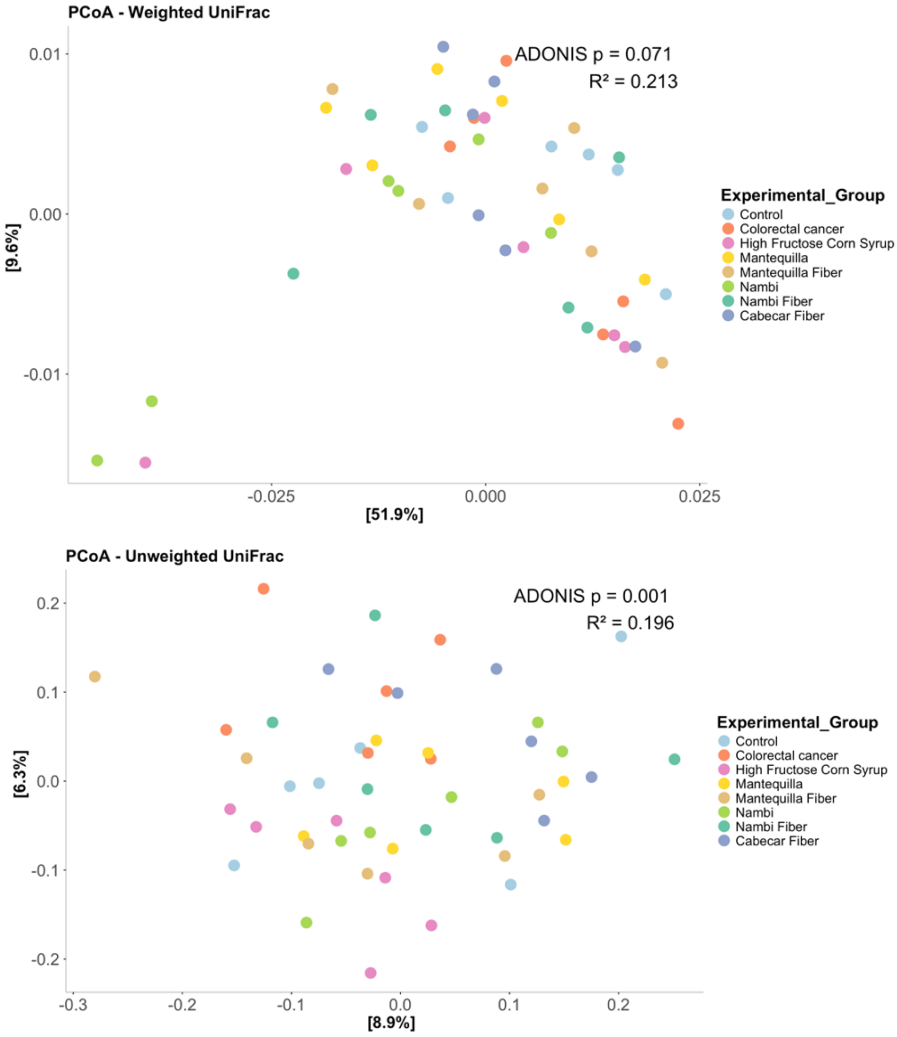

Figure 21.PCoA of gut microbial community composition based on Weighted and Unweighted Unifrac distances for experimental groups at week 12. Each point represents an individual sample, colored by experimental group. The Weighted UniFrac ADONIS analysis indicated no statistically significant differences among groups ($p = 0.071$, $R^2 = 0.213$). The Unweighted UniFrac (bottom) revealed significant differences among groups ($p = 0.001$, $R^2 = 0.196$).

To evaluate the impact of dietary interventions, samples of week 12 were categorized into five analytical groupings:

a) Experimental groups included eight distinct treatments: Control, Colorectal cancer, High Fructose Corn Syrup, Mantequilla, Mantequilla Fiber, Nambi, Nambi Fiber, and Cabecar Fiber.

b) Bean groups were defined based on the presence and type of bean: None, Mantequilla, Nambi, and Cabecar.

c) Fiber Type groups classified treatments by fiber content: None, cooked whole bean flour (Whole Bean), and total dietary fiber (Whole fiber).

d) Diet groups reflected overall dietary composition: standard rat diet, high caloric diet, cooked whole bean flour supplementation (Whole Bean), and total dietary fiber supplementation (Whole fiber).

e) Treatment groups summarized intervention strategies: Control, Cancer, Cancer + Fiber, and Cancer + Fructose.

These categorical definitions were used to stratify samples for diversity analyses, taxonomic comparisons, and Permutational Multivariate Analysis of Variance (PERMANOVA) testing, enabling assessment of both specific dietary components and broader intervention effects. The resulting pseudo-F values and p-values are summarized in Table 5, highlighting which factors significantly contributed to microbial compositional differences.

Table 5. PERMANOVA results for the experimental variables using Weighted Unifrac distance at week 12.

Experimental Variable	N	Groups	Pseudo-F (Weighted UniFrac)	p-value (Weighted UniFrac)	Permutations
Experimental Group[a]	48	8	1.35432	0.1	999
Bean[b]	48	4	1.562336	0.078	999
Fiber Type[c]	48	3	1.72292	0.07	999
Diet[d]	48	4	1.919084	**0.03****	999
Treatment[e]	48	4	1.860133	**0.024****	999

[a] Experimental groups were defined as control, colorectal cancer, high fructose corn syrup, mantequilla, mantequilla fiber, nambi, nambi fiber and cabecar fiber.
[b] Bean groups were defined as none, mantequilla, nambi and cabecar.
[c] Fiber Type groups were defined as none, whole fiber and whole bean.
[d] Diet groups were defined as Rat diet, High caloric, whole fiber supplementation and whole bean supplementation.
[e] Treatment groups were defined as control, cancer, cancer+fiber and cancer+fructose.

PERMANOVA analysis based on Weighted UniFrac distances demonstrated that diet and treatment significantly influenced gut microbial community structure. Specifically, diet grouping yielded a pseudo-F value of 1.919 ($p = 0.03$), while treatment grouping produced a pseudo-F value of 1.860 ($p = 0.024$). In contrast, other experimental variables—including bean type, fiber type, and the broader experimental group classification—did not reach statistical significance ($p > 0.05$) (**Table *5***).

To complement PERMANOVA, ADONIS and ANOSIM tests were also applied to assess the relative contribution of experimental and dietary variables to microbial community variation. These analyses provide additional measures of effect size and confirm the robustness of group differences.

ADONIS analysis revealed that diet ($R^2 = 0.106$, $p = 0.032$) and bean type ($R^2 = 0.086$, $p = 0.039$) significantly contributed to gut microbial community variation, while cancer status and fiber type did not reach statistical significance. Together, diet and bean origin explained ~19% of the variance, highlighting dietary context as the primary driver of microbial compositional differences (**Table *6***).

Table 6. ADONIS results for Experimental and Dietary variables on gut microbiota composition based on Weighted Unifrac distances at Week 12.

	Df	SS	MS	F. Model	R2	Pr(>F)
Diet+Cancer						
Cancer	1	0.040406	0.040406	1.382004	0.027824	0.226
Diet	3	0.154572	0.051524	1.762278	0.106442	0.032*
Residuals	43	1.257199	0.029237	NaN	0.865734	NaN
Total	47	1.452177	NaN	NaN	1.000000	NaN
Bean+Fiber Type						
Bean	3	0.139798	0.046599	1.554723	0.096268	0.087
Fiber_Type	1	0.023546	0.023546	0.785580	0.016214	0.554
Residuals	43	1.288833	0.029973	NaN	0.887518	NaN
Total	47	1.452177	NaN	NaN	1.000000	NaN
Cancer+Exp Group						
Cancer	1	0.040406	0.040406	1.375647	0.027824	0.180
Experimental_Group	6	0.236880	0.039480	1.344121	0.163120	0.109
Residuals	40	1.174892	0.029372	NaN	0.809055	NaN
Total	47	1.452177	NaN	NaN	1.000000	NaN

*NaN: not a number.

ANOSIM analysis revealed that none of the tested variables reached statistical significance ($p > 0.05$). These results are consistent with PERMANOVA and ADONIS findings, where diet and treatment emerged as the most influential factors shaping microbial community structure (**Table** *7*).

Table 7. ANOSIM results for experimental and dietary variables on Gut microbiota composition based on Weighted Unifrac distances at Week 12.

Variable	N	Groups	R statistic	p-value	Permutations
Experimental group	48	8	0.044759	0.17	999
Bean	48	4	0.021401	0.303	999
Diet	48	4	0.068704	0.066	999
Fiber type	48	3	0.014287	0.285	999
Treatment	48	4	0.108764	0.072	999

To assess genus-level differences in microbial composition across experimental groups, the CLR transformed abundances of the top 10 genera at Week 12 were compared using Kruskal–Wallis tests (Figure 22). Among these, *Turicibacter* showed the most pronounced variation ($p = 0.001$), with significantly higher abundance in fiber-supplemented groups —particularly Cabecar and Nambi— compared to high-fructose and carcinogen-exposed groups. Lactobacillaceae *HT002* also differed significantly across treatments ($p = 0.03$), with elevated levels in native bean fiber groups. The remaining genera, including *Bacteroides*, *Bifidobacterium*, *Lactobacillus*, *Muribaculaceae*, and *Ruminococcus*, did not show statistically significant differences ($p > 0.1$), though trends in *Lactobacillus* and Prevotellaceae_UCG-001*, Muribaculaceaea, Ruminococcus,* suggested preservation in fiber-rich diets.

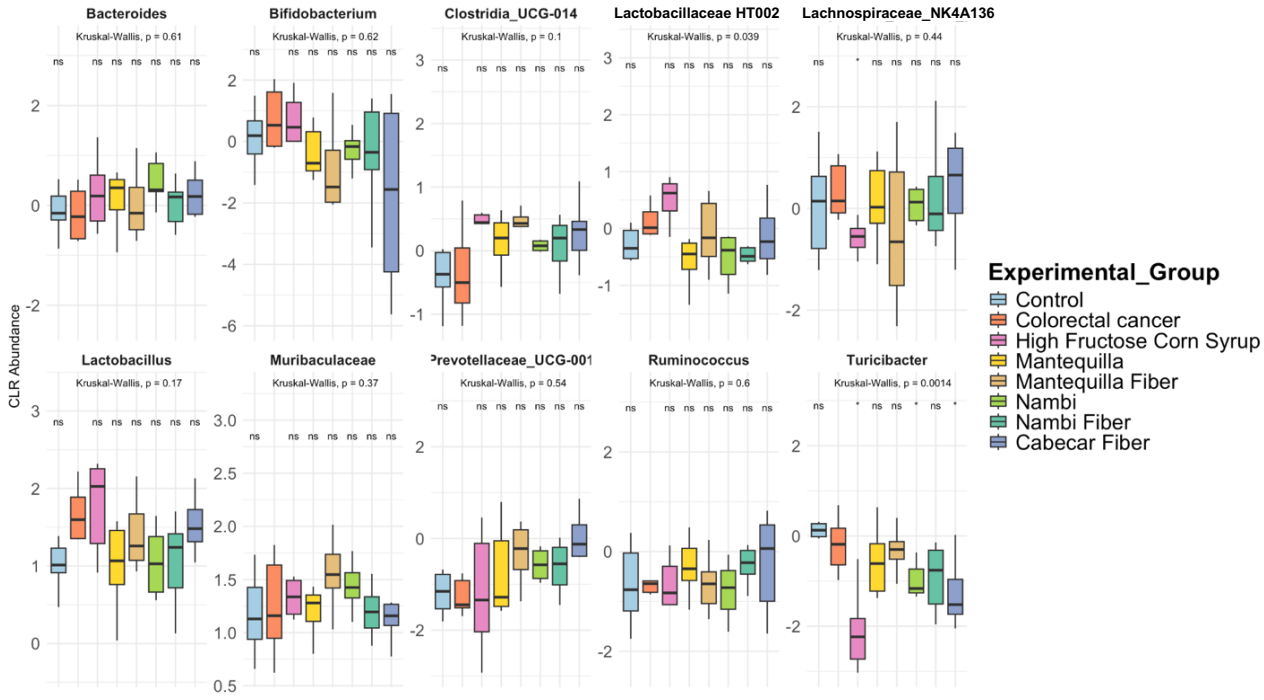

Figure 22.CLR-transformed abundance of the top 10 genera at Week 12. Boxplots display CLR-transformed abundances of the most abundant genera across eight experimental groups. Significant differences were detected for *Turicibacter* ($p = 0.001$) and Lactobacillaceae *HT002* ($p = 0.03$). Other genera showed no significant variation. Significance levels are indicated above each plot (*ns*, *, **).

To evaluate the influence of bean type on microbial composition, CLR-transformed abundances of the top 10 genera were compared across four bean types at Week 12. While Kruskal–Wallis tests did not reveal statistically significant differences for most genera ($p > 0.05$), visual trends suggest that Cabecar, Mantequilla and Nambi beans may support higher abundance of *Clostridia UCG-014*, Lachnospiraceae NK4A136, Prevotellaceae UCG-001 and *Ruminococcus* (Figure 23).

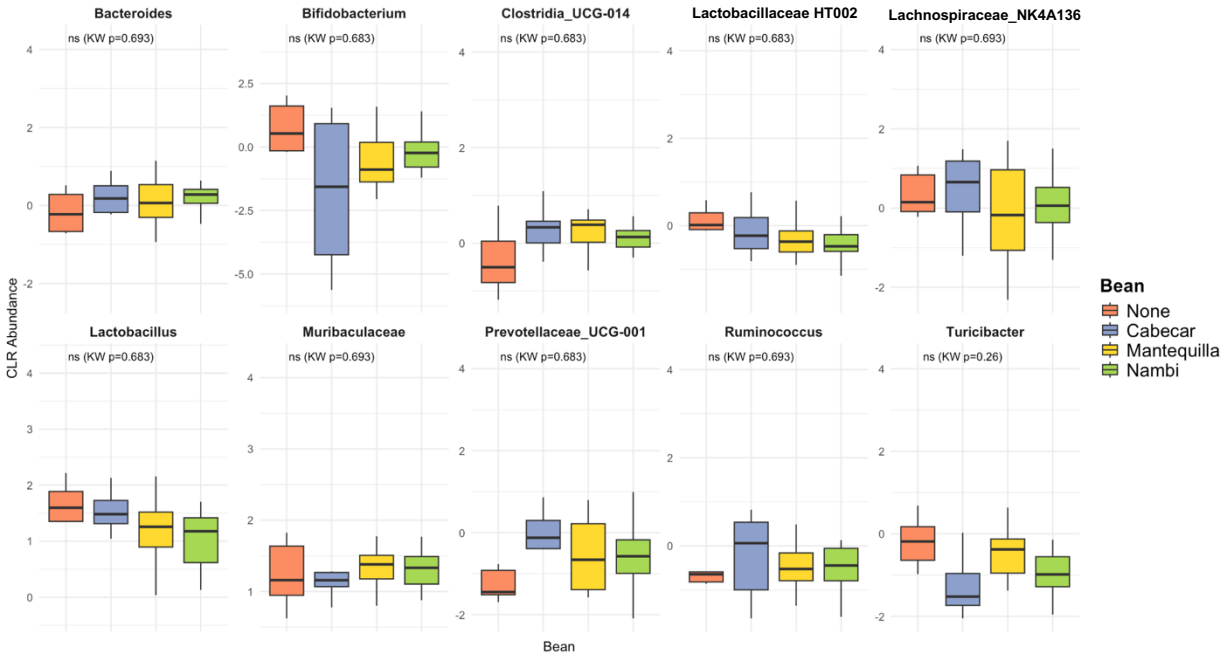

Figure 23. CLR-transformed abundance of the top 10 genera by bean type at Week 12. Boxplots display centered log-ratio (CLR) transformed abundances of the ten most abundant genera (*Bacteroides*, *Bifidobacterium*, *Clostridia_UCG-014*, Lactobacillaceae *HT002*, *Lachnospiraceae NK4A136*, *Lactobacillus*, *Muribaculaceae*, *Prevotellaceae_UCG-001*, *Ruminococcus*, and *Turicibacter*) across four bean types: None, Cabecar, Mantequilla, and Nambi. Statistical differences were assessed using the Kruskal–Wallis test, with significance indicated above each plot (*ns* = not significant).

To assess the impact of fiber type on microbial composition, CLR-transformed abundances of ten key genera were compared across three treatment groups: no fiber, whole fiber, and whole bean. Although Kruskal–Wallis tests revealed no statistically significant differences ($p > 0.05$), visual inspection of the boxplots suggests subtle shifts in abundance patterns. Genera such as *Clostridia UCG-014*, Lachnospiraceae NK4A136 , Prevotellaceae

UCG-001, and *Ruminococcus* appeared slightly elevated in fiber-supplemented groups, particularly in whole bean treatments (Figure 24).

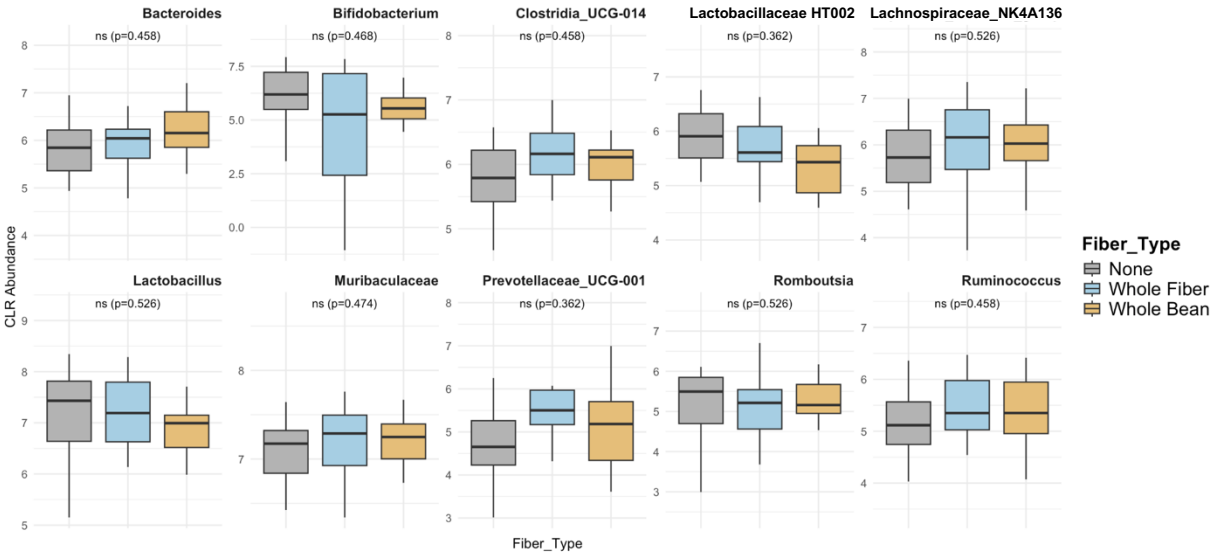

Figure 24. CLR-transformed abundance of the top 10 genera at Week 12 across fiber types. Boxplots display centered log-ratio (CLR) transformed abundances of ten representative bacterial genera (*Bacteroides*, *Bifidobacterium*, Clostridia_UCG-014, Lactobacillaceae HT002, Lachnospiraceae NK4A136, *Lactobacillus*, Muribaculaceae, Prevotellaceae_UCG-001, *Romboutsia*, and *Ruminococcus*) across three fiber treatments: None (gray), Whole Fiber (blue), and Whole Bean (yellow). Statistical comparisons were performed using the Kruskal–Wallis test, with all genera showing non-significant differences ($p > 0.05$).

The CLR-transformed abundance of ten bacterial taxa was compared across four dietary interventions: High Caloric, Rat Diet, Whole Fiber, and Whole Bean. Box plots illustrate the distribution of microbial abundance within each group. Most taxa, including *Bacteroides*, *Bifidobacterium*, *Clostridia UCG-014*, Lactobacillaceae HT002, Lachnospirace*ae NK4A136*, *Lactobacillus*, *Muribaculaceae*, Prevotellaceae UCG-001, and *Ruminococcus*, showed no statistically significant differences between diets ($p > 0.05$). However, *Romboutsia* exhibited a statistically significant variation in abundance across diet groups ($p = 0.0398$), suggesting a potential diet-dependent modulation of this genus (Figure 25).

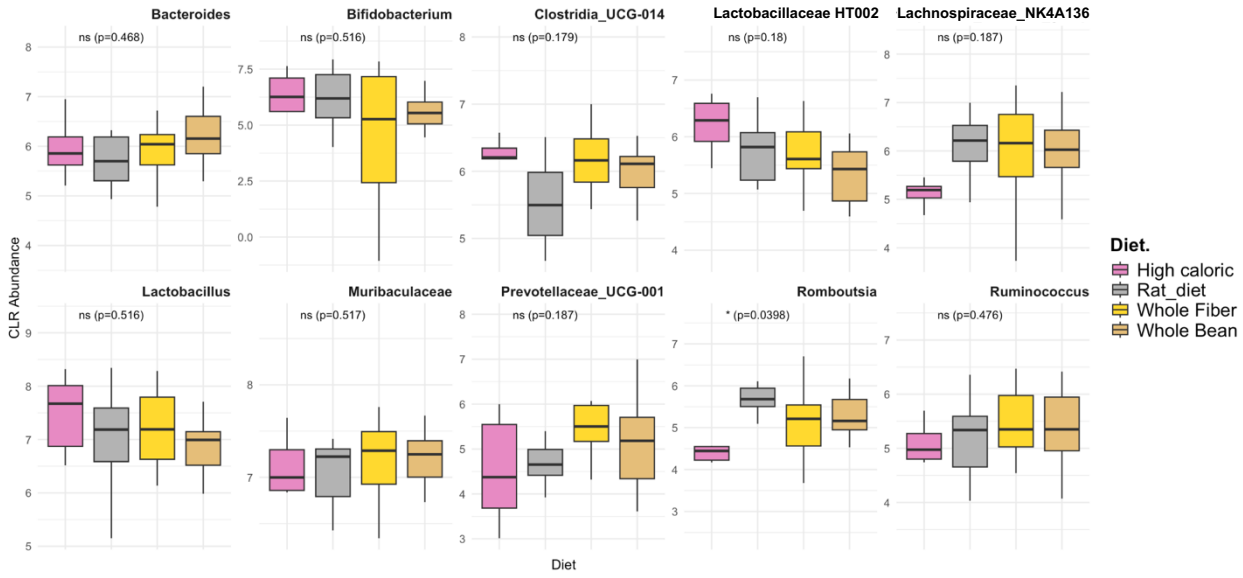

Figure 25. CLR-transformed abundance of the top 10 genera at Week 12 across different diets. Boxplots display centered log-ratio (CLR) transformed abundances of ten representative bacterial genera (*Bacteroides*, *Bifidobacterium*, *Clostridia UCG-014*, Lactobacillaceae *HT002*, *Lachnospiraceae NK4A136*, *Lactobacillus*, *Muribaculaceae*, *Prevotellaceae UCG-001*, *Romboutsia*, and *Ruminococcus*) across four diets. Statistical comparisons were performed using the Kruskal–Wallis test, Romboutsia stands out with a significant p-value of 0.0398, suggesting diet has a measurable impact on its abundance, while all other genera shows non-significant differences ($p > 0.05$).

The CLR-transformed abundance of top ten bacterial taxa was compared across four treatment groups: Control, Cancer, Cancer + Fructose, and Cancer + Fiber (Figure 26). Most taxa did not exhibit statistically significant differences among treatments, including *Bacteroides* ($p = 0.554$), *Bifidobacterium* ($p = 0.311$), *Clostridia UCG-014* ($p = 0.073$), Lachnospiraceae NK4A136 ($p = 0.311$), *Lactobacillus* ($p = 0.209$), *Muribaculaceae* ($p = 0.599$), Prevotellaceae UCG-001 ($p = 0.311$), *and Ruminococcus* ($p = 0.599$). However, two taxa showed significant modulation by treatment. Lactobacillaceae *HT002* abundance differed significantly among groups ($p = 0.0431$). Notably, *Turicibacter* abundance was highly affected ($p = 0.00354$), with marked differences particularly in the Cancer + Fiber group, indicating a strong response to fiber supplementation in the context of colorectal carcinogenesis.

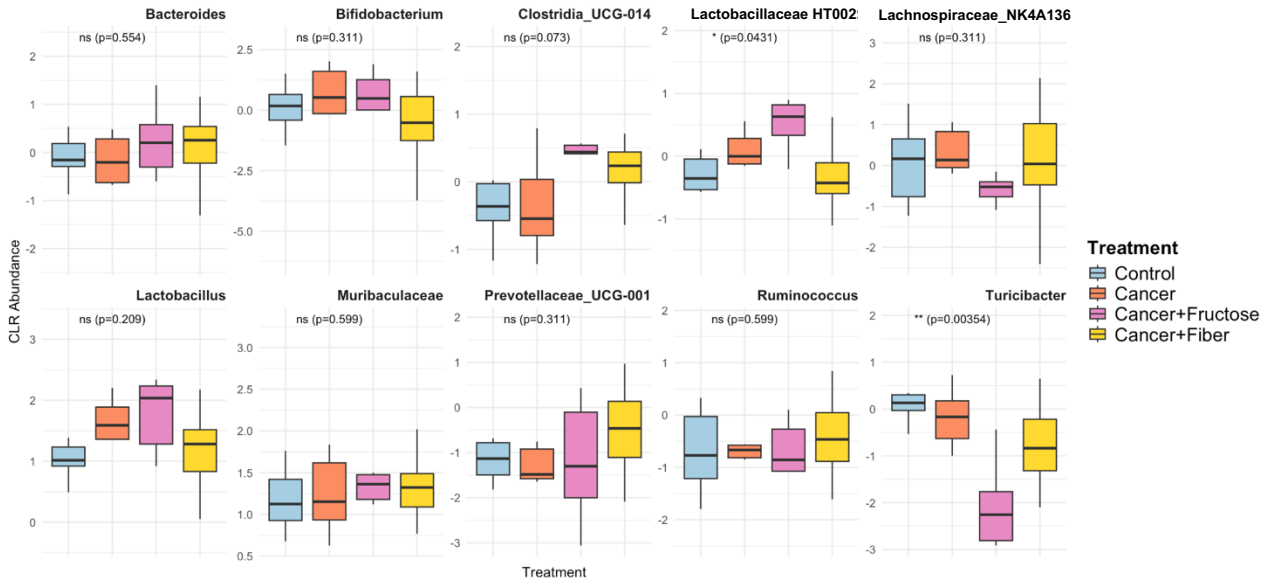

Figure 26. CLR-transformed abundance of top 10 bacterial taxa across treatment groups. Boxplots represent median-centered log-ratio (CLR) values for each taxon. Colors denote treatment groups: Control (blue), Cancer (orange), Cancer + Fructose (pink), and Cancer + Fiber (yellow). Statistical significance was assessed using Kruskal–Wallis test; p-values are indicated above each plot.

Then an analysis of Compositions of Microbiomes with Bias Correction (ANCOM-BC) was applied to each analytical grouping to identify taxa with differential abundance while correcting for compositional biases inherent to sequencing data. This method was chosen because it provides bias-adjusted estimates of absolute abundance changes, reduces false positives, and accommodates complex experimental designs. Thus, ANCOM-BC allowed us to robustly evaluate the impact of dietary interventions and treatment strategies on specific microbial taxa, complementing diversity analyses with taxon-level resolution. The following section summarizes the main findings obtained from ANCOM-BC of experimental variables previously described.

A) Experimental group:

In ANCOMBC analysis of experimental groups, Desulfovibrionaceae, *UCG-004*, Ruminococcaceae and *Fournierella* were significantly enriched in response to Cabecar bean fiber supplementation, with a Log Fold Change (LFC) of approximately +3 for the first two taxa and approximately +1 for the last two. Meanwhile, Staphylococcaceae and

Paenalcaligenes were depleted, with a LFC of approximately -3,5 and -2 respectively (Figure 27**).**

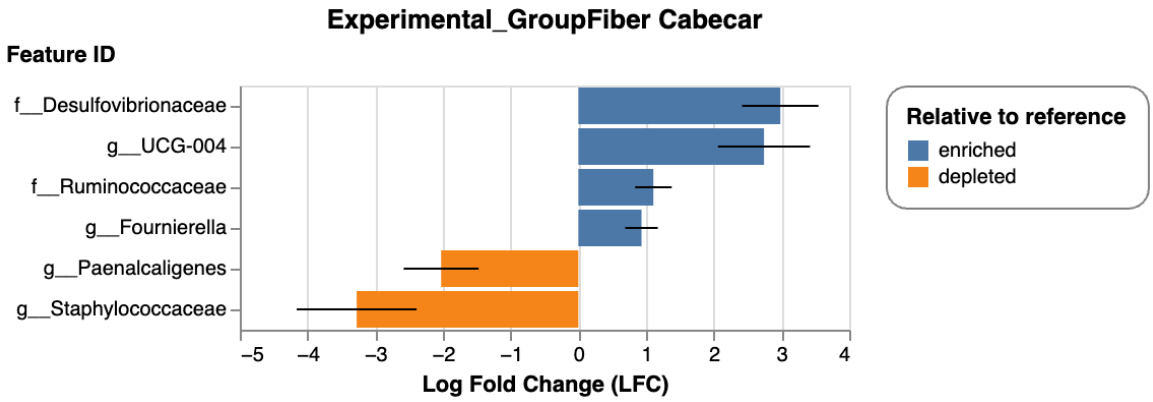

Figure 27. Differential abundance of microbial taxa in the Cabecar fiber experimental group relative to colorectal cancer group, estimated by ANCOM-BC. Log fold changes (LFC) represent bias-corrected differences in abundance for each taxon. Positive values (blue bars) indicate enrichment; negative values (orange bars) indicate depletion. Error bars denote confidence intervals.

Analysis of Mantequilla fiber experimental group revealed three taxa with significant differential abundance relative to the colorectal cancer reference group. The *Eubacterium ventriosum* group was enriched with a LFC of approximately +3, while family Planococcaceae and *Jeotgalicoccus* were depleted with a LFC of approximately -2 (Figure 28).

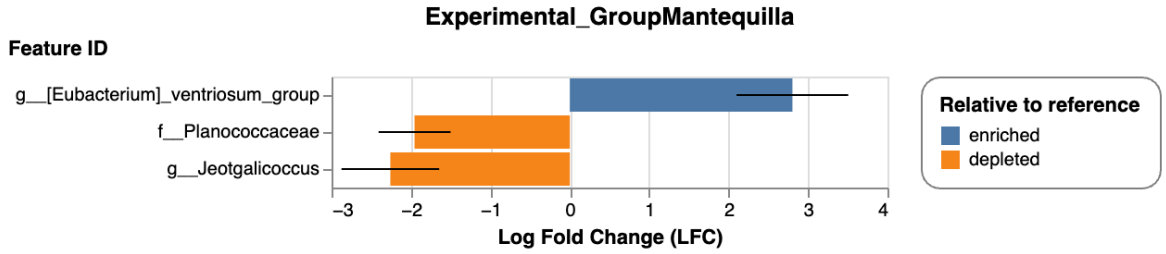

Figure 28. Differential abundance of microbial taxa in the Mantequilla experimental group relative to colorectal cancer group, estimated by ANCOM-BC. Log fold changes (LFC) represent bias-corrected differences in abundance for each taxon. Positive values (blue bars) indicate enrichment; negative values (orange bars) indicate depletion. Error bars denote confidence intervals.

ANCOM-BC analysis of the Nambi treatment group identified several microbial taxa with significant differential abundance relative to the colorectal cancer reference group. Enriched taxa included *Bacteroides pectinophilus* group, which showed the highest positive LFC, suggesting strong enrichment under whole Nambi beans supplementation, followed by Desulfovibrionaceae, *Gastranaerophilales*, *Anaerotruncus*, *Barnesiella*, Bacteroidia, *Fourniella*. Depleted taxa with a LFC of about -2 included Eggerthellaceae, Planococcaceae, consistent with its depletion in other fiber groups, and *Tyzzerella* (Figure 29).

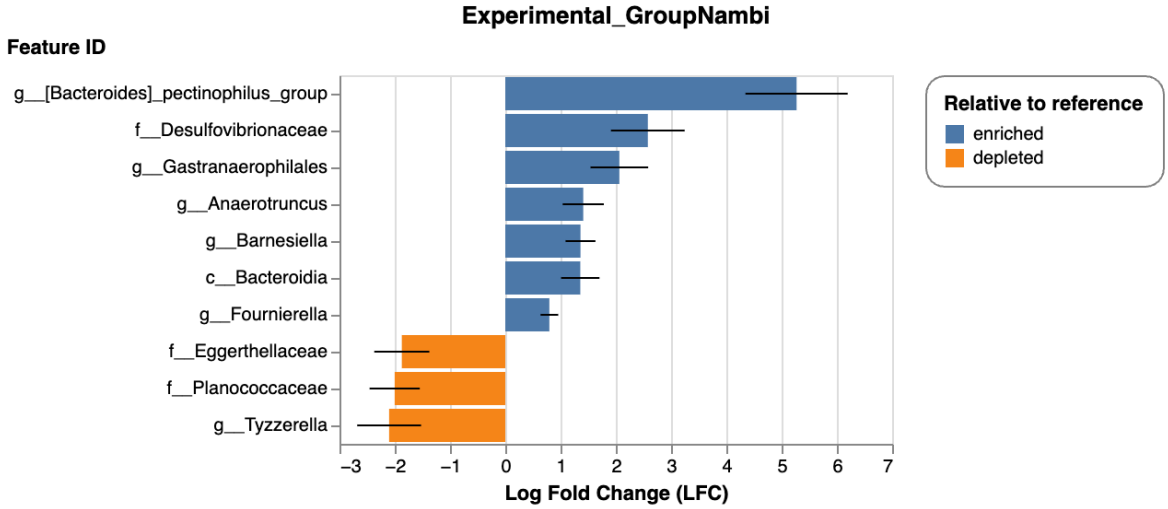

Figure 29. Differential abundance of microbial taxa in the Nambi experimental group relative to colorectal cancer group, estimated by ANCOM-BC. Log fold changes (LFC) represent bias-corrected differences in abundance for each taxon. Positive values (blue bars) indicate enrichment; negative values (orange bars) indicate depletion. Error bars denote confidence intervals.

ANCOM-BC analysis revealed significant shifts in microbial abundance in the Nambi fiber group compared to the colorectal cancer reference group. Enriched taxa included *Bacteroides pectinophilus* group, which showed the highest positive log fold change (LFC ≈ +5), indicating strong enrichment under Nambi fiber supplementation*, Eubacterium ventriosum* group (LFC ≈ +2) and *UCG-010* (LFC ≈ +1). Depleted taxa included Planococcaceae, *Paeniclaligenes*, *Jeotgalicoccus* and *Corynebacterium*, all showing negative LFC values (–2 to –3,5), suggesting reduced abundance under fiber supplementation (Figure 30).

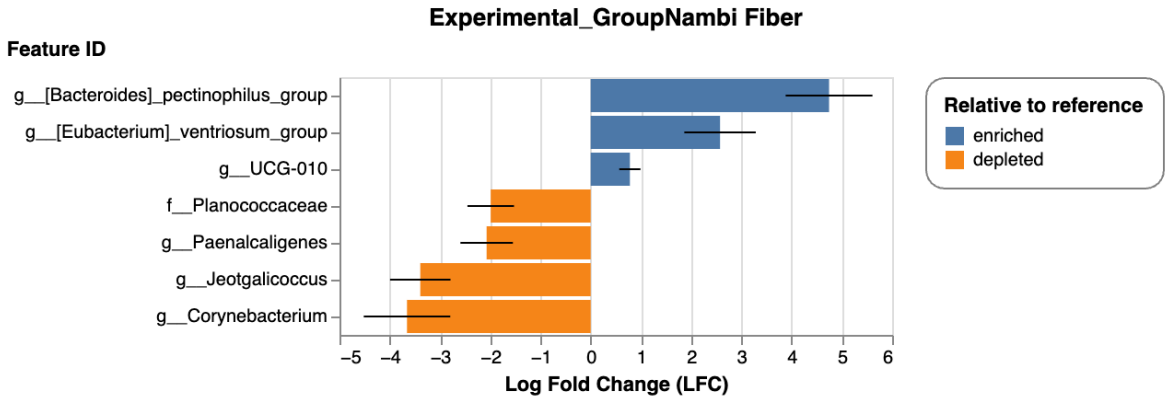

Figure 30. Differential abundance of microbial taxa in the Nambi Fiber experimental group relative to colorectal cancer group, estimated by ANCOM-BC. Log fold changes (LFC) represent bias-corrected differences in abundance for each taxon. Positive values (blue bars) indicate enrichment; negative values (orange bars) indicate depletion. Error bars denote confidence intervals.

B) Fiber Type:

To assess whether whole bean supplementation exerted distinct microbiota effects compared to isolated bean fiber, we performed a differential abundance analysis using ANCOM-BC. With whole bean supplementation enriched taxa included: *Eubacterium ventriosum* group (LFC ≈ +3), Desulfovibrionaceae, *Anaerotruncus*, *Barnesiella* and class Bacteroidia. Depleted taxa included Planococcaceae and *Jeotgalicoccu*s, both showing negative LFC values (≈ –2 to –2.5). In contrast, with whole fiber (soluble and insoluble) supplementation only *Anaeroplasma* was enriched, suggesting a fiber-responsive profile distinct from that observed with whole bean, while *Paenalcaligenes, Jeotgalicoccus*, and

Corynebacterium were significantly depleted (LFC ≈ –2 to –3.5), indicating suppression of low-abundance opportunistic taxa (Figure 31).

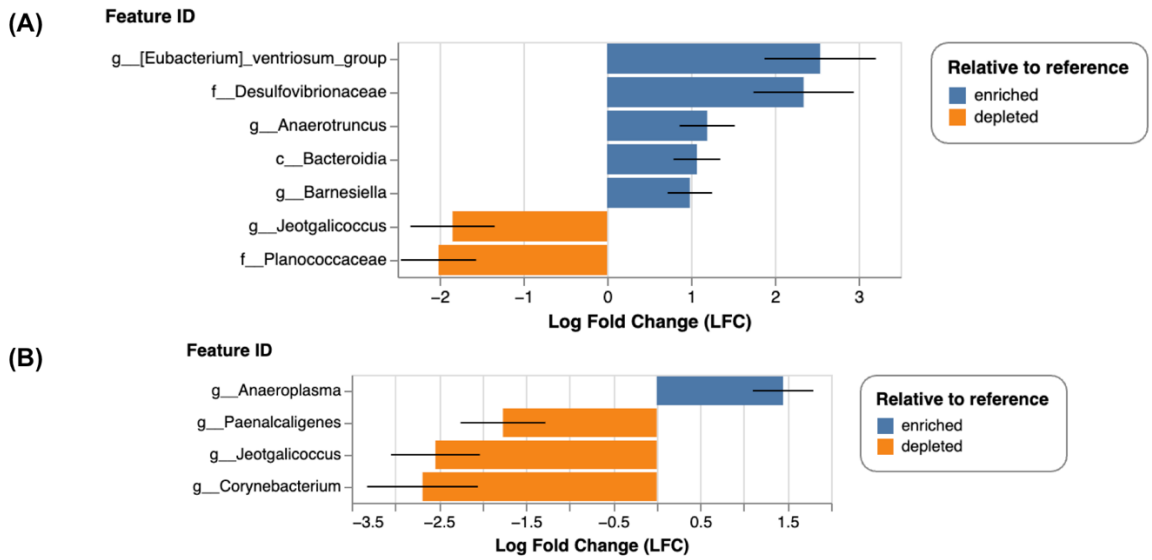

Figure 31. Differential abundance of microbial taxa according to fiber type supplementation relative to colorectal cancer group estimated by ANCOM-BC. (A)Supplementation with cooked whole beans flour including Cabecar, Mantequilla and Nambi; (B) Supplementation with total dietary fiber from beans Cabecar, Mantequilla and Nambi. Log fold changes (LFC) represent bias-corrected differences in abundance for each taxon. Positive values (blue bars) indicate enrichment; negative values (orange bars) indicate depletion. Error bars denote confidence intervals.

C) Diet

To evaluate how different dietary interventions influence gut microbiota composition during colorectal carcinogenesis, we compared the effects of a HFCS diet (Figure 32). Differential abundance analysis using ANCOM-BC showed Enterobacteriaceae (LFC ≈ +6) was the most enriched taxa, followed by *Anaerostipes*, *Acinetobacter*, *Enterococcus*, Oscillospiraceae UCG-007, *Empedobacter, Helicobacter,* Ruminococcaceae *UBA1819 and Anaeroplasma* among others. Depleted taxa included *Corynebacterium, Jeotgalicoccus,* Staphylococcaceae, *Paenalcaligenes and Turicibacter* among others.

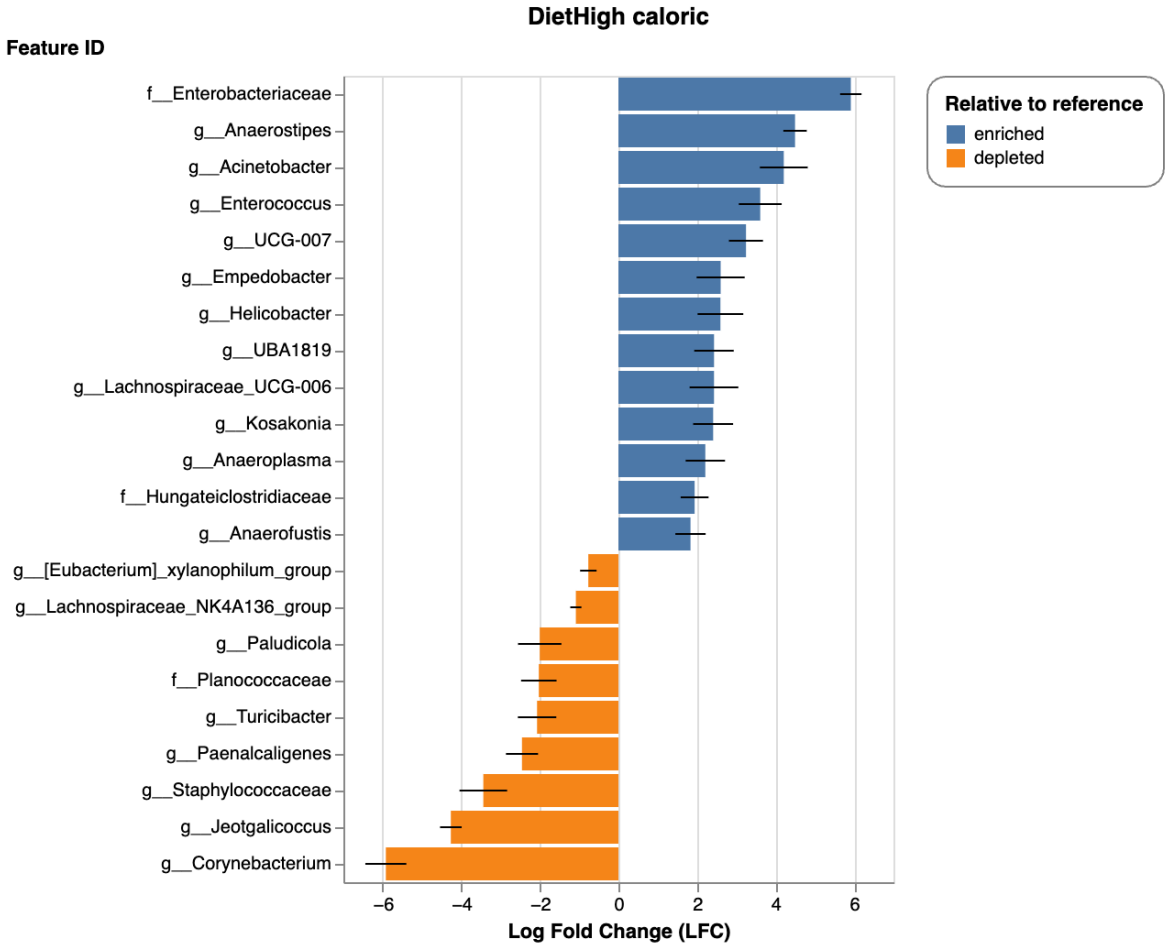

Figure 32. Differential abundance of gut microbial taxa in mice fed a high fructose corn syrup diet compared to the colorectal cancer group, as determined by ANCOM-BC analysis. Bars represent log fold change (LFC) values, with blue indicating taxa enriched under HFCS and orange indicating taxa depleted. Error bars denote confidence intervals. Enriched taxa included Enterobacteriaceae, *Acinetobacter, Enterococcus, Helicobacter, Anaerostipes, Kosakonia, Anaeroplasma*, and others, while depleted taxa included SCFA-producing genera (*Eubacterium xylanophilum* group, Lachnospiraceae NK4A136, *Paludicola*) and opportunistic taxa (Planococcaceae, *Paenalcaligenes, Jeotgalicoccus, Corynebacterium, Turicibacter,* Staphylococcaceae).

D) Treatment

ANCOM-BC analysis was performed across four treatment groups: control (no carcinogenesis), cancer (carcinogenesis without dietary intervention), cancer+fiber (carcinogenesis with cooked whole bean flour and total dietary fiber supplementation), and cancer+fructose (carcinogenesis with high-fructose corn syrup intake). The cancer group was used as the reference condition for all comparisons.

For the control group, no differential features were retained after filtering, and consequently no plot could be generated. In the cancer+fiber group, several taxa were significantly enriched, including *Eubacterium ventriosum*_group, Desulfovibrionaceae, *Helicobacter* with a LFC of ~+2 and Anaeroplasma with a LFC of ~+1.5. Conversely, several taxa were significantly depleted, including Eggerthellaceae (LFC~-1), Planococcaceae (LFC~-2), *Jeotgalicoccus*, and *Corynebacterium* (LFC~-2.5) (Figure 33).

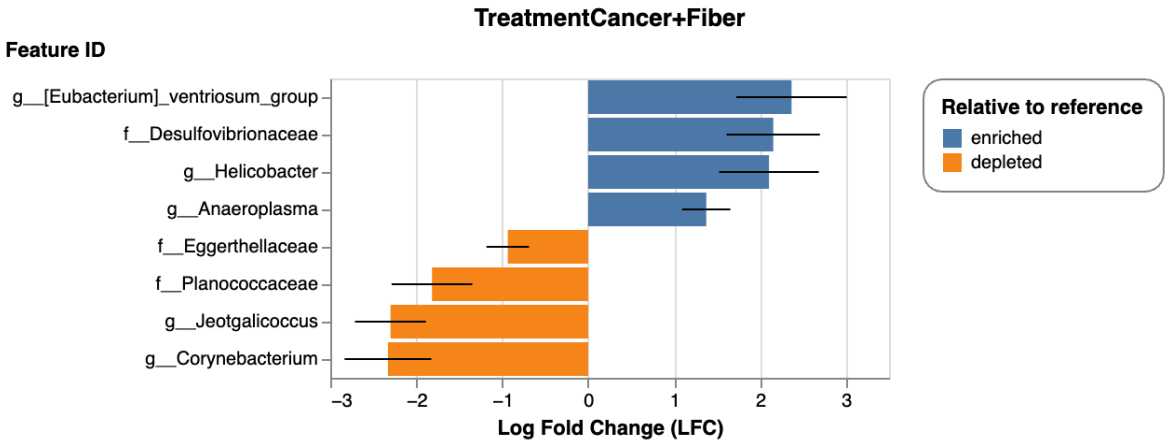

Figure 33. Differentially abundant taxa in the cancer+fiber group relative to cancer reference group, estimated by ANCOM-BC.
Horizontal bars represent log fold change (LFC) values, with positive values indicating enrichment and negative values indicating depletion compared to the cancer group. Blue bars denote taxa enriched under fiber supplementation *Eubacterium ventriosum* group, Desulfovibrionaceae, *Helicobacter, Anaeroplasma*), while orange bars denote taxa depleted (Eggerthellaceae, Planococcaceae, *Jeotgalicoccus, Corynebacterium*). Error bars indicate confidence intervals for each estimate.

The cancer+Fructose group exhibited a distinct microbial profile characterized by significant shifts in both enriched and depleted taxa. Enriched taxa (positive log fold change, LFC > 0) included Enterobacteriaceae (LFC +6), *Anaerostipes* (LFC +4), *Acinetobacter* (LFC +4), *Enterococcus* (LFC +3.5), *Helicobacter* (LFC +2.5), *Kosakonia* (LFC +2), *Anaerofustis* (LFC +2), and *Anaeroplasma* (LFC +2). Conversely, several taxa were significantly depleted (negative log fold change, LFC < 0), including *Eubacterium xylanophilum* group (LFC –2.2), Lachnospiraceae NK4A136 (LFC –2.0), *Paludicola* (LFC –1.8), *Planococcaceae* (LFC –2.5), *Turicibacter* (LFC –2.3), *Paenalcaligenes* (LFC –2.1), *Staphylococcaceae* (LFC –3.0), *Jeotgalicoccus* (LFC –4.0), and *Corynebacterium* (LFC –6.0) (Figure 34).

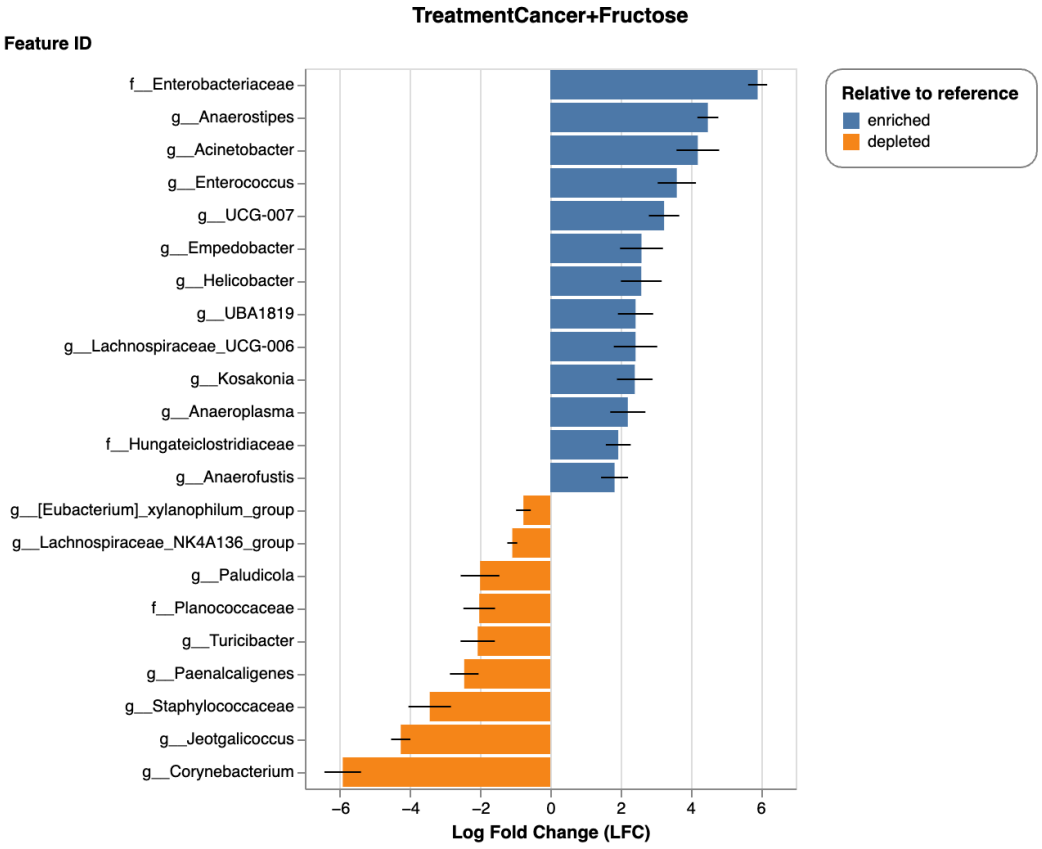

Figure 34. Differentially abundant taxa in the cancer+fructose group relative to cancer reference group, estimated by ANCOM-BC. Horizontal bars represent log fold change (LFC) values, with positive values indicating enrichment and negative values indicating depletion compared to the cancer group. Blue bars denote taxa enriched under HFCS supplementation while orange bars denote taxa depleted. Error bars indicate confidence intervals for each estimate.

The generalized mixed effects model (GLMM) with a Poisson distribution was applied to normalized read counts for each bacterial genera across treatments and time points. This approach allows visualization of how microbial read counts evolve over time under different dietary and carcinogenic conditions, while controlling repeated measures and variability across samples. Temporal comparisons within treatments revealed distinct trajectories across the six genera

To highlight temporal dynamics within each treatment group, the initial analysis was conducted using fixed groups (Figure 35). *Lactobacillus* read counts increased steadily in the CRC and HFCS groups, while it decreased in the Mantequilla, Mantequilla Fiber, and Nambi Fiber groups. The Nambi group showed transient increases of *Lactobacillus* at weeks 3 and 9 before returning to baseline at week 12, whereas Cabecar Fiber displayed a consistent increase throughout the experiment. *Bifidobacterium* decreased in the control group, remained stable in CRC, and fluctuated in HFCS with an early rise followed by decline and stabilization. It decreased steadily in the Mantequilla and Mantequilla Fiber groups. The Nambi group showed transient increases before declining at week 12, and both Nambi Fiber and Cabecar Fiber decreased overall, with Cabecar Fiber moderately higher at the end. *Roseburia* showed variable patterns, with the control group increasing at week 12 compared to baseline, CRC, HFCS, and Cabecar Fiber maintaining increasing trends, Mantequilla and Mantequilla Fiber showing moderate variation, Nambi increasing at weeks 3 and 9, and Nambi Fiber rising sharply at week 3 but declining at week 9. *Ruminococcus* exhibited non-monotonic changes in HFCS, while fiber treatments showed clearer temporal separation. Mantequilla group increased in later weeks; Cabecar Fiber and Nambi Fiber displayed the strongest temporal effects, and Nambi and Mantequilla Fiber showed intermediate variation. Lachnospiraceae NK4A136 revealed increases in Nambi Fiber and Cabecar Fiber at week 3, while other groups decreased. By weeks 9 and 12, all groups except HFCS increased compared to baseline, with Nambi Fiber and Cabecar Fiber maintaining consistent increases across the experiment. *Helicobacter* showed the highest read counts at week 1, followed by a sharp decline at week 3 and persistently low values thereafter, with only a small transient increase in HFCS at week 9. The charts of this analysis applied to the rest of the genera are in the appendix A section.

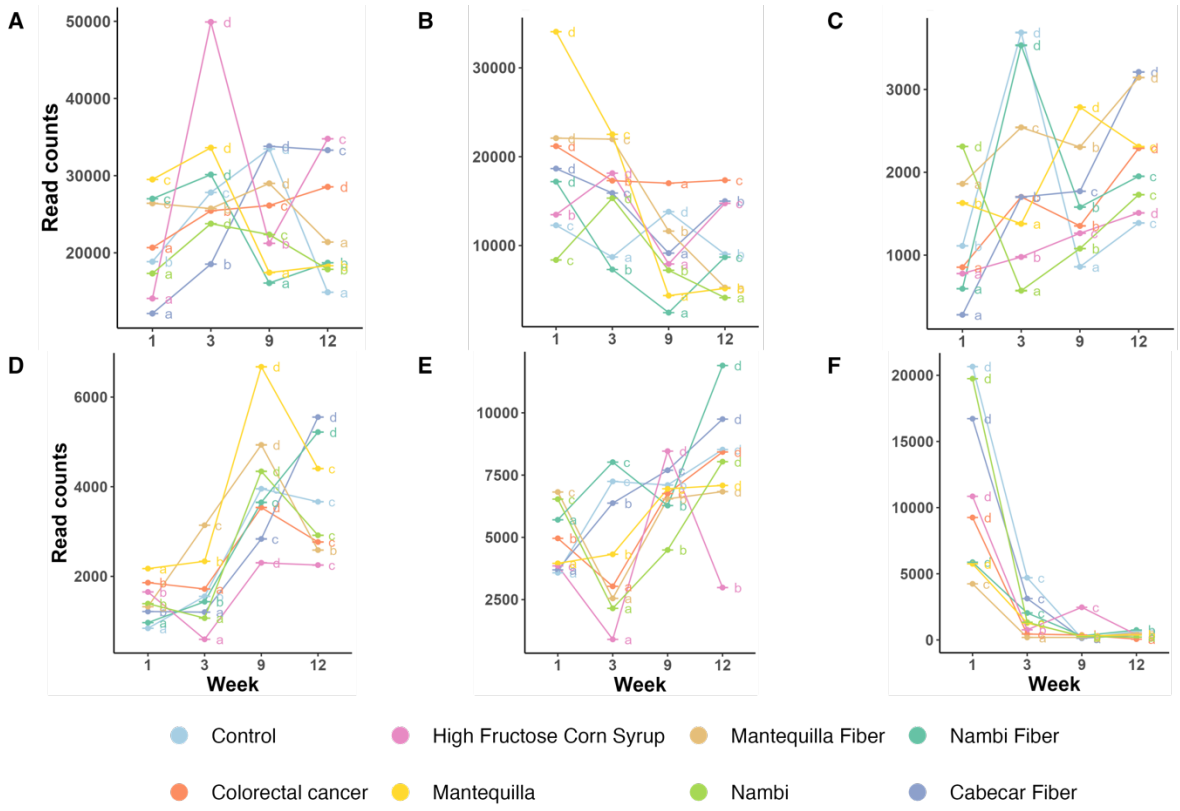

Figure 35. Temporal changes in normalized read counts of selected gut bacterial genera in Wistar rats microbiota under different dietary interventions. Genera analyzed include (A) *Lactobacillus*, (B) *Bifidobacterium* (C) *Roseburia,* (D) *Ruminococcus*, (E) Lachnospiraceae NK4A136, and (H) *Helicobacter*. Read counts were modeled using a generalized mixed effects model (GLMM) with a Poisson distribution, normalized by total reads. Deviance analysis tested the effects of treatment and time, followed by pairwise Z-tests. Statistical differences from the previous timepoint are indicated by compact letter display (CLD): groups sharing the same letter are not significantly different, while distinct letters denote significant differences. Graphs are presented as fixed groups, comparing timepoints, to highlight temporal dynamics within each treatment. Treatments include Control, Colorectal cancer, High Fructose Corn Syrup, Mantequilla, Mantequilla Fiber, Nambi, Nambi Fiber, and Cabecar Fiber.

Cross-sectional comparisons at fixed weeks highlighted increasing separation among treatments as the study progressed (Figure 36). For *Lactobacillus*, groups overlapped at week 1, but by week 12 CRC and HFCS displayed the highest read counts, while fiber supplemented- groups clustered lower, with Cabecar Fiber consistently higher than other fibers. *Bifidobacterium* showed clearer differences at week 3, with CRC and HFCS higher than fiber groups. At week 9, separation was more pronounced, and by week 12 CRC, HFCS, and Cabecar Fiber maintained elevated values, while other treatments clustered

separately. *Roseburia* exhibited progressive separation, with CRC consistently higher, HFCS, Control, and Nambi lower by week 12, and fiber interventions such as Cabecar Fiber, Mantequilla Fiber, and Mantequilla showing higher values at later weeks. *Ruminococcus* were similar at week 1, but by week 3 HFCS was lower and Mantequilla Fiber higher. The greatest separation occurred on week 9, when Mantequilla and fiber groups were higher than Control and HFCS. At week 12, Cabecar Fiber and Nambi Fiber showed the highest values, while HFCS remained among the lowest. Lachnospiraceae NK4A136 showed progressive separation, with Mantequilla and Mantequilla Fiber lower by week 12, Nambi Fiber and Cabecar Fiber maintaining higher read counts, and HFCS significantly lower than all other groups. *Helicobacter* differed markedly at week 1, with Control and Nambi highest, Cabecar Fiber intermediate, and CRC and HFCS lower. By week 3, counts dropped sharply across treatments, reducing differences. At week 9, most groups were near baseline, with HFCS showing a modest relative increase, while by week 12 statistical differences persisted, but overall abundances remained low. The charts of this analysis applied to the rest of the genera are in the appendix A section.

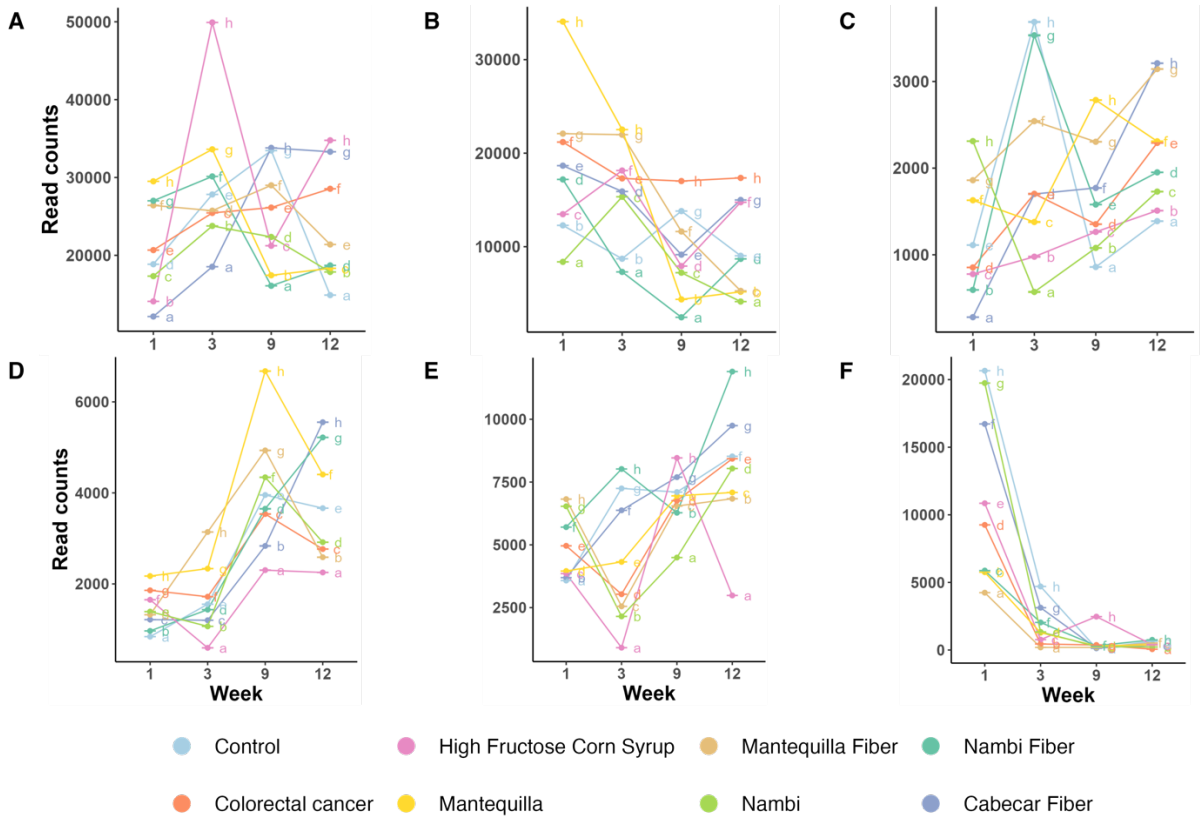

Figure 36. Normalized read counts of selected gut bacterial genera in Wistar rats under different dietary treatments, compared across groups at fixed timepoints to highlight cross-sectional differences among experimental groups at each sampling week. Read counts were modeled using a generalized mixed effects model (GLMM) with a Poisson distribution, normalized by total reads. Deviance analysis tested the effects of treatment and time, followed by pairwise Ztests. Statistical differences are indicated by compact letter display (CLD): groups sharing the same letter are not significantly different, while distinct letters denote significant differences. Genera analyzed include (A)*Lactobacillus*, (B)*Bifidobacterium*, (C)*Roseburia,* (D)*Ruminococcus,* (E)Lachnospiraceae NK4A136, and (H) *Helicobacter*. Treatments include Control, Colorectal cancer (CRC), High Fructose Corn Syrup (HFCS), Mantequilla, Mantequilla Fiber, Nambi, Nambi Fiber, and Cabecar Fiber.

CHAPTER V. DISCUSSION

Colorectal cancer (CRC) poses a significant public health challenge worldwide, with a shift in its epidemiology evident in recent decades. While the incidence has declined among older adults due to enhanced screening and preventive strategies, a worrisome increase has been observed among younger populations under 50 years of age. This early-onset CRC trend is particularly concerning because it often presents at more advanced stages and with aggressive biological features. This phenomenon is primarily influenced by lifestyle and dietary modifications (Gupta et al., 2024). An increase in the consumption of processed foods, refined sugars, and HFCS has coincided with a decrease in the consumption of traditional, fiber rich foods such as beans, whole grains, and autochthonous staples (Caceres-Matos et al., 2024; Varre et al., 2025). Beans have historically constituted a cornerstone of the diet in Costa Rica and throughout the Latin American continent. They provide affordable access to resistant starch, non-starch polysaccharides, and polyphenols. The observed decline in their consumption can be attributed to a more widespread nutritional transition towards dietary patterns reminiscent of those prevalent in Westernized societies. This dietary shift may, in turn, contribute to the increasing prevalence of CRC in younger demographics. Therefore, it is imperative to comprehend the way these dietary modifications affect the composition of the gut microbiota and the development of colorectal carcinogenesis.

To address this issue, the present study employed a Wistar rat model of colorectal carcinogenesis induced with DMH/DSS. This model was selected for its reproducibility, and its ability to mimic both the histological and the molecular alterations characteristic of human colorectal cancer (Arigesavan & Sudhandiran, 2015; Kinjo et al., 2006; Onose et al., 2003). Although many microbiome studies use AOM/DSS protocols (Tanaka, 2009; Tanaka et al., 2003), the DMH/DSS model allows controlled induction of carcinogenic stress while preserving physiological stability when appropriately dosed. The experimental design included dietary interventions with total bean fiber and cooked whole bean flour from native Costa Rican varieties, and HFCS supplementation as a condition to mimic a Westernized diet.

The rats showed normal health and growth trajectories across groups validating the experiment. No signs of malnutrition or dysbiosis were observed during the 12 weeks of this study. The HFCS group showed lower food intake but increased water intake, consistent with

the osmotic load of the sugar solution and similar to previous reports where HFCS consumption increased fluid intake while maintaining body weight (Meyers et al., 2017). Fiber-rich diets produced overlapping intake trajectories, likely reflecting increased satiety. The observed physiological stability in Wistar rats throughout the experiment underscores its suitability as a model for colorectal carcinogenesis.

Fiber retains water in the feces, improving their transit across the colon. Evidence from previous studies using rodent colorectal carcinogenesis models indicates that excessive fiber intake can substantially alter gut microbiota composition. High-fiber diets are known to increase SCFAs production and reshape microbial communities, often in ways that reduce carcinogenesis risk (Bestari et al., 2023; Donohoe et al., 2015). However, when administered at very high doses, soluble fiber may exert unintended pressures to the microbiota. Reports have shown that excessive fiber can reduce microbial diversity, eliminate commensal and probiotic taxa, and favor the expansion of pathobionts. These changes are frequently accompanied by alterations in bile acid metabolism, which can stimulate epithelial proliferation and activate oncogenic signaling pathways (J. Yang et al., 2024). The results obtained in this study demonstrate that the bean fiber supplementation in this model was not excessive. The supplementation was well tolerated, did not induce major shifts in microbial composition, and did not altered taxa in a manner consistent with fiber overload. Instead, the observed feeding patterns and microbiota outcomes suggest that the dietary fiber fraction modulated intake behavior without compromising microbial diversity or systemic stability.

The temporal trajectory of microbiota maturation was also evident in this experiment, with early developmental stages characterized by lower richness and later stabilization of SCFA-producing families, consistent with human and rodent microbiome development (Hanski et al., 2024; Pantoja-Feliciano et al., 2013). Fiber supplemented groups followed similar developmental patterns, suggesting support of natural ecological maturation rather than disruption.

Wistar rats harbor a gut community dominated by Bacteroidota and Bacillota with a consistent set of carbohydrate-fermenting taxa that support the high-fiber, plant-polysaccharide processing typical of rodent chow-based diets. Dominant families included Lactobacillaceae, Lachnospiraceae, and Bifidobacteriaceae. Also, genera such as *Lactobacillus, Bifidobacterium*, and *Prevotella* were among the most abundant. Importantly,

the native microbial community of the rats contained both fiber-fermenting bacteria (e.g., *Bacteroides, Lactobacillus, Prevotella*) and SCFA producers (e.g., *Eubacterium, Ruminococcus, Roseburia, Blautia*). These results are consistent with previous studies that reported that the core microbiota of the large intestine of healthy rats include anaerobic bacteria from Lachnospiraceae and Ruminococcaceae (D. Li et al., 2017). Also, other less abundant but relevant bacterial families such as Bacteroidaceae, Clostridiales, Helicobacteraceae, Prevotellaceae were detected, similar to other previous reports (Nagpal et al., 2018). In line with the findings of the study of Brooks et al., the *Lactobacillus* was confirmed as the most abundant bacterial genus in the Wistar rat feces (Brooks et al., 2011).

Although the gut microbiome of rats and humans differ taxonomically, they share functional microbial guilds capable of fermenting complex carbohydrates and producing SCFAs. This functional similarity is more relevant than exact taxonomic overlap when studying dietary fiber effects (D. Li et al., 2017; Nagpal et al., 2018). Pooled fiber-intervention analyses show that different fibers drive distinct but functionally overlapping butyrate-producing consortia, illustrating functional redundancy and strong dependence on baseline microbiota (Van-Wehle & Vital, 2024). In the present study, the stability of the baseline gut microbiota across experimental groups suggests that the subsequent microbial divergence was driven by dietary ecological selection rather than pre-existing differences.

A significant challenge in rodent carcinogenesis models is the presence of systemic inflammation and dysbiosis, which complicates the distinction between dietary influences and disease effects. In the present study, however, carcinogen exposure did not produce any evident systemic deterioration and did not generate significant reductions in microbial diversity or broad compositional disruption. In models exhibiting robust inflammation, dysbiosis has been identified as a pivotal factor influencing both tumor and microbial outcomes(Ahmad Kendong et al., 2021; Janney et al., 2020; C. Yang et al., 2024). Unlike these models, this design maintained a core microbiota capable of preserving fermentative lineages even under carcinogenic stress. This resilience of the microbiota allowed us to attribute observed microbial shifts primarily to dietary interventions rather than systemic illness or inflammation. The present findings underscore the value of Wistar rats in studying

diet–microbiota interactions in CRC. They provide further evidence of how this is a physiologically stable background that avoids confounding systemic impairment.

Although the overall composition of the gut microbiota remained stable, dietary intervention with bean fiber and bean flour promoted the enrichment of relevant fermentative lineages, allowing exploration of their functional implications in SCFA production and in the modulation of inflammatory responses. Bean fiber and whole bean flour supplementation enriched fermentative lineages such as Muribaculaceae, Ruminococcaceae, Lachnospiraceae, and Prevotellaceae, all associated with SCFA production and anti-inflammatory effects. Protective taxa including *Bifidobacterium, Lactobacillus, Turicibacter*, and *Eubacterium ventriosum* were selectively promoted. Comparable studies demonstrated that cooked black bean consumption enriched Clostridia-related fermenters and improved metabolic and inflammatory markers (Sánchez-Tapia et al., 2020). Although the specific taxa identified in our dataset differ, likely due to methodological and taxonomic resolution differences, the ecological pattern is consistent across investigations. Beans provide complex substrates such as resistant starch and non-starch polysaccharides that selectively enrich carbohydrate fermenters, thereby supporting SCFA mediated host benefits (Lutsiv et al., 2022).

The comparison between whole bean flour and whole bean fiber supplementation revealed that both interventions produced similar outcomes, suggesting that the fiber fraction was the main determinant of microbial modulation. However, native bean varieties such as Cabecar and Nambi appeared to support higher relative abundance of taxa associated with fiber fermentation and SCFA production. These findings underscore the importance of considering both isolated fiber fractions and whole food sources when evaluating dietary interventions in carcinogenesis models. A notable enriched lineage with whole bean flour supplementation was the *Eubacterium ventriosum* group, a Gram-positive anaerobe from the family Lachnospiraceae. This lineage is recognized as a prominent producer of SCFAs, which have been demonstrated to support epithelial integrity and gut health. Its enrichment under bean supplementation aligns with previous evidence linking this genus to reduced risk of IBD and UC (B. Liu et al., 2022).

Polyphenols are plant-derived compounds, classified as secondary metabolites or phytonutrients, that can be divided into several categories. The main categories are phenolic

acids, flavonoids, lignans and stilbens (Quirós-Sauceda et al., 2014). They can act as modulators of gut microbiota, and their interaction with dietary fiber is particularly relevant. Although fiber and polyphenols are distinct compounds, in whole foods they are structurally bound within the plant cell wall matrix. Furthermore, fiber can act as a carrier for non-extractable polyphenols, which remain trapped or chemically bonded to cellulose, hemicellulose, and pectin (Jakobek & Matić, 2019). This natural association means that fiber intake often delivers polyphenols to the colon, where they can be easily uptake by fermenters and absorbed by the epithelial gut cells. Indeed, daily polyphenol consumption has been linked to enrichment of taxa such as *Lactobacillus, Bacteroides, Enterococcus, Eubacterium ventriosum* (Vita et al., 2024) and *Akkermansia muciniphila* (Soheilipour et al., 2025; Van Buiten et al., 2024). Thus, the enrichment of *Eubacterium ventriosum* with bean fiber supplementation can possibly reflect a combined fiber–polyphenol effect, where the structural binding of polyphenols to bean fiber enhances the selective promotion of beneficial fermenters. This highlights the relevance of bean fiber supplementation, in which fiber and phytochemicals act synergistically to foster an anti-inflammatory microbial profile.

Another important observation of the fiber-associated supplementation was the depletion of taxa that can act as opportunists or inflammation-associated lineages in dysbiosis contexts. The depletion of Eggerthellaceae and the reductions observed in Planococcaceae, Jeotgalicoccus, and *Corynebacterium* suggest that bean fiber supplementation may reduce ecological opportunities for taxa that thrive under oxidative stress, epithelial disruption, or altered substrate availability (Cai et al., 2025; Elmagzoub et al., 2024; Y.-C. Shi et al., 2019; Tian et al., 2021). From a biological viewpoint, suppression of these lineages may matter because colorectal carcinogenesis is facilitated by cycles of epithelial damage, local immune activation, and altered nutrient availability (e.g., increased nitrate or oxygen diffusion into the lumen) that advantage facultative anaerobes and inflammation-adapted taxa (El Tekle et al., 2024; Hanus et al., 2021; Lamaudière et al., 2023). Diets rich in complex carbohydrates can counteract this process by supporting obligated anaerobic fermenters and maintaining a low-oxygen, SCFA-rich environment that favors barrier integrity and immune tolerance.

The enrichment of *Desulfovibrionaceae* in the fiber-supplemented groups requires context-dependent interpretation. As sulfate-reducing bacteria (SRB), members of this family produce hydrogen sulfide (H_2S), which at high concentrations has been linked to

mucosal injury, inflammation, and genotoxicity (Yazici et al., 2017). However, the impact of sulfate reducers is strongly influenced by sulfur availability, mucin dynamics, host detoxification capacity, and interactions with other microbial fermenters (Wolf et al., 2022). In a fiber-rich environment that promotes SCFAs production—particularly butyrate—moderate increases in *Desulfovibrionaceae* may reflect shifts in fermentation networks rather than a direct pro-tumorigenic signal. Importantly, taxa such as *Desulfovibrio* rely on electron donors (e.g., hydrogen and lactate) generated by primary fermenters, indicating that their abundance is shaped by community-level cross-feeding rather than direct fiber utilization (Mukhopadhya & Louis, 2025). Overall, these findings highlight that individual taxa should not be interpreted in isolation; biological outcomes depend on the collective metabolic activity of the microbial consortium (G. Li et al., 2024; Shen et al., 2023; Yue et al., 2022). Without functional measurements—such as luminal H_2S concentrations, sulfur flux, or inflammatory markers—it is not possible to conclude whether this enrichment represents a detrimental, neutral, or adaptive response.

In contrast to bean fiber, HFCS supplementation fostered a pro inflammatory, pro carcinogenic microbial profile. Fructose rich diets are known to increase intestinal permeability, alter microbial metabolism, and enhance tumor growth in experimental mouse models showing that HFCS directly accelerates intestinal tumorigenesis (Goncalves et al., 2019). Enrichment of Enterobacteriaceae, *Enterococcus, Helicobacter, Acinetobacter,* and *Kosakonia* was observed (Cheng et al., 2020), alongside depletion of protective fermenters such as Lachnospiraceae NK4A136 and *Eubacterium xylanophilum* (Cheng et al., 2020). This profile is consistent with sugar-rich diets that favor facultative anaerobes, impair barrier function, and promote carcinogenesis. Although *Anaerostipes*, a butyrate producer, was enriched under HFCS, its presence did not restore protective metabolic balance, underscoring that fiber related protection requires a supportive consortium rather than isolated taxa (Donohoe et al., 2015).

Helicobacter was another taxon enriched under HFCS that warrants attention. Multiple mouse models demonstrate that *Helicobacter* species can promote or modulate colorectal tumorigenesis, often in interaction with host genetics and the broader microbiota (Daniel et al., 2017; Dingemanse et al., 2015; Fox et al., 2011; Maggio-Price et al., 2006; Nagamine et al., 2008; Ralser et al., 2023). Enterohepatic species such as *H. hepaticus* and

H. typhlonius are consistently pro-tumorigenic in murine CRC models, while gastric *H. pylori* can indirectly accelerate intestinal tumorigenesis by reshaping distal microbiota.

Diet strongly influences *Helicobacter* abundance. High-fat or high-fructose diets generally favor its expansion, whereas fiber-rich interventions often reduce it (Jiang et al., 2025; Vratarić et al., 2025). In our study, however, *Helicobacter* was enriched not only in the HFCS group but also in some bean fiber groups. This dual pattern may reflect the complex ecological consequences of fiber fermentation: while fiber promotes beneficial fermenters, it can also alter mucosal conditions or release substrates that opportunistic taxa exploit. Polyphenols bound to bean fiber and fermentation by products may create niches that support *Helicobacter* growth, even within otherwise protective dietary contexts. Thus, the HFCS-associated enrichment likely represents a diet-induced imbalance that enhances pro-inflammatory signaling, while the enrichment in bean fiber groups underscores that fiber interventions can have taxon-specific effects. These findings highlight *Helicobacter* as a diet-responsive genus whose expansion may contribute to a pro-inflammatory, carcinogenesis-promoting environment, while also illustrating the complex ecological outcomes of fiber supplementation.

Finally, the enrichment of *Kosakonia* was noteworthy. Although this genus is typically associated with plants and rarely dominant in the gut, *Kosakonia* has been reported in opportunistic infections (Berinson et al., 2020)(Berinson et al., 2020). Its detection in this colorectal carcinogenesis model appears uncommon in published rodent CRC microbiome literature, suggesting HFCS may select for low abundance, context dependent pathobionts. This finding underscores the importance of longitudinal sampling, as such taxa may be transient or condition specific.

The GLMM analysis demonstrated that changes in bacterial read counts were not random fluctuations, but structured responses associated with both time and diet supplementation. Significant temporal separation among weeks indicates that the gut microbiota evolved along the biological stages of the DMH/DSS carcinogenesis model, from baseline conditions through the inflammatory phase and into the preneoplastic period. However, the magnitude of microbial change depended primarily on treatment: carcinogen exposure alone produced relatively modest and transient alterations, whereas dietary interventions, particularly fiber supplementation, generated clearer and sustained shifts in

bacterial abundance. The significant time-by-treatment interaction further suggests that diet did not simply alter the microbiota immediately but modified its trajectory during tumor development, with fermentative taxa becoming enriched mainly at later stages. Because the Poisson GLMM evaluates count data rather than proportions, these differences reflect true shifts in beneficial fermentative and probiotic-associated genera followed clear dietary patterns rather than carcinogen exposure alone.

Lactobacillus generally declined through time in most groups, a pattern consistent with ecological maturation and competitive replacement within the gut microbiota, as also seen in the control animals. The CRC group maintained relatively stable levels, suggesting that DMH/DSS exposure alone did not strongly suppress this genus. In contrast, HFCS supplementation produced a transient increase compatible with selective expansion of lactic-acid bacteria under simple carbohydrate availability, whereas fiber interventions diverged: Mantequilla Fiber and Nambi Fiber followed the declining trend. However, Cabecar Fiber maintained higher counts. A similar diet-dependent behavior was observed for *Bifidobacterium*, whose abundance was sensitive to substrate composition and carcinogenic exposure. Cabecar Fiber again showed the clearest enrichment, supporting varietal differences in fermentable components capable of sustaining *Bifidobacterium* growth. Evidence from probiotic and dietary studies strongly supports the protective role of *Lactobacillus* and *Bifidobacterium* in colorectal carcinogenesis. Experimental models have shown that *Bifidobacterium* strains can directly inhibit colon cancer cell growth and reduce tumor incidence (Parisa et al., 2020), while *B. longum* supplementation suppresses CRC progression through modulation of gut microbes, with higher abundance of Lachnospiraceae and immune function. *B. longum* could initiate Natural Killer (NK)/Dendritic cells (DC) interactions via DC maturation and the catalytic potential of NK cells to produce interferon-γ (IFN-γ), which proved to contribute to tumor prevention and treatment at the cellular level (Shang et al., 2024). Dietary interventions, such as fiber-rich diets, promote *Lactobacillus* and *Bifidobacterium* abundance and counteract dysbiosis, thereby reducing CRC risk (Bestari et al., 2023). Epidemiological studies further support these findings, with long-term yogurt intake linked to lower CRC incidence, particularly in individuals with higher tumor-associated *Bifidobacterium* abundance (Ugai et al., 2025). Mechanistic reviews confirm that these genera exert protective effects by enhancing SCFAs production, regulating immune

responses, detoxifying carcinogens, and inducing apoptosis in malignant cells (Esfandiari et al., 2024). Collectively, these findings highlighting their translational potential in CRC prevention and management.

These responses were consistent with the broader fermentative community. Fiber-supplemented treatments progressively increased members of Lachnospiraceae and Ruminococcaceae, including *Roseburia, Ruminococcus*, and Lachnospiraceae NK4A136, taxa associated with fiber fermentation and SCFAs production (Y.-J. Kim et al., 2024; M.-R. Wu et al., 2020). In particular, Lachnospiraceae NK4A136 showed sustained enrichment in Nambi Fiber and Cabecar Fiber, supporting its emerging role as a fiber-responsive and potentially protective taxon through SCFA production and bile-acid–related immunomodulation. Conversely, HFCS generally occupied lower statistical groupings for these fermentative organisms, suggesting reduced saccharolytic activity under high simple-sugar intake. Notably, *Helicobacter* exhibited an early peak followed by a sharp decline across treatments, indicating a transient response to the inflammatory DSS phase rather than a persistent tumor-associated pattern.

Together, these findings indicate that the Wistar DMH/DSS model did not generate a uniform dysbiosis but rather a diet-dependent restructuring of microbial metabolism. Fiber type, particularly Cabecar Fiber, selectively supported bifidogenic and butyrate-producing taxa, while HFCS favored lactic-acid bacteria without promoting fermentative consortia. Therefore, the microbial signatures observed during carcinogenesis appear to reflect substrate availability and metabolic cross-feeding more than tumor induction itself, reinforcing the concept that dietary composition can modulate microbial ecological trajectories and potentially influence colorectal cancer progression.

Several limitations should be noted that shape how strongly biological conclusions can be drawn. Fecal sampling provides a valuable window into luminal community dynamics but may underrepresent mucosa-associated microbes that have closer contact with epithelial and immune cells. In carcinogenesis, these mucosa-associated communities can be particularly relevant. Furthermore, 16S profiling provides taxonomic inference but limited direct functional resolution; two communities with similar taxa can differ substantially in gene content and metabolite output. As a result, functional validation through targeted metabolomics (e.g., SCFA quantification), host immune profiling (e.g., Treg/Th17 balance,

IL-18/IL-22 signaling), and histopathological correlation with preneoplastic lesions would strengthen mechanistic interpretation. Finally, some taxa detected as “enriched” include species with divergent biological effects, reinforcing the need for species-level confirmation.

In conclusion, the results of this study demonstrate that dietary composition was a stronger determinant of gut microbial structure during colorectal carcinogenesis than carcinogenic exposure itself, with bean-derived fiber promoting fermentative microbial communities and HFCS favoring inflammation-associated profiles.

CONCLUSIONS

This study addresses the growing concern of EOCRC, particularly in younger populations, and links this trend to dietary transitions marked by increased consumption of processed foods and sugars and reduced intake of beans and other traditional staples. By establishing and validating a DMH/DSS-induced colorectal carcinogenesis Wistar rat model, we demonstrated that this model provides physiological stability and resilience, allowing dietary effects on the gut microbiota to be studied without confounding systemic distress. Importantly, the gut microbiota remained resilient under carcinogenic stress, with DMH/DSS induction not causing major dysbiosis, and bean fiber supplementation avoiding the detrimental effects sometimes linked to excessive fiber intake. Characterization of the basal microbiota confirmed the presence of fiber-fermenting and SCFA-producing taxa, showing strong parallels with the human gut microbiota and supporting the translational relevance of the model.

Cooked whole-bean fiber and total dietary fiber from beans foster fermentative, SCFA producing communities that support epithelial integrity and immune homeostasis, while HFCS promotes opportunistic, inflammation adapted taxa linked to carcinogenesis, underscoring the divergent ecological outcomes of traditional versus Westernized diets. Together, these findings validate the protective role of bean fiber and demonstrate that culturally relevant foods can foster microbial resilience and anti-inflammatory fermentative communities, while HFCS drives pro-carcinogenic profiles. This thesis therefore contributes both mechanistic insights and culturally grounded recommendations for public health nutrition in populations facing dietary transitions, offering a clear path toward integrating traditional dietary practices into modern strategies for colorectal carcinogenesis prevention.

BIBLIOGRAPHY

Ahmad Kendong, S. M., Raja Ali, R. A., Nawawi, K. N. M., Ahmad, H. F., & Mokhtar, N. M. (2021). Gut Dysbiosis and Intestinal Barrier Dysfunction: Potential Explanation for Early-Onset Colorectal Cancer. *Frontiers in Cellular and Infection Microbiology*, *11*, 744606. https://doi.org/10.3389/fcimb.2021.744606

Alzahrani, K. M., Fallatah, S. M., Almehmadi, R. A., Alghamdi, J. S., Alsulaimani, A. I., Alkhaldi, L. M., & Alsuwayhi, A. G. (2022). Colorectal Cancer and Its Screening Among Public in the Western Region of Saudi Arabia. *Cureus*, *14*(7), e27404. https://doi.org/10.7759/cureus.27404

Arigesavan, K., & Sudhandiran, G. (2015). Carvacrol exhibits anti-oxidant and anti-inflammatory effects against 1, 2-dimethyl hydrazine plus dextran sodium sulfate induced inflammation associated carcinogenicity in the colon of Fischer 344 rats. *Biochemical and Biophysical Research Communications*, *461*(2), 314–320. https://doi.org/10.1016/j.bbrc.2015.04.030

Arpaia, N., Campbell, C., Fan, X., Dikiy, S., Van Der Veeken, J., deRoos, P., Liu, H., Cross, J. R., Pfeffer, K., Coffer, P. J., & Rudensky, A. Y. (2013). Metabolites produced by commensal bacteria promote peripheral regulatory T-cell generation. *Nature*, *504*(7480), 451–455. https://doi.org/10.1038/nature12726

Atarashi, K., Tanoue, T., Shima, T., Imaoka, A., Kuwahara, T., Momose, Y., Cheng, G., Yamasaki, S., Saito, T., Ohba, Y., Taniguchi, T., Takeda, K., Hori, S., Ivanov, I. I., Umesaki, Y., Itoh, K., & Honda, K. (2011). Induction of Colonic Regulatory T Cells by Indigenous Clostridium Species. *Science*. (world). https://doi.org/10.1126/science.1198469

Awoyinka, O. A., Ileola, A., Imeoria, C. N., Omonisi, A. E., Oladele, F. C., & Asaolu, M. F. (2016). Comparative Study on Nigerian Wild and Edible Beans in Reversing Incidence of Colon Cancer in Albino Rats. *OALib*, *03*(07), 1–7. https://doi.org/10.4236/oalib.1102708

Beaugerie, L., & Itzkowitz, S. H. (2015). Cancers Complicating Inflammatory Bowel Disease. *New England Journal of Medicine*, *372*(15), 1441–1452. https://doi.org/10.1056/NEJMra1403718

Berinson, B., Bellon, E., Christner, M., Both, A., Aepfelbacher, M., & Rohde, H. (2020). Identification of Kosakonia cowanii as a rare cause of acute cholecystitis: Case report and review of the literature. *BMC Infectious Diseases*, *20*(1), 366. https://doi.org/10.1186/s12879-020-05084-6

Bestari, S. A., Fulyani, F., Kusuma, R. J., & Lestari, E. S. (2023). A diet high in protein and fiber changes the gut microbiota of colorectal cancerrat model. *Food Research*, *7*(3), 221–226. https://doi.org/10.26656/fr.2017.7(3).575

Biarc, J., Nguyen, I. S., Pini, A., Gossé, F., Richert, S., Thiersé, D., Van Dorsselaer, A., Leize-Wagner, E., Raul, F., Klein, J.-P., & Schöller-Guinard, M. (2004). Carcinogenic properties of proteins with pro-inflammatory activity from Streptococcus infantarius (formerly S.bovis). *Carcinogenesis*, *25*(8), 1477–1484. https://doi.org/10.1093/carcin/bgh091

Bonnet, M., Buc, E., Sauvanet, P., Darcha, C., Dubois, D., Pereira, B., Déchelotte, P., Bonnet, R., Pezet, D., & Darfeuille-Michaud, A. (2014). Colonization of the Human Gut by *E. coli* and Colorectal Cancer Risk. *Clinical Cancer Research*, *20*(4), 859–867. https://doi.org/10.1158/1078-0432.CCR-13-1343

Bray, F., Laversanne, M., Sung, H., Ferlay, J., Siegel, R. L., Soerjomataram, I., & Jemal, A. (2024). Global cancer statistics 2022: GLOBOCAN estimates of incidence and mortality worldwide for 36 cancers in 185 countries. *CA: A Cancer Journal for Clinicians*, *74*(3), 229–263. https://doi.org/10.3322/caac.21834

Brooks, S. P. J., McAllister, M., Sandoz, M., & Kalmokoff, M. L. (2011). Culture-independent phylogenetic analysis of the faecal flora of the rat. *Canadian Journal of Microbiology*. (Ottawa, Canada). https://doi.org/10.1139/w03-075

Caceres-Matos, R., Castro-Méndez, A., Domínguez, M., Pabón-Carrasco, D., & Pabón-Carrasco, M. (2024). The Influence of Ultra-Processed Food on Colorectal Cancer: A Systematic Review. *Gastrointestinal Disorders*, *6*(1), 164–179. https://doi.org/10.3390/gidisord6010012

Cahenzli, J., Köller, Y., Wyss, M., Geuking, M. B., & McCoy, K. D. (2013). Intestinal Microbial Diversity during Early-Life Colonization Shapes Long-Term IgE Levels. *Cell Host & Microbe*, *14*(5), 559–570. https://doi.org/10.1016/j.chom.2013.10.004

Cai, P., Yang, Q., Lu, J., Dai, X., & Xiong, J. (2025). Fecal bacterial biomarkers and blood biochemical indicators as potential key factors in the development of colorectal cancer. *mSystems*, *10*(3), e00043-25. https://doi.org/10.1128/msystems.00043-25

Cantarel, B. L., Lombard, V., & Henrissat, B. (2012). Complex Carbohydrate Utilization by the Healthy Human Microbiome. *PLoS ONE*, *7*(6), e28742. https://doi.org/10.1371/journal.pone.0028742

Chandra, H., Sharma, K. K., Tuovinen, O. H., Sun, X., & Shukla, P. (2021). Pathobionts: Mechanisms of survival, expansion, and interaction with host with a focus on Clostridioides difficile. *Gut Microbes*, *13*(1), 1979882. https://doi.org/10.1080/19490976.2021.1979882

Chang, P. V., Hao, L., Offermanns, S., & Medzhitov, R. (2014). The microbial metabolite butyrate regulates intestinal macrophage function via histone deacetylase inhibition. *Proceedings of the National Academy of Sciences*, *111*(6), 2247–2252. https://doi.org/10.1073/pnas.1322269111

Cheng, Y., Ling, Z., & Li, L. (2020). The Intestinal Microbiota and Colorectal Cancer. *Frontiers in Immunology*, *11*, 615056. https://doi.org/10.3389/fimmu.2020.615056

Cheong, Y. J., & Trefely, S. (2025). Divergent roles for propionate and butyrate in colorectal cancer epigenetics. *Nature Metabolism*, *7*(1), 11–13. https://doi.org/10.1038/s42255-024-01186-6

Chung, L., Thiele Orberg, E., Geis, A. L., Chan, J. L., Fu, K., DeStefano Shields, C. E., Dejea, C. M., Fathi, P., Chen, J., Finard, B. B., Tam, A. J., McAllister, F., Fan, H., Wu, X., Ganguly, S., Lebid, A., Metz, P., Van Meerbeke, S. W., Huso, D. L., … Housseau, F. (2018). Bacteroides fragilis Toxin Coordinates a Pro-carcinogenic Inflammatory Cascade via Targeting of Colonic Epithelial Cells. *Cell Host & Microbe*, *23*(2), 203-214.e5. https://doi.org/10.1016/j.chom.2018.01.007

Daniel, S. G., Ball, C. L., Besselsen, D. G., Doetschman, T., & Hurwitz, B. L. (2017). Functional Changes in the Gut Microbiome Contribute to Transforming Growth Factor β-Deficient Colon Cancer. *mSystems*, *2*(5), e00065-17. https://doi.org/10.1128/mSystems.00065-17

De Vos, W. M., Tilg, H., Van Hul, M., & Cani, P. D. (2022). Gut microbiome and health: Mechanistic insights. *Gut*, *71*(5), 1020–1032. https://doi.org/10.1136/gutjnl-2021-326789

Devaux, A., Villéger, R., Roche, G., Diémé, B., Rodrigues, M., Juban, C., Lagrée, M., Venisse, N., Jousse, C., Barnich, N., & Bonnet, M. (2025). L-serine promotes pro-carcinogenic effects of colibactin-producing E. coli. *Gut Microbes*, *17*(1), 2515480. https://doi.org/10.1080/19490976.2025.2515480

Dharwadkar, P., Zaki, T. A., & Murphy, C. C. (2022). Colorectal cancer in younger adults. *Hematology/Oncology Clinics of North America*, *36*(3), 449–470. https://doi.org/10.1016/j.hoc.2022.02.005

Dingemanse, C., Belzer, C., van Hijum, S. A. F. T., Günthel, M., Salvatori, D., Dunnen, J. T. den, Kuijper, E. J., Devilee, P., de Vos, W. M., van Ommen, G. B., & Robanus-Maandag, E. C. (2015). Akkermansia muciniphila and Helicobacter typhlonius modulate intestinal tumor development in mice. *Carcinogenesis*, *36*(11), 1388–1396. https://doi.org/10.1093/carcin/bgv120

Donohoe, D. R., Holley, D., Collins, L. B., Montgomery, S. A., Whitmore, C., Hillhouse, A., Curry, K. P., Renner, S. W., Greenwalt, A., Ryan, E. P., Godfrey, V., Heise, M. T., Threadgill, D. S., Han, A., Swenberg, J. A., Threadgill, D. W., & Bultman, S. J. (2015). *A Gnotobiotic Mouse Model Demonstrates that Dietary Fiber Protects Against Colorectal Tumorigenesis in a Microbiota- and Butyrate–Dependent Manner*.

Donohoe, D. R., Wali, A., Brylawski, B. P., & Bultman, S. J. (2012). Microbial Regulation of Glucose Metabolism and Cell-Cycle Progression in Mammalian Colonocytes. *PLoS ONE*, *7*(9), e46589. https://doi.org/10.1371/journal.pone.0046589

El Tekle, G., Andreeva, N., & Garrett, W. S. (2024). The Role of the Microbiome in the Etiopathogenesis of Colon Cancer. *Annual Review of Physiology*, *86*(1), 453–478. https://doi.org/10.1146/annurev-physiol-042022-025619

Elmagzoub, W. A., Idris, S. M., Elnaiem, M. H. E., Mukhtar, M. E., Eltayeb, E., Bakhiet, S. M., Okuni, J. B., Ojok, L., El Sanousi, S. M., El Wahed, A. A., Gameel, A. A., & Eltom, K. H. (2024). Faecal microbial diversity in a cattle herd infected by Mycobacterium avium subsp. paratuberculosis: A possible effect of production

status. *World Journal of Microbiology and Biotechnology*, *40*(9), 276. https://doi.org/10.1007/s11274-024-04080-1

Esfandiari, F., Bakhshi, B., Shahbazi, T., Derakhshan-nezhad, E., Bahroudi, M., Minaeeian, S., Boustanshenas, M., Alborzi, F., Behboudi, B., & Fazeli, M. S. (2024). Significant difference in gut microbiota Bifidobacterium species but not Lactobacillus species in colorectal cancer patients in comparison with healthy volunteers using quantitative real-time PCR. *PLOS ONE*, *19*(11), e0294053. https://doi.org/10.1371/journal.pone.0294053

Fernández Rojas, R. (2008). *Consumo de frijoles en familias costarricenses y relación con condición geográfica y características de la persona encargada de la preparación. Por Shirley Rodríguez González y Xinia Fernández Rojas.* ResearchGate. https://www.researchgate.net/publication/258762575_Consumo_de_frijoles_en_familias_costarricenses_y_relacion_con_condicion_geografica_y_caracteristicas_de_la_persona_encargada_de_la_preparacion_Por_Shirley_Rodriguez_Gonzalez_y_Xinia_Fernandez_Rojas

Foley, M. H., Cockburn, D. W., & Koropatkin, N. M. (2016). The Sus operon: A model system for starch uptake by the human gut Bacteroidetes. *Cellular and Molecular Life Sciences*, *73*(14), 2603–2617. https://doi.org/10.1007/s00018-016-2242-x

Foster, J. R., & Frost, D. (2018). Chapter 3—The History of the Rat. In A. W. Suttie (Ed.), *Boorman's Pathology of the Rat (Second Edition)* (Second Edition, pp. 7–12). Academic Press. https://doi.org/10.1016/B978-0-12-391448-4.00003-4

Fox, J. G., Ge, Z., Whary, M. T., Erdman, S. E., & Horwitz, B. H. (2011). Helicobacter hepaticus infection in mice: Models for understanding lower bowel inflammation and cancer. *Mucosal Immunology*, *4*(1), 22–30. https://doi.org/10.1038/mi.2010.61

Furusawa, Y., Obata, Y., Fukuda, S., Endo, T. A., Nakato, G., Takahashi, D., Nakanishi, Y., Uetake, C., Kato, K., Kato, T., Takahashi, M., Fukuda, N. N., Murakami, S., Miyauchi, E., Hino, S., Atarashi, K., Onawa, S., Fujimura, Y., Lockett, T., … Ohno, H. (2013). Commensal microbe-derived butyrate induces the differentiation of colonic regulatory T cells. *Nature*, *504*(7480), 446–450. https://doi.org/10.1038/nature12721

Garvey, M. (2024). Intestinal Dysbiosis: Microbial Imbalance Impacts on Colorectal Cancer Initiation, Progression and Disease Mitigation. *Biomedicines*, *12*(4), 740. https://doi.org/10.3390/biomedicines12040740

Ge, J., Yin, X., & Chen, L. (2024). Regulatory T cells: Masterminds of immune equilibrium and future therapeutic innovations. *Frontiers in Immunology*, *15*, 1457189. https://doi.org/10.3389/fimmu.2024.1457189

Goncalves, M. D., Lu, C., Tutnauer, J., Hartman, T. E., Hwang, S.-K., Murphy, C. J., Pauli, C., Morris, R., Taylor, S., Bosch, K., Yang, S., Wang, Y., Van Riper, J., Lekaye, H. C., Roper, J., Kim, Y., Chen, Q., Gross, S. S., Rhee, K. Y., … Yun, J. (2019). High-fructose corn syrup enhances intestinal tumor growth in mice. *Science*, *363*(6433), 1345–1349. https://doi.org/10.1126/science.aat8515

González, S., & Fernandez-Rojas, X. (2015). Prácticas culinarias asociadas al consumo de frijoles en familias costarricenses. *Agronomía Mesoamericana*, *26*, 145. https://doi.org/10.15517/am.v26i1.16937

Gupta, S., May, F. P., & Murphy, C. C. (2024). Birth Cohort Colorectal Cancer (CRC): Implications for Research and Practice. *Clinical Gastroenterology and Hepatology*, *22*(3), 455-469.e7. https://doi.org/10.1016/j.cgh.2023.11.040

Hanski, E., Raulo, A., & Knowles, S. C. L. (2024). Early-life gut microbiota assembly patterns are conserved between laboratory and wild mice. *Communications Biology*, *7*, 1456. https://doi.org/10.1038/s42003-024-07039-y

Hanus, M., Parada-Venegas, D., Landskron, G., Wielandt, A. M., Hurtado, C., Alvarez, K., Hermoso, M. A., López-Köstner, F., & De La Fuente, M. (2021). Immune System, Microbiota, and Microbial Metabolites: The Unresolved Triad in Colorectal Cancer Microenvironment. *Frontiers in Immunology*, *12*, 612826. https://doi.org/10.3389/fimmu.2021.612826

Haydé, V.-C., Ramón, G.-G., Lorenzo, G.-O., Dave, O. B., Rosalía, R.-C., Paul, W., & Guadalupe, L.-P. (2012). Non-digestible fraction of beans (*Phaseolus vulgaris* L.) modulates signalling pathway genes at an early stage of colon cancer in Sprague–Dawley rats. *British Journal of Nutrition*, *108*(S1), S145–S154. https://doi.org/10.1017/S0007114512000785

Janney, A., Powrie, F., & Mann, E. H. (2020). Host–microbiota maladaptation in colorectal cancer. *Nature*, *585*(7826), 509–517. https://doi.org/10.1038/s41586-020-2729-3

Jiang, L., Wu, Q., Lu, Z., Zhang, J., Zhao, D., Liu, D., & Zhang, C. (2025). Fermented broccoli stalk by-product with lactic acid bacteria ameliorates high-fat diet-induced obesity in C57BL/6 mice. *Frontiers in Nutrition*, *12*, 1670009. https://doi.org/10.3389/fnut.2025.1670009

Kato, I., & Sun, J. (2023). Microbiome and diet in colon cancer development and treatment. *Cancer Journal (Sudbury, Mass.)*, *29*(2), 89–97. https://doi.org/10.1097/PPO.0000000000000649

Keum, N., & Giovannucci, E. (2019). Global burden of colorectal cancer: Emerging trends, risk factors and prevention strategies. *Nature Reviews Gastroenterology & Hepatology*, *16*(12), 713–732. https://doi.org/10.1038/s41575-019-0189-8

Kilua, A., Chihiro, H., Han, K.-H., Homma, K., Fukuma, N., Kamitani, T., Suzuki, T., & Fukushima, M. (2020). Whole kidney bean (Phaseolus vulgaris) and bean hull reduce the total serum cholesterol, modulate the gut microbiota and affect the caecal fermentation in rats. *Bioactive Carbohydrates and Dietary Fibre*, *24*, 100232. https://doi.org/10.1016/j.bcdf.2020.100232

Kim, E., Coelho, D., & Blachier, F. (2013). Review of the association between meat consumption and risk of colorectal cancer. *Nutrition Research*, *33*(12), 983–994. https://doi.org/10.1016/j.nutres.2013.07.018

Kim, J., & Lee, H. K. (2022). Potential Role of the Gut Microbiome In Colorectal Cancer Progression. *Frontiers in Immunology*, *12*, 807648. https://doi.org/10.3389/fimmu.2021.807648

Kim, Y.-J., Jung, D.-H., & Park, C.-S. (2024). Important roles of Ruminococcaceae in the human intestine for resistant starch utilization. *Food Science and Biotechnology*, *33*(9), 2009–2019. https://doi.org/10.1007/s10068-024-01621-0

Kinjo, T., Suzui, M., Morioka, T., Nabandith, V., Inamine, M., Kaneshiro, T., Arakaki, J., Nishimaki, T., & Yoshimi, N. (2006). Distribution of preneoplastic lesions and tumors, and beta-catenin gene mutations in colon carcinomas induced by 1,2-dimethylhydrazine plus dextran sulfate sodium. *Journal of Experimental & Clinical Cancer Research: CR*, *25*(1), 89–95.

Kordahi, M. C., Stanaway, I. B., Avril, M., Chac, D., Blanc, M.-P., Ross, B., Diener, C., Jain, S., McCleary, P., Parker, A., Friedman, V., Huang, J., Burke, W., Gibbons, S. M., Willis, A. D., Darveau, R. P., Grady, W. M., Ko, C. W., & DePaolo, R. W. (2021). Genomic and functional characterization of a mucosal symbiont involved in early-stage colorectal cancer. *Cell Host & Microbe*, *29*(10), 1589-1598.e6. https://doi.org/10.1016/j.chom.2021.08.013

Lamaudière, M. T. F., Arasaradnam, R., Weedall, G. D., & Morozov, I. Y. (2023). The Colorectal Cancer Microbiota Alter Their Transcriptome To Adapt to the Acidity, Reactive Oxygen Species, and Metabolite Availability of Gut Microenvironments. *mSphere*, *8*(2), e00627-22. https://doi.org/10.1128/msphere.00627-22

Le, D. T., Kumar, G., Williamson, G., Devkota, L., & Dhital, S. (2024). (Poly)phenols and dietary fiber in beans: Metabolism and nutritional impact in the gastrointestinal tract. *Food Hydrocolloids*, *156*, 110350. https://doi.org/10.1016/j.foodhyd.2024.110350

Lenth, R. V., & Piaskowski, J. (2017). *emmeans: Estimated Marginal Means, aka Least-Squares Means* (p. 2.0.1) [Dataset]. https://doi.org/10.32614/CRAN.package.emmeans

Li, D., Chen, H., Mao, B., Yang, Q., Zhao, J., Gu, Z., Zhang, H., Chen, Y. Q., & Chen, W. (2017). Microbial Biogeography and Core Microbiota of the Rat Digestive Tract. *Scientific Reports*, *7*(1), 45840. https://doi.org/10.1038/srep45840

Li, G., Liu, H., Yu, Y., Wang, Q., Yang, C., Yan, Y., Wang, F., & Mao, Y. (2024). Desulfovibrio desulfuricans and its derived metabolites confer resistance to FOLFOX through METTL3. *eBioMedicine*, *102*, 105041. https://doi.org/10.1016/j.ebiom.2024.105041

Lin, Q., Guan, S.-W., & Yu, H.-B. (2023). Immuno-oncology-microbiome axis of gastrointestinal malignancy. *World Journal of Gastrointestinal Oncology*, *15*(5), 757–775. https://doi.org/10.4251/wjgo.v15.i5.757

Liu, B., Ye, D., Yang, H., Song, J., Sun, X., Mao, Y., & He, Z. (2022). Two-Sample Mendelian Randomization Analysis Investigates Causal Associations Between Gut Microbial Genera and Inflammatory Bowel Disease, and Specificity Causal Associations in Ulcerative Colitis or Crohn's Disease. *Frontiers in Immunology*, *13*, 921546. https://doi.org/10.3389/fimmu.2022.921546

Liu, Z., Zhou, X., Kuang, L., Chen, Q., Zhao, J., Yin, H., Zhou, Z., Liu, X., Liu, D., Wu, S., & Wu, L. (2025). Novel insights into immune-gut microbiota interactions in colorectal cancer: A Mendelian randomization study. *Infectious Agents and Cancer*, *20*(1), 27. https://doi.org/10.1186/s13027-025-00653-3

Long, X., Wong, C. C., Tong, L., Chu, E. S. H., Ho Szeto, C., Go, M. Y. Y., Coker, O. O., Chan, A. W. H., Chan, F. K. L., Sung, J. J. Y., & Yu, J. (2019). Peptostreptococcus anaerobius promotes colorectal carcinogenesis and modulates tumour immunity. *Nature Microbiology*, *4*(12), 2319–2330. https://doi.org/10.1038/s41564-019-0541-3

Louis, P., & Flint, H. J. (2017). Formation of propionate and butyrate by the human colonic microbiota. *Environmental Microbiology*, *19*(1), 29–41. https://doi.org/10.1111/1462-2920.13589

Lutsiv, T., McGinley, J. N., Neil-McDonald, E. S., Weir, T. L., Foster, M. T., & Thompson, H. J. (2022). Relandscaping the Gut Microbiota with a Whole Food: Dose–Response Effects to Common Bean. *Foods*, *11*(8), 1153. https://doi.org/10.3390/foods11081153

Ma, Y., Zhang, Y., Qu, R., Zhou, X., Sun, L., Wang, K., Jiang, C., Zhang, Z., & Fu, W. (2022). Promotion of Deoxycholic Acid Effect on Colonic Cancer Cell Lines In Vitro by Altering the Mucosal Microbiota. *Microorganisms*, *10*(12), 2486. https://doi.org/10.3390/microorganisms10122486

Macia, L., Tan, J., Vieira, A. T., Leach, K., Stanley, D., Luong, S., Maruya, M., Ian McKenzie, C., Hijikata, A., Wong, C., Binge, L., Thorburn, A. N., Chevalier, N., Ang, C., Marino, E., Robert, R., Offermanns, S., Teixeira, M. M., Moore, R. J., … Mackay, C. R. (2015). Metabolite-sensing receptors GPR43 and GPR109A facilitate dietary fibre-induced gut homeostasis through regulation of the inflammasome. *Nature Communications*, *6*(1), 6734. https://doi.org/10.1038/ncomms7734

Maggio-Price, L., Treuting, P., Zeng, W., Tsang, M., Bielefeldt-Ohmann, H., & Iritani, B. M. (2006). *Helicobacter* Infection Is Required for Inflammation and Colon Cancer in Smad3-Deficient Mice. *Cancer Research*, *66*(2), 828–838. https://doi.org/10.1158/0008-5472.CAN-05-2448

Martínez-Ríos, J., López-Pacheco, C. P., García-Zepeda, E. A., & Soldevila, G. (2025). CCR9 shapes the immune microenvironment of colorectal cancer modulating the

balance between intratumoral CD8+ T cell and FoxP3+ Helios+ Treg subpopulations. *PLOS One*, *20*(4), e0321930. https://doi.org/10.1371/journal.pone.0321930

McGillycuddy, M., Warton, D. I., Popovic, G., & Bolker, B. M. (2025). Parsimoniously Fitting Large Multivariate Random Effects in **glmmTMB**. *Journal of Statistical Software*, *112*(1). https://doi.org/10.18637/jss.v112.i01

Meyers, A. M., Mourra, D., & Beeler, J. A. (2017). High fructose corn syrup induces metabolic dysregulation and altered dopamine signaling in the absence of obesity. *PLOS ONE*, *12*(12), e0190206. https://doi.org/10.1371/journal.pone.0190206

Mukhopadhya, I., & Louis, P. (2025). Gut microbiota-derived short-chain fatty acids and their role in human health and disease. *Nature Reviews Microbiology*, *23*(10), 635–651. https://doi.org/10.1038/s41579-025-01183-w

Nagamine, C. M., Sohn, J. J., Rickman, B. H., Rogers, A. B., Fox, J. G., & Schauer, D. B. (2008). *Helicobacter hepaticus* Infection Promotes Colon Tumorigenesis in the BALB/c- *Rag2*$^{-/-}$ *Apc* $^{Min\ /+}$ Mouse. *Infection and Immunity*, *76*(6), 2758–2766. https://doi.org/10.1128/IAI.01604-07

Nagpal, R., Wang, S., Solberg Woods, L. C., Seshie, O., Chung, S. T., Shively, C. A., Register, T. C., Craft, S., McClain, D. A., & Yadav, H. (2018). Comparative Microbiome Signatures and Short-Chain Fatty Acids in Mouse, Rat, Non-human Primate, and Human Feces. *Frontiers in Microbiology*, *9*. https://doi.org/10.3389/fmicb.2018.02897

Nascimento-Gonçalves, E., Mendes, B. A. L., Silva-Reis, R., Faustino-Rocha, A. I., Gama, A., & Oliveira, P. A. (2021). Animal Models of Colorectal Cancer: From Spontaneous to Genetically Engineered Models and Their Applications. *Veterinary Sciences*, *8*(4), 59. https://doi.org/10.3390/vetsci8040059

Nguyen, L. H., Goel, A., & Chung, D. C. (2020). Pathways of Colorectal Carcinogenesis. *Gastroenterology*, *158*(2), 291–302. https://doi.org/10.1053/j.gastro.2019.08.059

Nitsche, U., Zimmermann, A., Späth, C., Müller, T., Maak, M., Schuster, T., Slotta-Huspenina, J., Käser, S. A., Michalski, C. W., Janssen, K.-P., Friess, H., Rosenberg, R., & Bader, F. G. (2013). Mucinous and Signet-Ring Cell Colorectal Cancers Differ from Classical Adenocarcinomas in Tumor Biology and Prognosis. *Annals of Surgery*, *258*(5), 775–783. https://doi.org/10.1097/SLA.0b013e3182a69f7e

Onose, J., Imai, T., Hasumura, M., Ueda, M., & Hirose, M. (2003). Rapid induction of colorectal tumors in rats initiated with 1,2-dimethylhydrazine followed by dextran sodium sulfate treatment. *Cancer Letters*, *198*(2), 145–152. https://doi.org/10.1016/S0304-3835(03)00316-1

Pantoja-Feliciano, I. G., Clemente, J. C., Costello, E. K., Perez, M. E., Blaser, M. J., Knight, R., & Dominguez-Bello, M. G. (2013). Biphasic assembly of the murine intestinal microbiota during early development. *The ISME Journal*, *7*(6), 1112–1115. https://doi.org/10.1038/ismej.2013.15

Parisa, A., Roya, G., Mahdi, R., Shabnam, R., Maryam, E., & Malihe, T. (2020). Anti-cancer effects of Bifidobacterium species in colon cancer cells and a mouse model of carcinogenesis. *PLOS ONE*, *15*(5), e0232930. https://doi.org/10.1371/journal.pone.0232930

Petersen, C., & Round, J. L. (2014). Defining dysbiosis and its influence on host immunity and disease. *Cellular Microbiology*, *16*(7), 1024–1033. https://doi.org/10.1111/cmi.12308

Pignatelli, P., Nuccio, F., Piattelli, A., & Curia, M. C. (2023). The Role of Fusobacterium nucleatum in Oral and Colorectal Carcinogenesis. *Microorganisms*, *11*(9), 2358. https://doi.org/10.3390/microorganisms11092358

Prado, S. B. R. D., Castro-Alves, V. C., Ferreira, G. F., & Fabi, J. P. (2019). Ingestion of Non-digestible Carbohydrates From Plant-Source Foods and Decreased Risk of Colorectal Cancer: A Review on the Biological Effects and the Mechanisms of Action. *Frontiers in Nutrition*, *6*, 72. https://doi.org/10.3389/fnut.2019.00072

Quirós-Sauceda, A. E., Palafox-Carlos, H., Sáyago-Ayerdi, S. G., Ayala-Zavala, J. F., Bello-Perez, L. A., Álvarez-Parrilla, E., De La Rosa, L. A., González-Córdova, A. F., & González-Aguilar, G. A. (2014). Dietary fiber and phenolic compounds as functional ingredients: Interaction and possible effect after ingestion. *Food Funct.*, *5*(6), 1063–1072. https://doi.org/10.1039/C4FO00073K

Ralser, A., Dietl, A., Jarosch, S., Engelsberger, V., Wanisch, A., Janssen, K. P., Middelhoff, M., Vieth, M., Quante, M., Haller, D., Busch, D. H., Deng, L., Mejías-Luque, R., & Gerhard, M. (2023). *Helicobacter pylori* promotes colorectal carcinogenesis by

deregulating intestinal immunity and inducing a mucus-degrading microbiota signature. *Gut*, *72*(7), 1258–1270. https://doi.org/10.1136/gutjnl-2022-328075

Rastall, R. A., Diez-Municio, M., Forssten, S. D., Hamaker, B., Meynier, A., Moreno, F. J., Respondek, F., Stahl, B., Venema, K., & Wiese, M. (2022). Structure and function of non-digestible carbohydrates in the gut microbiome. *Beneficial Microbes*, *13*(2), 95–168. https://doi.org/10.3920/BM2021.0090

Roshandel, G., Ghasemi-Kebria, F., & Malekzadeh, R. (2024). Colorectal Cancer: Epidemiology, Risk Factors, and Prevention. *Cancers*, *16*(8), 1530. https://doi.org/10.3390/cancers16081530

Round, J. L., & Mazmanian, S. K. (2010). Inducible Foxp3^{+} regulatory T-cell development by a commensal bacterium of the intestinal microbiota. *Proceedings of the National Academy of Sciences*, *107*(27), 12204–12209. https://doi.org/10.1073/pnas.0909122107

Sánchez-Tapia, M., Hernández-Velázquez, I., Pichardo-Ontiveros, E., Granados-Portillo, O., Gálvez, A., R Tovar, A., & Torres, N. (2020). Consumption of Cooked Black Beans Stimulates a Cluster of Some Clostridia Class Bacteria Decreasing Inflammatory Response and Improving Insulin Sensitivity. *Nutrients*, *12*(4), 1182. https://doi.org/10.3390/nu12041182

Shah, S. C., Camargo, M. C., Lamm, M., Bustamante, R., Roumie, C. L., Wilson, O., Halvorson, A. E., Greevy, R., Liu, L., Gupta, S., & Demb, J. (2024). The impact of Helicobacter pylori infection and treatment on colorectal cancer in a large, nationwide cohort. *Journal of Clinical Oncology : Official Journal of the American Society of Clinical Oncology*, *42*(16), 1881–1889. https://doi.org/10.1200/JCO.23.00703

Shang, F., Jiang, X., Wang, H., Guo, S., Kang, S., Xu, B., Wang, X., Chen, S., Li, N., Liu, B., & Zhao, Z. (2024). Bifidobacterium longum suppresses colorectal cancer through the modulation of intestinal microbes and immune function. *Frontiers in Microbiology*, *15*, 1327464. https://doi.org/10.3389/fmicb.2024.1327464

Shen, Y., Song, M., Wu, S., Zhao, H., & Zhang, Y. (2023). Plant-Based Dietary Fibers and Polysaccharides as Modulators of Gut Microbiota in Intestinal and Lung Inflammation: Current State and Challenges. *Nutrients*, *15*(15), 3321. https://doi.org/10.3390/nu15153321

Shi, P., Yu, Y., Xie, H., Yin, X., Chen, X., Zhao, Y., & Zhao, H. (2025). Recent advances in regulatory immune cells: Exploring the world beyond Tregs. *Frontiers in Immunology*, *16*, 1530301. https://doi.org/10.3389/fimmu.2025.1530301

Shi, Y.-C., Cai, S.-T., Tian, Y.-P., Zhao, H.-J., Zhang, Y.-B., Chen, J., Ren, R.-R., Luo, X., Peng, L.-H., Sun, G., & Yang, Y.-S. (2019). Effects of Proton Pump Inhibitors on the Gastrointestinal Microbiota in Gastroesophageal Reflux Disease. *Genomics, Proteomics & Bioinformatics*, *17*(1), 52–63. https://doi.org/10.1016/j.gpb.2018.12.004

Silva-Reis, R., Castro-Ribeiro, C., Gonçalves, M., Ferreira, T., Pires, M. J., Iglesias-Aguirre, C. E., Cortés-Martín, A., Selma, M. V., Espín, J. C., Nascimento-Gonçalves, E., Moreira-Pais, A., Neuparth, M. J., Peixoto, F., Rosa, E., Gama, A., Ferreira, R., Oliveira, P. A., & Faustino-Rocha, A. I. (2022). An Integrative Approach to Characterize the Early Phases of Dimethylhydrazine-Induced Colorectal Carcinogenesis in the Rat. *Biomedicines*, *10*(2), Article 2. https://doi.org/10.3390/biomedicines10020409

Smith, P. M., Howitt, M. R., Panikov, N., Michaud, M., Gallini, C. A., Bohlooly-Y, M., Glickman, J. N., & Garrett, W. S. (2013). The microbial metabolites, short chain fatty acids, regulate colonic Treg cell homeostasis. *Science (New York, N.Y.)*, *341*(6145), 10.1126/science.1241165. https://doi.org/10.1126/science.1241165

Soheilipour, M., Noursina, A., Nekookhoo, M., Malekpour, E., Mirzaei, S. A., Shafieyoun, M. H., Rouzbahani, H., Chitsazi, M. R., & Safari, F. (2025). The pathobiont role of Akkermansia muciniphila in colorectal cancer: A systematic review. *BMC Gastroenterology*, *25*(1), 702. https://doi.org/10.1186/s12876-025-04293-0

Stribling, P., & Ibrahim, F. (2023). Dietary fibre definition revisited—The case of low molecular weight carbohydrates. *Clinical Nutrition ESPEN*, *55*, 340–356. https://doi.org/10.1016/j.clnesp.2023.04.014

Tanaka, T. (2009). Colorectal carcinogenesis: Review of human and experimental animal studies. *Journal of Carcinogenesis*, *8*(1), 5. https://doi.org/10.4103/1477-3163.49014

Tanaka, T., Kohno, H., Suzuki, R., Yamada, Y., Sugie, S., & Mori, H. (2003). A novel inflammation-related mouse colon carcinogenesis model induced by azoxymethane

and dextran sodium sulfate. *Cancer Science*, *94*(11), 965–973. https://doi.org/10.1111/j.1349-7006.2003.tb01386.x

Testa, U., Pelosi, E., & Castelli, G. (2018). Colorectal Cancer: Genetic Abnormalities, Tumor Progression, Tumor Heterogeneity, Clonal Evolution and Tumor-Initiating Cells. *Medical Sciences*, *6*(2), 31. https://doi.org/10.3390/medsci6020031

Tian, T., Zhang, X., Luo, T., Wang, D., Sun, Y., & Dai, J. (2021). Effects of Short-Term Dietary Fiber Intervention on Gut Microbiota in Young Healthy People. *Diabetes, Metabolic Syndrome and Obesity: Targets and Therapy*, *Volume 14*, 3507–3516. https://doi.org/10.2147/DMSO.S313385

Tortora, S. C., Bodiwala, V. M., Quinn, A., Martello, L. A., & Vignesh, S. (2022). Microbiome and colorectal carcinogenesis: Linked mechanisms and racial differences. *World Journal of Gastrointestinal Oncology*, *14*(2), 375–395. https://doi.org/10.4251/wjgo.v14.i2.375

Tsoi, H., Chu, E. S. H., Zhang, X., Sheng, J., Nakatsu, G., Ng, S. C., Chan, A. W. H., Chan, F. K. L., Sung, J. J. Y., & Yu, J. (2017). Peptostreptococcus anaerobius Induces Intracellular Cholesterol Biosynthesis in Colon Cells to Induce Proliferation and Causes Dysplasia in Mice. *Gastroenterology*, *152*(6), 1419-1433.e5. https://doi.org/10.1053/j.gastro.2017.01.009

Tudela, H., Claus, S. P., & Saleh, M. (2021). *Next Generation Microbiome Research: Identification of Keystone Species in the Metabolic Regulation of Host-Gut Microbiota Interplay*.

Ugai, S., Liu, L., Kosumi, K., Kawamura, H., Hamada, T., Mima, K., Arima, K., Okadome, K., Yao, Q., Matsuda, K., Zhong, Y., Mizuno, H., Chan, A. T., Garrett, W. S., Song, M., Giannakis, M., Giovannucci, E. L., Zhang, X., Ogino, S., & Ugai, T. (2025). Long-term yogurt intake and colorectal cancer incidence subclassified by Bifidobacterium abundance in tumor. *Gut Microbes*, *17*(1), 2452237. https://doi.org/10.1080/19490976.2025.2452237

Valerin, J. (2020). *INFORME SITUACIONAL GRANOS BASICOS 2019-2022: FRIJOL-MAIZ.* Ministerio de Agricultura y Ganadería de Costa Rica.

Van Buiten, C. B., Seitz, V. A., Metcalf, J. L., & Raskin, I. (2024). Dietary Polyphenols Support Akkermansia muciniphila Growth via Mediation of the Gastrointestinal

Redox Environment. *Antioxidants*, *13*(3), 304. https://doi.org/10.3390/antiox13030304

Van Hul, M., Cani, P. D., Petitfils, C., De Vos, W. M., Tilg, H., & El-Omar, E. M. (2024). What defines a healthy gut microbiome? *Gut*, *73*(11), 1893–1908. https://doi.org/10.1136/gutjnl-2024-333378

Van-Wehle, T., & Vital, M. (2024). Investigating the response of the butyrate production potential to major fibers in dietary intervention studies. *Npj Biofilms and Microbiomes*, *10*(1), 63. https://doi.org/10.1038/s41522-024-00533-5

Varre, J. V., Dustin, M., & Van Vliet, S. (2025). Dietary transformations and health implications in migrant populations: A global perspective. *Frontiers in Nutrition*, *12*, 1623556. https://doi.org/10.3389/fnut.2025.1623556

Vdoviaková, K., Petrovová, E., Maloveská, M., Krešáková, L., Teleky, J., Elias, M. Z. J., & Petrášová, D. (2016). Surgical Anatomy of the Gastrointestinal Tract and Its Vasculature in the Laboratory Rat. *Gastroenterology Research and Practice*, *2016*(1), 2632368. https://doi.org/10.1155/2016/2632368

Vita, A. A., Roberts, K. M., Gundersen, A., Farris, Y., Zwickey, H., Bradley, R., & Weir, T. L. (2024). Relationships between Habitual Polyphenol Consumption and Gut Microbiota in the INCLD Health Cohort. *Nutrients*, *16*(6), 773. https://doi.org/10.3390/nu16060773

von Schillde, M.-A., Hörmannsperger, G., Weiher, M., Alpert, C.-A., Hahne, H., Bäuerl, C., van Huynegem, K., Steidler, L., Hrncir, T., Pérez-Martínez, G., Kuster, B., & Haller, D. (2012). Lactocepin Secreted By Lactobacillus Exerts Anti-Inflammatory Effects By Selectively Degrading Proinflammatory Chemokines. *Cell Host & Microbe*, *11*(4), 387–396. https://doi.org/10.1016/j.chom.2012.02.006

Vratarić, M., Teofilović, A., Vojnović Milutinović, D., Veličković, N., Đmura, G., & Djordjevic, A. (2025). Gut microbiota composition combined with reduced intestinal fatty acid uptake prevents hepatic steatosis in obesity-resistant mice fed a high-fat diet. *Scientific Reports*, *15*(1), 37040. https://doi.org/10.1038/s41598-025-20768-2

Wang, B., Morinobu, A., Horiuchi, M., Liu, J., & Kumagai, S. (2008). Butyrate inhibits functional differentiation of human monocyte-derived dendritic cells. *Cellular Immunology*, *253*(1–2), 54–58. https://doi.org/10.1016/j.cellimm.2008.04.016

Wang, H., Shi, P., Zuo, L., Dong, J., Zhao, J., Liu, Q., & Zhu, W. (2016). Dietary Non-digestible Polysaccharides Ameliorate Intestinal Epithelial Barrier Dysfunction in IL-10 Knockout Mice. *Journal of Crohn's and Colitis*, *10*(9), 1076–1086. https://doi.org/10.1093/ecco-jcc/jjw065

Wang, J., Zhao, Q., Zhang, S., Liu, J., Fan, X., Han, B., Hou, Y., & Ai, X. (2025). Microbial short chain fatty acids: Effective histone deacetylase inhibitors in immune regulation (Review). *International Journal of Molecular Medicine*, *57*(1), 16. https://doi.org/10.3892/ijmm.2025.5687

Wickham, H., Averick, M., Bryan, J., Chang, W., McGowan, L., François, R., Grolemund, G., Hayes, A., Henry, L., Hester, J., Kuhn, M., Pedersen, T., Miller, E., Bache, S., Müller, K., Ooms, J., Robinson, D., Seidel, D., Spinu, V., … Yutani, H. (2019). Welcome to the Tidyverse. *Journal of Open Source Software*, *4*(43), 1686. https://doi.org/10.21105/joss.01686

Wolf, P. G., Cowley, E. S., Breister, A., Matatov, S., Lucio, L., Polak, P., Ridlon, J. M., Gaskins, H. R., & Anantharaman, K. (2022). Diversity and distribution of sulfur metabolic genes in the human gut microbiome and their association with colorectal cancer. *Microbiome*, *10*(1), 64. https://doi.org/10.1186/s40168-022-01242-x

Wu, M.-R., Chou, T.-S., Huang, C.-Y., & Hsiao, J.-K. (2020). *A potential probiotic-Lachnospiraceae NK4A136 group: Evidence from the restoration of the dietary pattern from a high-fat diet*. In Review. https://doi.org/10.21203/rs.3.rs-48913/v1

Wu, N., Yang, X., Zhang, R., Li, J., Xiao, X., Hu, Y., Chen, Y., Yang, F., Lu, N., Wang, Z., Luan, C., Liu, Y., Wang, B., Xiang, C., Wang, Y., Zhao, F., Gao, G. F., Wang, S., Li, L., … Zhu, B. (2013). Dysbiosis Signature of Fecal Microbiota in Colorectal Cancer Patients. *Microbial Ecology*, *66*(2), 462–470. https://doi.org/10.1007/s00248-013-0245-9

Wu, S., Rhee, K.-J., Albesiano, E., Rabizadeh, S., Wu, X., Yen, H.-R., Huso, D. L., Brancati, F. L., Wick, E., McAllister, F., Housseau, F., Pardoll, D. M., & Sears, C. L. (2009). A human colonic commensal promotes colon tumorigenesis via activation of T helper type 17 T cell responses. *Nature Medicine*, *15*(9), 1016–1022. https://doi.org/10.1038/nm.2015

Yang, C., Wusigale, You, L., Li, X., Kwok, L.-Y., & Chen, Y. (2024). Inflammation, Gut Microbiota, and Metabolomic Shifts in Colorectal Cancer: Insights from Human and Mouse Models. *International Journal of Molecular Sciences*, *25*(20), 11189. https://doi.org/10.3390/ijms252011189

Yang, J., Wei, H., Lin, Y., Chu, E. S. H., Zhou, Y., Gou, H., Guo, S., Lau, H. C. H., Cheung, A. H. K., Chen, H., To, K. F., Sung, J. J. Y., Wang, Y., & Yu, J. (2024). High Soluble Fiber Promotes Colorectal Tumorigenesis Through Modulating Gut Microbiota and Metabolites in Mice. *Gastroenterology*, *166*(2), 323-337.e7. https://doi.org/10.1053/j.gastro.2023.10.012

Yang, W., Yu, T., Huang, X., Bilotta, A. J., Xu, L., Lu, Y., Sun, J., Pan, F., Zhou, J., Zhang, W., Yao, S., Maynard, C. L., Singh, N., Dann, S. M., Liu, Z., & Cong, Y. (2020). Intestinal microbiota-derived short-chain fatty acids regulation of immune cell IL-22 production and gut immunity. *Nature Communications*, *11*(1), 4457. https://doi.org/10.1038/s41467-020-18262-6

Yazici, C., Wolf, P. G., Kim, H., Cross, T.-W. L., Vermillion, K., Carroll, T., Augustus, G. J., Mutlu, E., Tussing-Humphreys, L., Braunschweig, C., Xicola, R. M., Jung, B., Llor, X., Ellis, N. A., & Gaskins, H. R. (2017). Race-dependent association of sulfidogenic bacteria with colorectal cancer. *Gut*, *66*(11), 1983–1994. https://doi.org/10.1136/gutjnl-2016-313321

Yu, H., Yang, R., Li, M., Li, D., & Xu, Y. (2025). The role of Treg cells in colorectal cancer and the immunotherapy targeting Treg cells. *Frontiers in Immunology*, *16*, 1574327. https://doi.org/10.3389/fimmu.2025.1574327

Yue, C., Chu, C., Zhao, J., Zhang, H., Chen, W., & Zhai, Q. (2022). Dietary strategies to promote the abundance of intestinal Akkermansia muciniphila, a focus on the effect of plant extracts. *Journal of Functional Foods*, *93*, 105093. https://doi.org/10.1016/j.jff.2022.105093

Zhu, Q., Jin, Z., Wu, W., Gao, R., Guo, B., Gao, Z., Yang, Y., & Qin, H. (2014). Analysis of the Intestinal Lumen Microbiota in an Animal Model of Colorectal Cancer. *PLoS ONE*, *9*(3), e90849. https://doi.org/10.1371/journal.pone.0090849

Zuo, Z., Pang, W., Sun, W., Lu, B., Zou, L., Zhang, D., & Wang, Y. (2023). Metallothionein–Kidney Bean Polyphenol Complexes Showed Antidiabetic Activity in Type 2

Diabetic Rats by Improving Insulin Resistance and Regulating Gut Microbiota. *Foods*, *12*(16), 3139. https://doi.org/10.3390/foods12163139

APPENDIX A

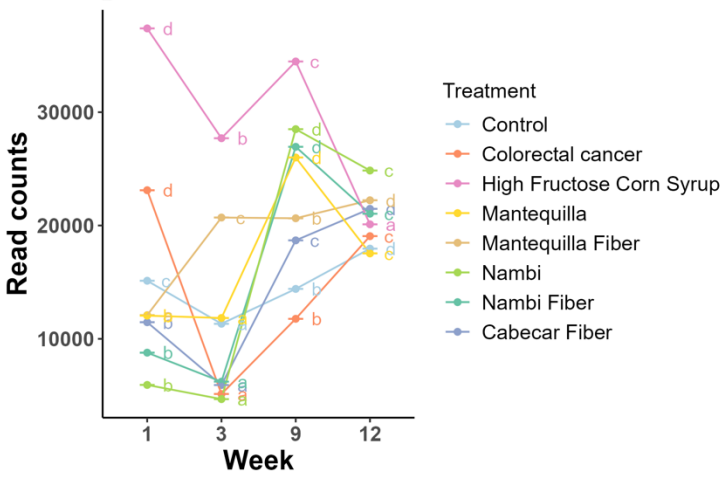

Figure A1. Temporal changes in normalized read counts of *Muribaculaceae.* Read counts were modeled using a generalized mixed effects model (GLMM) with a Poisson distribution, normalized by total reads. Deviance analysis tested the effects of treatment and time, followed by pairwise Z-tests. Statistical differences from the previous timepoint are indicated by compact letter display (CLD): groups sharing the same letter are not significantly different, while distinct letters denote significant differences. Graphs are presented as fixed groups, comparing timepoints, to highlight temporal dynamics within each treatment. Treatments include Control, Colorectal cancer, High Fructose Corn Syrup, Mantequilla, Mantequilla Fiber, Nambi, Nambi Fiber, and Cabecar Fiber.

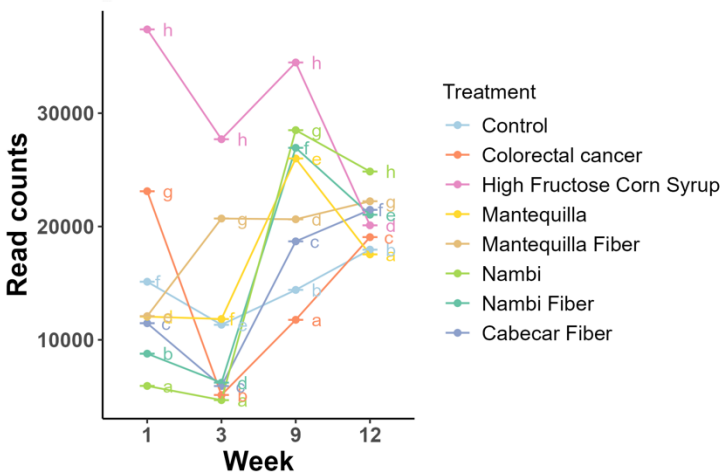

Figure A2. Normalized read counts of *Muribaculaceae* in Wistar rats under different dietary treatments, compared across groups at fixed timepoints to highlight cross-sectional differences among interventions at each sampling week. Read counts were modeled using a generalized mixed effects model (GLMM) with a Poisson distribution, normalized by total reads. Deviance analysis tested the effects of treatment and time, followed by pairwise Ztests. Statistical differences are indicated by compact letter display (CLD): groups sharing the same letter are not significantly different, while distinct letters denote significant differences. Treatments include Control, Colorectal cancer (CRC), High Fructose Corn Syrup (HFCS), Mantequilla, Mantequilla Fiber, Nambi, Nambi Fiber, and Cabecar Fiber.

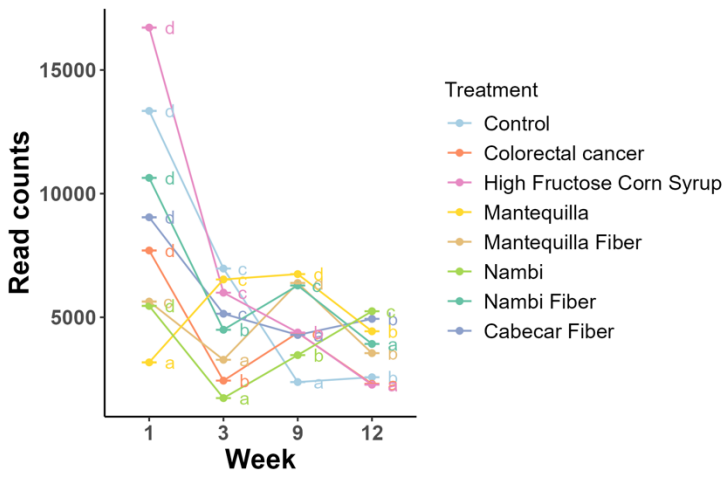

Figure A3. Temporal changes in normalized read counts of Prevotellaceae_UCG-001. Read counts were modeled using a generalized mixed effects model (GLMM) with a Poisson distribution, normalized by total reads. Deviance analysis tested the effects of treatment and time, followed by pairwise Z-tests. Statistical differences from the previous timepoint are indicated by compact letter display (CLD): groups sharing the same letter are not significantly different, while distinct letters denote significant differences. Graphs are presented as fixed groups, comparing timepoints, to highlight temporal dynamics within each treatment. Treatments include Control, Colorectal cancer, High Fructose Corn Syrup, Mantequilla, Mantequilla Fiber, Nambi, Nambi Fiber, and Cabecar Fiber.

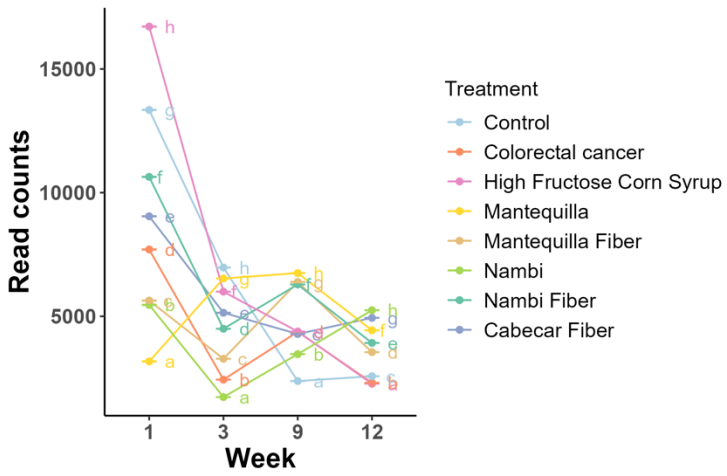

Figure A4. Normalized read counts of Prevotellaceae_UCG-001 in Wistar rats under different dietary treatments, compared across groups at fixed timepoints to highlight cross-sectional differences among interventions at each sampling week. Read counts were modeled using a generalized mixed effects model (GLMM) with a Poisson distribution, normalized by total reads. Deviance analysis tested the effects of treatment and time, followed by pairwise Ztests. Statistical differences are indicated by compact letter display (CLD): groups sharing the same letter are not significantly different, while distinct letters denote significant differences. Treatments include Control, Colorectal cancer (CRC), High Fructose Corn Syrup (HFCS), Mantequilla, Mantequilla Fiber, Nambi, Nambi Fiber, and Cabecar Fiber.

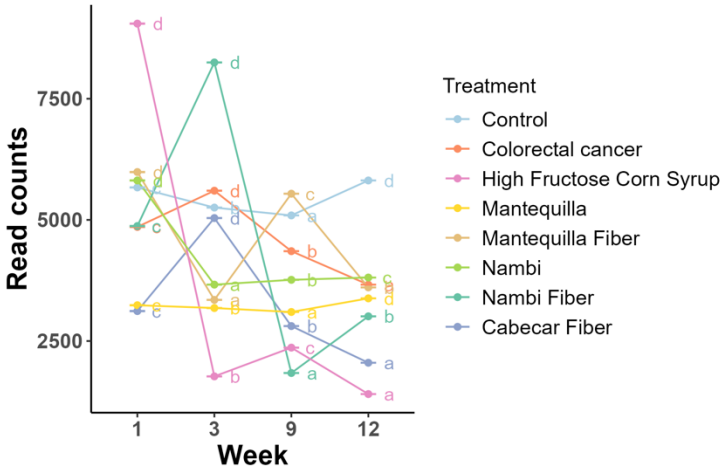

Figure A5. Temporal changes in normalized read counts of *Rombutsia.* Read counts were modeled using a generalized mixed effects model (GLMM) with a Poisson distribution, normalized by total reads. Deviance analysis tested the effects of treatment and time, followed by pairwise Z-tests. Statistical differences from the previous timepoint are indicated by compact letter display (CLD): groups sharing the same letter are not significantly different, while distinct letters denote significant differences.
Graphs are presented as fixed groups, comparing timepoints, to highlight temporal dynamics within each treatment. Treatments include Control, Colorectal cancer, High Fructose Corn Syrup, Mantequilla, Mantequilla Fiber, Nambi, Nambi Fiber, and Cabecar Fiber.

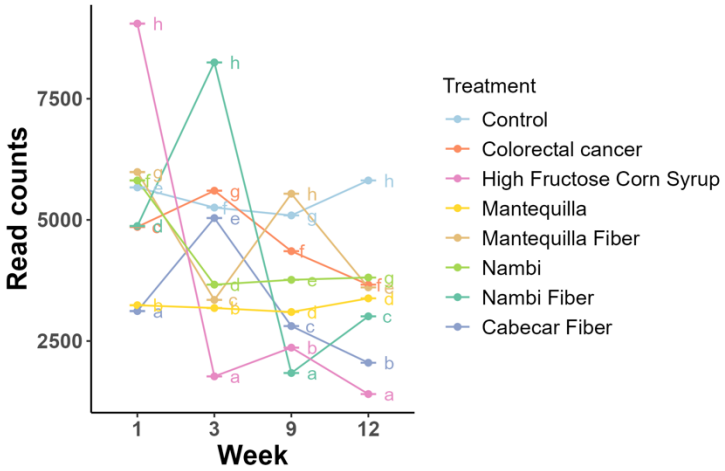

Figure A6. Normalized read counts of *Rombutsia* in Wistar rats under different dietary treatments, compared across groups at fixed timepoints to highlight cross-sectional differences among interventions at each sampling week. Read counts were modeled using a generalized mixed effects model (GLMM) with a Poisson distribution, normalized by total reads. Deviance analysis tested the effects of treatment and time, followed by pairwise Ztests. Statistical differences are indicated by compact letter display (CLD): groups sharing the same letter are not significantly different, while distinct letters denote significant differences. Treatments include Control, Colorectal cancer (CRC), High Fructose Corn Syrup (HFCS), Mantequilla, Mantequilla Fiber, Nambi, Nambi Fiber, and Cabecar Fiber.

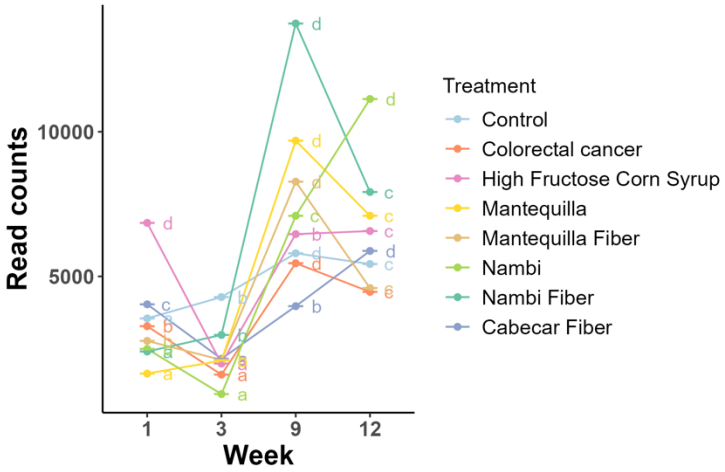

Figure A7. Temporal changes in normalized read counts of *Bacteroides.* Read counts were modeled using a generalized mixed effects model (GLMM) with a Poisson distribution, normalized by total reads. Deviance analysis tested the effects of treatment and time, followed by pairwise Z-tests. Statistical differences from the previous timepoint are indicated by compact letter display (CLD): groups sharing the same letter are not significantly different, while distinct letters denote significant differences.
Graphs are presented as fixed groups, comparing timepoints, to highlight temporal dynamics within each treatment. Treatments include Control, Colorectal cancer, High Fructose Corn Syrup, Mantequilla, Mantequilla Fiber, Nambi, Nambi Fiber, and Cabecar Fiber.

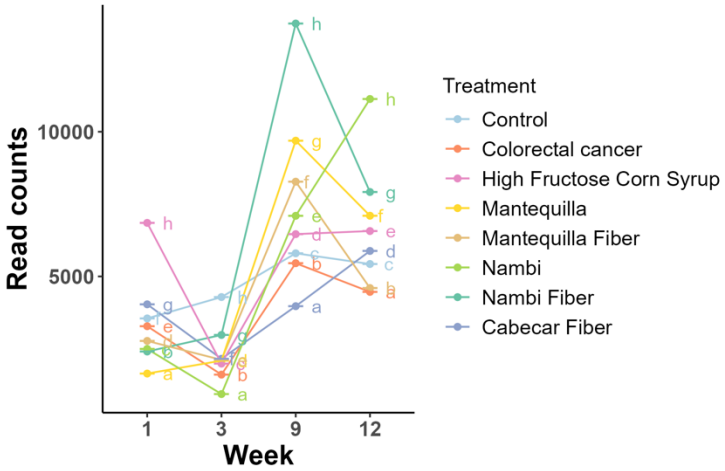

Figure A8. Normalized read counts of *Bacteroides* in Wistar rats under different dietary treatments, compared across groups at fixed timepoints to highlight cross-sectional differences among interventions at each sampling week. Read counts were modeled using a generalized mixed effects model (GLMM) with a Poisson distribution, normalized by total reads. Deviance analysis tested the effects of treatment and time, followed by pairwise Ztests. Statistical differences are indicated by compact letter display (CLD): groups sharing the same letter are not significantly different, while distinct letters denote significant differences. Treatments include Control, Colorectal cancer (CRC), High Fructose Corn Syrup (HFCS), Mantequilla, Mantequilla Fiber, Nambi, Nambi Fiber, and Cabecar Fiber.

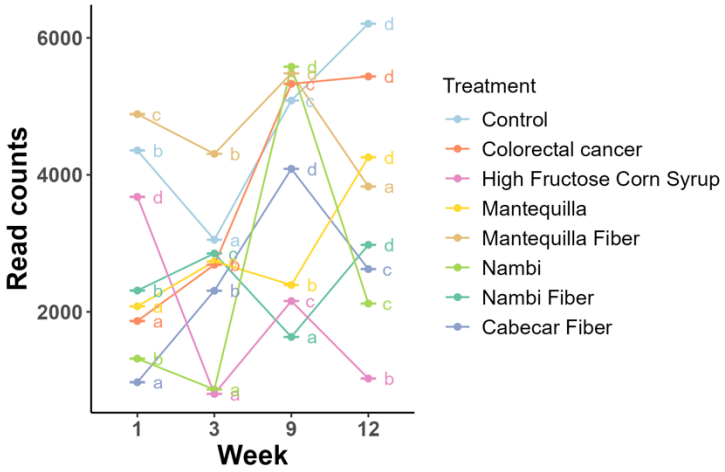

Figure A9. Temporal changes in normalized read counts of *Turicibacter*. Read counts were modeled using a generalized mixed effects model (GLMM) with a Poisson distribution, normalized by total reads. Deviance analysis tested the effects of treatment and time, followed by pairwise Z-tests. Statistical differences from the previous timepoint are indicated by compact letter display (CLD): groups sharing the same letter are not significantly different, while distinct letters denote significant differences.
Graphs are presented as fixed groups, comparing timepoints, to highlight temporal dynamics within each treatment. Treatments include Control, Colorectal cancer, High Fructose Corn Syrup, Mantequilla, Mantequilla Fiber, Nambi, Nambi Fiber, and Cabecar Fiber.

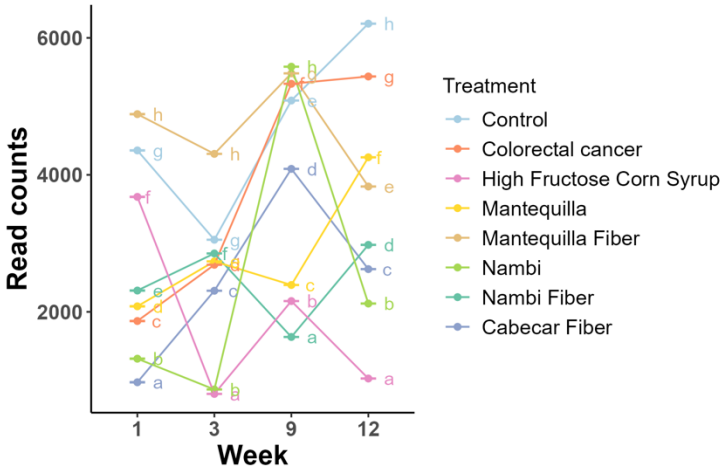

Figure A10. Normalized read counts of *Turicibacter* in Wistar rats under different dietary treatments, compared across groups at fixed timepoints to highlight cross-sectional differences among interventions at each sampling week. Read counts were modeled using a generalized mixed effects model (GLMM) with a Poisson distribution, normalized by total reads. Deviance analysis tested the effects of treatment and time, followed by pairwise Ztests. Statistical differences are indicated by compact letter display (CLD): groups sharing the same letter are not significantly different, while distinct letters denote significant differences. Treatments include Control, Colorectal cancer (CRC), High Fructose Corn Syrup (HFCS), Mantequilla, Mantequilla Fiber, Nambi, Nambi Fiber, and Cabecar Fiber.

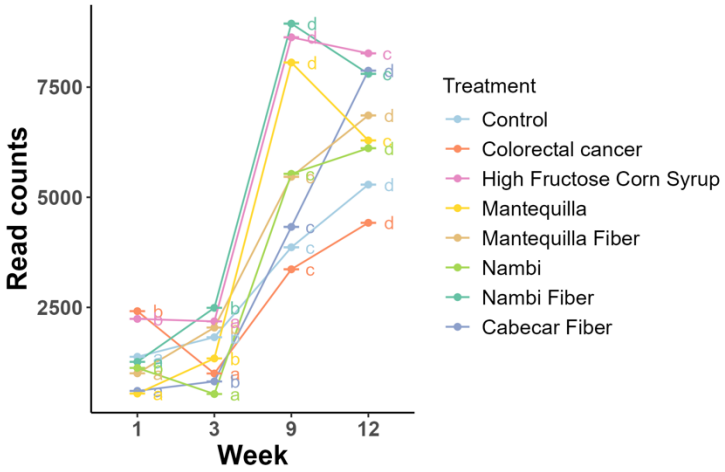

Figure A11. Temporal changes in normalized read counts of *Clostridia_UCG-014.* Read counts were modeled using a generalized mixed effects model (GLMM) with a Poisson distribution, normalized by total reads. Deviance analysis tested the effects of treatment and time, followed by pairwise Z-tests. Statistical differences from the previous timepoint are indicated by compact letter display (CLD): groups sharing the same letter are not significantly different, while distinct letters denote significant differences. Graphs are presented as fixed groups, comparing timepoints, to highlight temporal dynamics within each treatment. Treatments include Control, Colorectal cancer, High Fructose Corn Syrup, Mantequilla, Mantequilla Fiber, Nambi, Nambi Fiber, and Cabecar Fiber.

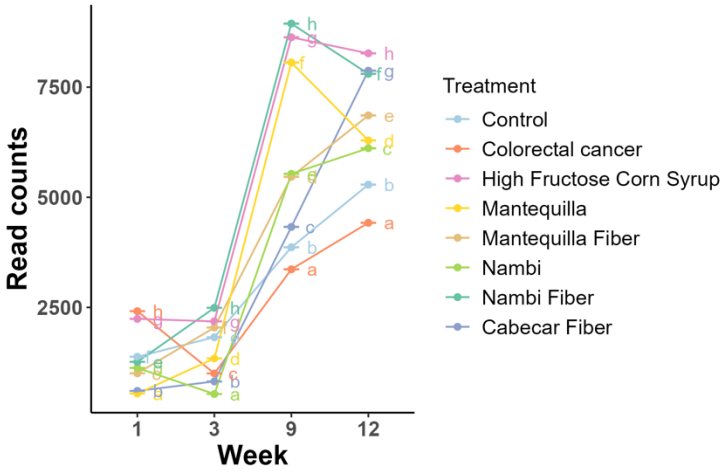

Figure A12. Normalized read counts of *Clostridia UCG-014* in Wistar rats under different dietary treatments, compared across groups at fixed timepoints to highlight cross-sectional differences among interventions at each sampling week. Read counts were modeled using a generalized mixed effects model (GLMM) with a Poisson distribution, normalized by total reads. Deviance analysis tested the effects of treatment and time, followed by pairwise Ztests. Statistical differences are indicated by compact letter display (CLD): groups sharing the same letter are not significantly different, while distinct letters denote significant differences. Treatments include Control, Colorectal cancer (CRC), High Fructose Corn Syrup (HFCS), Mantequilla, Mantequilla Fiber, Nambi, Nambi Fiber, and Cabecar Fiber.

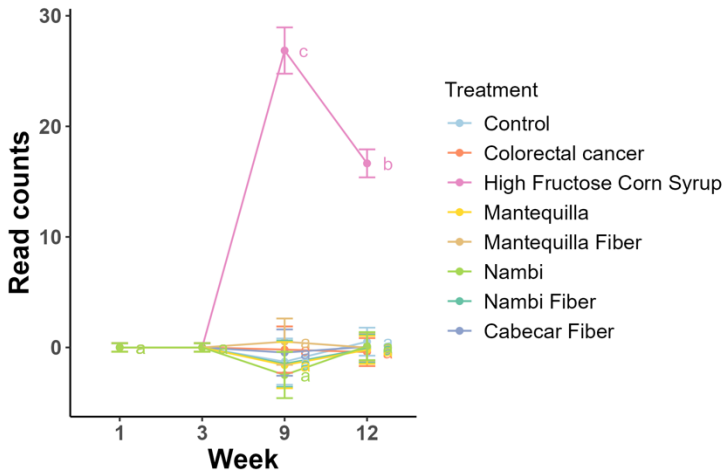

Figure A13. Temporal changes in normalized read counts of *Kosakonia.* Read counts were modeled using a generalized mixed effects model (GLMM) with a Poisson distribution, normalized by total reads. Deviance analysis tested the effects of treatment and time, followed by pairwise Z-tests. Statistical differences from the previous timepoint are indicated by compact letter display (CLD): groups sharing the same letter are not significantly different, while distinct letters denote significant differences.
Graphs are presented as fixed groups, comparing timepoints, to highlight temporal dynamics within each treatment. Treatments include Control, Colorectal cancer, High Fructose Corn Syrup, Mantequilla, Mantequilla Fiber, Nambi, Nambi Fiber, and Cabecar Fiber.

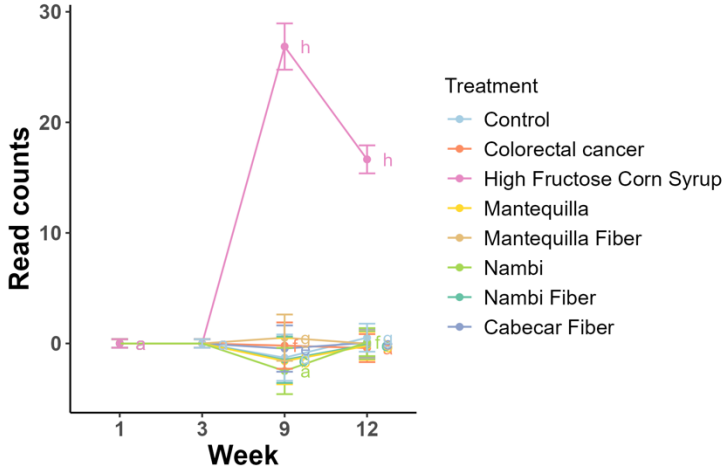

Figure A14. Normalized read counts of *Kosakonia* in Wistar rats under different dietary treatments, compared across groups at fixed timepoints to highlight cross-sectional differences among interventions at each sampling week. Read counts were modeled using a generalized mixed effects model (GLMM) with a Poisson distribution, normalized by total reads. Deviance analysis tested the effects of treatment and time, followed by pairwise Ztests. Statistical differences are indicated by compact letter display (CLD): groups sharing the same letter are not significantly different, while distinct letters denote significant differences. Treatments include Control, Colorectal cancer (CRC), High Fructose Corn Syrup (HFCS), Mantequilla, Mantequilla Fiber, Nambi, Nambi Fiber, and Cabecar Fiber.

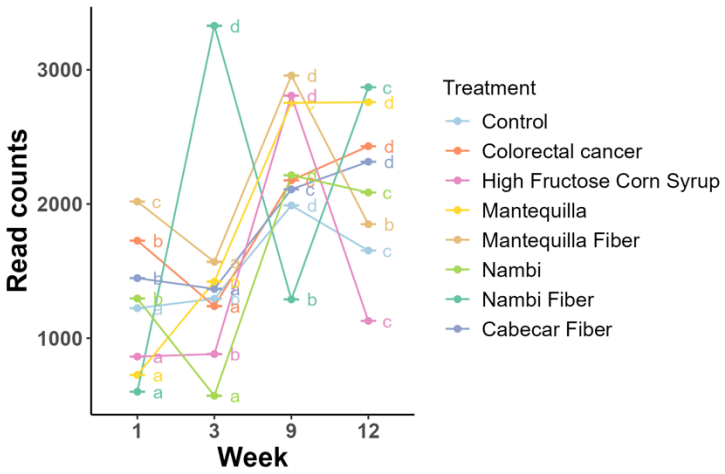

Figure A15. Temporal changes in normalized read counts of *Eubacterium_xylanophilum_group*. Read counts were modeled using a generalized mixed effects model (GLMM) with a Poisson distribution, normalized by total reads. Deviance analysis tested the effects of treatment and time, followed by pairwise Z-tests. Statistical differences from the previous timepoint are indicated by compact letter display (CLD): groups sharing the same letter are not significantly different, while distinct letters denote significant differences. Graphs are presented as fixed groups, comparing timepoints, to highlight temporal dynamics within each treatment. Treatments include Control, Colorectal cancer, High Fructose Corn Syrup, Mantequilla, Mantequilla Fiber, Nambi, Nambi Fiber, and Cabecar Fiber.

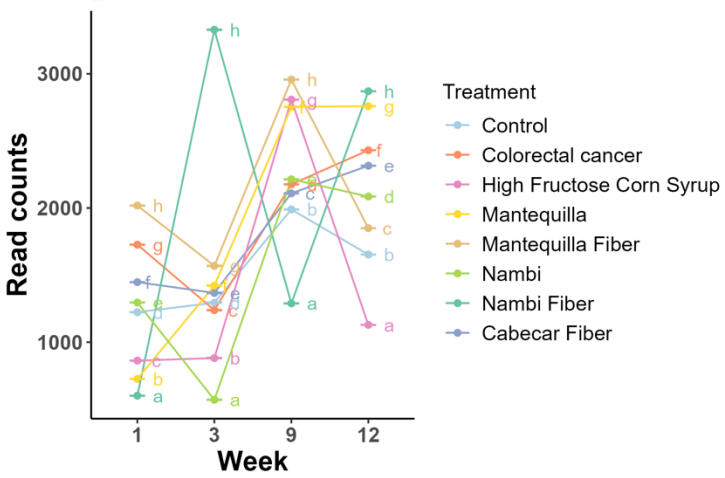

Figure A16. Normalized read counts of *Eubacterium_xylanophilum_group* in Wistar rats under different dietary treatments, compared across groups at fixed timepoints to highlight cross-sectional differences among interventions at each sampling week. Read counts were modeled using a generalized mixed effects model (GLMM) with a Poisson distribution, normalized by total reads. Deviance analysis tested the effects of treatment and time, followed by pairwise Ztests. Statistical differences are indicated by compact letter display (CLD): groups sharing the same letter are not significantly different, while distinct letters denote significant differences. Treatments include Control, Colorectal cancer (CRC), High Fructose Corn Syrup (HFCS), Mantequilla, Mantequilla Fiber, Nambi, Nambi Fiber, and Cabecar Fiber.